AN ABSTRACT OF THE THESIS OF

Ki - Seog Chang for the degree of Doctor of Philosophy in Chemistry presented on February 5, 1998.

Title: New, Complex Group 13 Borates: Synthesis, Structures, and Properties

Redacted for Privacy

Abstract approved: _____

Douglas A. Keszler

The results presented in this dissertation encompass synthesis, crystal structures, solid solutions, and two types of optical materials - luminescent hosts and nonlinear optical crystals. Several new alkali and alkaline-earth metal group 13 borates have been synthesized by using high-temperature techniques. Products have been characterized by single-crystal X-ray diffraction methods and luminescence measurements. The anionic-group theory with symbolic addition has been used to predict the second-order nonlinear susceptibility coefficients of the noncentrosymmetric materials. Following the introductory chapter, results are presented in Chapter 2 on the synthesis, structure, and Eu^{2+} luminescence of $SrAlBO_4$. The structural characteristics and optical properties have been especially important for development of a simple model relating Eu^{2+} emission color and O coordination environments.

The synthesis and study of the structurally related materials $MAl_2(BO_3)_2O$ (M = Ca, Sr, Ba) and $Na_2Al_2(BO_3)_2O$ are considered in Chapters 3 - 6. The materials provide a rich chemistry for examination of nonlinear optical properties,

luminescence, solid-solution behavior, and negative thermal expansion.

The structure and intrinsic luminescence of the pyroborate oxide $SrGa_2(B_2O_5)O_2$ are described in Chapter 7. In Chapter 8, the structure of two new lithium aluminum borates, $Li_2Al(BO_3)O$ and $LiAlB_2O_5$, are described. The latter represents the first example of the condensation of AlB_2O_7 rings.

New, Complex Group 13 Borates:

Synthesis, Structures, and Properties

by

Ki-Seog Chang

A THESIS

submitted to

Oregon State University

in partial fulfillment of

the requirements for the

degree of

Doctor of Philosophy

Completed February 5, 1998

Commencement June 1998

Doctor of Philosophy thesis of Ki-Seog Chang presented on February 5, 1998

APPROVED:

Redacted for Privacy

Major Professor, representing Chemistry

Redacted for Privacy

Head of Department of Chemistry

Redacted for Privacy

Dean of Graduate School

I understand that my thesis will become part of the permanent collection of Oregon State University libraries. My signature below authorizes release of my thesis of any reader upon request.

Redacted for Privacy

Ki-Seog Chang, Author

ACKNOWLEDGMENTS

First of all, I want to thank Professor Douglas A. Keszler for his guidance and assistance throughout my entire program. Without his expertise and direction, my Ph.D. thesis may have never been completed. I will forever owe a debt of gratitude to him.

I would also like to acknowledge my gratitude to my committee members, Prof. James H. Kruger, Prof. Michael M. Lerner, Prof. Kevin P. Gable, Prof. Kelly K. Falkner, and Prof. Kristiina Iisa(Dept. of Chemical Engineering, Georgia Institute of Technology) for their ongoing support of my doctoral program.

Very special thanks are offered to my colleagues Dr. Jun-Ming Tu, Dr. Anna Akella, M.S. Kimberly H. Dahm, M.S. Ken Vandenberghe, Dr. Ho-Kun Kim, Dr. John Evans, Dr. Anthony Diaz, and M.S. Stephen Crossno for their valuable assistance.

My warmest thanks to my colleagues Greg Peterson, Dong Li, Ben Clark, Dr. Judith Kissick, and Dr. Tae-Hwan Cho for their helpful discussions and fun in the research group.

I also wish to thank all the faculty and staff of Department of Chemistry, Oregon State University for their continued assistance.

I would further like to acknowledge my gratitude to my fatherland Korea and Republic of Korea Air Force Academy, Prof. Sung-Kee Chung and colleagues in the Department of the Chemistry, Pohang Institute of Science and Technology, and Prof. Ha-Seog Kim in Chemistry Department of Seoul National University. They believe I am special.

Lastly, I want to acknowledge my deep debt of gratitude to my M.D. Ingle family andNordlund family friends, Charles Kent, Bonnie Clair, Jennifer Rachael, and Timothy Hal, my parents Jai-Yol Chang and Duck-Hwa La, my brother Chung-Seog Chang, my parents in law Nak-Hee Lee and Sun-Ee Park, my wife Eun-Ja Lee, and my daughters Joo-Young Chang and Joo-Yo Chang for their consistent encouragement and support.

TABLE OF CONTENTS

TABLE OF CONTENTS (Continued)

TABLE OF CONTENTS (Continued)

TABLE OF CONTENTS (Continued)

LIST OF FIGURES

LIST OF FIGURES (Continued)

LIST OF TABLES

LIST OF TABLES (Continued)

New, Complex Group 13 Borates: Synthesis, Structures, and Properties

CHAPTER 1

INTRODUCTION

The preparation and study of inorganic optical materials underwent a rapid growth phase following the advent of the laser in the early 1960s. The development of laser crystals, nonlinear optical materials, and phosphors has led to many commercial applications for exploiting light in communications, image processing, and general purpose computing. With the aid of frequency conversion materials it is possible to exploit new wavelengths extending from the far-infrared to the vacuum ultraviolet for the utilization of lasers. Light emitting solid-state materials have also found in a wide range of display technologies, e.g., television and fluorescent lamps. Clearly, the investigation of new materials issues forth a means of replacing older, and less cost effective devices, with modern energy efficient ones, in addition to spurring the discovery and development of optical materials for new applications.

Since Al and Ga are more electronegative and more covalent than alkali and alkaline-earth metals, we can expect the large energy gap of a isolated BO_3 group and the wide range transparency (VUV) for NLO properties in the aluminum borates. The Ga^{3+} ion is an unusual activator and has potential for luminescent

material. The alkaline-earth metal of the alkaline-earth metal aluminum borates has good activator doping sites in the size and charge of luminescent materials, such as Eu^{2+}, Pb^{2+}, Ce^{3+}, Eu^{3+}, and Tb^{3+} ions with charge compensation ions if necessary. The alkaline-earth metals have no electronic transition in the BO_3 group energy gap range for relevant real application of NLO materials. Since alkali or alkaline-earth metals have a usually isotropic environment, no polarization by a high symmetry with high coordination number, they have no electronic transitions in the ultraviolet-transparent range, but borate groups usually have anisotropic environments. We estimate nonlinearity about borate groups. In my research it has been identified that new family of alkali or alkaline-earth aluminum borates have variable composition for manipulation, linear and nonlinear optical properties, thermal contraction, and open framework structure for the ionic conductor and that they are new hosts for luminescent materials.

The work described in this dissertation is focused on the development of the crystal chemistry of alkali-metal and alkaline-earth metal group 13 borates and their solid solutions, thermal expansion, optical frequency conversion and luminescence. The motivation for studying these systems derives from fusing the chemical, structural, and optical properties of known materials and projecting a likely improved performance for new materials.

A few borates have been shown to exhibit favorable nonlinear optical properties at high powers and short wavelengths, and capabilities as efficient frequency converters. Among them, β-BaB_2O_4 (BBO) and LiB_3O_5 (LBO) have been extensively used for frequency conversion of high-power laser light.[1] Crystals of

LBO are relatively free of inclusions, which greatly decrease the optical damage threshold, giving LBO a damage threshold higher than that of any other commercially available converter. Borates are also used as phosphors. These include $MgGdB_5O_{10}$, $MgLaB_5O_{10}$, SrB_4O_7, and $InBO_3$ which are currently used in fluorescent lamps and cathode-ray tubes.[2] Eu^{2+} doped phosphors are used in a variety of applications. $SrB_4O_7:Eu^{2+}$ is used in suntanning lamps to produce near-UV light. $BaMgAl_{10}O_{17}:Eu^{2+}$ is used in fluorescent lamps, and is also the blue component of plasma displays. $SrGa_2S_4:Eu^{2+}$ has been proposed for use as the green component in field emission and electroluminescent displays. The Ga^{3+} ion also has a d^{10} configuration in the central ion as a unusual example of luminescent complexes.[3] The compound $MgGaBO_4$ shows a blue luminescence under excitation by cathode-ray radiation. The gallium compounds $LnGa_3B_4O_{12}$ (Ln = Y, Sm, Eu, Gd, Tb, or Dy) show a very broad emission band with a maximum at 450 nm. The development of luminescent materials for lighting, cathode-ray tubes, scintillator, X-ray screens, and most recently, flat-panel displays, is dependent on the discovery of materials that possess desirable properties such as high efficiency, UV durability, desirable color rendition, and thermal stability.

Borate anions exist in numerous structural types since the B atom is found in either three-or four-fold coordination modes. In this dissertation, I will describe several new structural types that result from different combinations of these three-coordinate B atoms. These new structures encompass the orthoborate BO_3 and pyroborate B_2O_5, triborate B_3O_5. In Chapters 2 - 4 and 7, the crystal chemistry, structures, and characteristics of new luminescent materials are presented. In

Chapter 2, 3, and 7, Eu^{2+} or Ga^{3+} luminescence results are also described. In Chapter 3, 4, 5, and 6, the new layered orthoborates $MAl_2(BO_3)_2O$ (M = Ca, Sr, Ba, and Na_2), resembling those of 3-dimensional β-alumina-type structures, are described. Among the nonlinear optical converters currently in discovery, $KBe_2BO_3F_2$ (KBBF) and $Sr_2Be_2(BO_3)_2O$ (SBBO) exhibit some favorable optical properties at high powers and short wavelength. These desirable features stem from the specific electronic structure of BO_3 triangles and anionic group orientations in the crystal. The layered borate materials such as $YAl_3(BO_3)_4$ (YAB), KBBF, and SBBO showed that the active group responsible for the NLO properties is the $(BO_3)^{3-}$ anion.[4, 5, 6] As part of my efforts to discover new nonlinear optical materials, I found three structures containing the BO_3 triangle; these results are detailed in Chapters 3 - 5. Among them, $SrAl_2(BO_3)_2O$ (SABO) and $BaAl_2(BO_3)_2O$ (BABO), exhibit desirable optical properties and crystal-growth characteristics. Both our calculations with free anionic group theory and optical frequency-conversion measurements indicated that this compound is an attractive and promising nonlinear optical material. The new crystals of aluminum borate could replace other materials in lasers used in medicine and industry.

Solid-state synthesis has been used for the preparation of new materials. As previously mentioned, a strong need exists for new optical materials. Imitating the Keszler Group philosophy, I approach my research horizontally -- I look for new compounds that satisfy my materials research goals, characterize their structural nature, and study them further for their practical utility. Thus, potential new optical materials will eventually be tested in some degree for their performance in their

targeted purpose.

To carry out these objectives, I attempt to "design" a new compound based upon the following: (1) the desired properties of the proposed material, (2) a "void" where a compound is not known to exist, but might exist, and (3) chemical knowledge of structure-property relationships, intuition, and creativity.

The previous structural studies of layered borate materials such as KBBF and SBBO showed that the active group responsible for the NLO properties is the $(BO_3)^{3-}$ anion. To search new nonlinear optical materials, my continued synthetic efforts were directed to the preparation of aluminum borates containg isolated BO_3 groups. This effort has led to the discovery of three new materials built from isolated planar BO_3 triangles - SABO, BABO, and NABO. While attempting to prepare the Ca analog, a new centrosymmetric structure type was identified.

Section I. Crystal Chemistry of Borates

Borate anions exist in numerous structural types since the B atom is found in either three- or four-fold coordination modes. These structures encompass the orthoborates BO_3, pyroborates B_2O_5, triborates B_3O_5, tetraborates B_4O_7, pentaborates B_5O_9, and polyborates B_6O_{10}, B_8O_{13}, B_9O_{15}, and $B_{10}O_{17}$

Anhydrous borates comprise those B-O species of synthetic or natural origin in the crystalline or vitreous states that exhibit B atoms linked to either three O atoms at the corners of a triangular plane or four O atoms at the vertices of a tetrahedron. Borates have been widely used in glass, cleaning agents, paints, anticorrosive agents, phosphors, laser hosts, and nonlinear optical materials. During the past few years, greater interest has developed in crystalline borates

because of their favorable high optical damage thresholds and UV transparency for optical applications. I have undertaken the study of new alkali-metal or alkaline-earth metal aluminum (or gallium) borates of potential interest as optical materials. From the different combinations of 3-coordinate of B atoms, several new anhydrous borates have been discovered. A classification scheme of these new structures is given below:

1. Orthoborates containing the monometric, triangular-planar unit BO_3. Compounds $SrAl(BO_3)O$, SABO, BABO, $Na_2Al_2(BO_3)_2O$ (NABO), $CaAl_2(BO_3)_2O$ (CABO), and $Li_2Al(BO_3)O$ exhibit such borate units and are described in Chapters 2, 3, 4, 5, 6, and 8.

2. Pyroborates containing the unit B_2O_5 that consists of two triangles joined by a common oxygen atom. Compounds $SrGa_2(B_2O_5)O_2$ and $LiAlB_2O_5$ exhibit only pyroborate groups, and they are discussed in Chapters 7 and 8.

3. Triborates containing B_3O_7 rings that comprise two triangular BO_3 and one tetrahedral BO_4 group. The B_3O_7 rings are completely condensed into a 3-dimensional framework by sharing vertices. The chemical formula of the anion in structures can be simply obtained by counting the O atoms $B_3O_{3+4/2} = B_3O_5$. Compounds LiB_3O_5 (LBO), $SrLi(B_3O_5)_3$, and $CsLi(B_3O_5)_2$ (CLBO) exhibit such borate rings. From the different combinations of 3-coordinate of B atoms and 4-coordinate of Al atom, a new anhydrous borate $LiAlB_2O_5$ has been discovered. A AlB_2O_7 ring of $LiAlB_2O_5$ is very similar to B_3O_7 ring. The compound $LiAlB_2O_5$ exhibits such aluminum borate ring and is described in chapter 8.

Section II. Electronic Structures of Isolated Borates

The electronic structure of the BO_3 group calculated by the DV-SCM-Xα

quantum-chemical method shows 173 nm for absorption of n to π^* and 150 nm for absorption of π to π^*.[7] Crystalline borates exhibit a number of properties that make them attractive as optical materials: wide range of transparency, high damage threshold, chemical stability, low thermal expansion, and high optical quality.

Layered $(BO_3)^{3-}$ anions are responsible for the NLO properties in NABO, SABO, and BABO. The ultraviolet-transparent range of layered borate materials is determined mainly by the energy gap of the anionic groups[8] if the cations are alkali or alkaline-earth metals which have no electronic transitions in this range. Figure1.1 shows the electronic structure of the$(BO_3)^{3-}$ ion calculated by the DV-SCM-Xα quantum-chemical method.[9] Absorption in this group occurs at 173 nm.

If the dangling bonds of the three terminal oxygen atoms are interlinked with cations such as Ca, Sr, Ba, and Na, the absorption band should be shifted. In the cation, Be, the absorption band shifts to 150 - 160 nm.[4] As the atomic radii of alkaline-earth elements, Be, Ca, Sr, and Ba, increases down a group, the polarizabilities of them increase and the absorption bands of them shift to larger wavelengths.

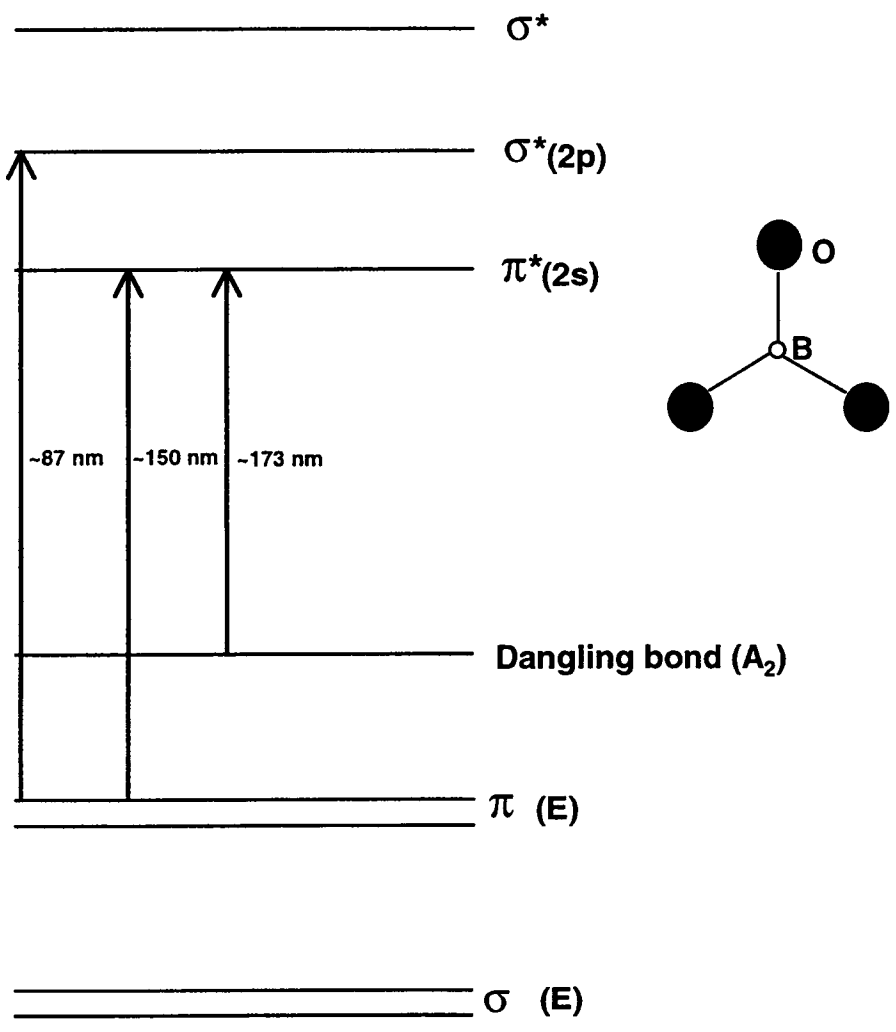

Figure 1.1 Electronic structure of the $(BO_3)^{3-}$ group.

Section III. Optical Frequency Converters (SHG)

Nonlinear optical (NLO) crystals are unique in allowing generation of new wavelengths extending from the far-infrared to the ultraviolet by second harmonic generation, sum and difference mixing, and stimulated Raman scattering of laser light. Desirable characteristics of new nonlinear optical materials include sufficient birefringence for phase matching, mechanical and chemical stability, a wide rang of transparency, high optical quality, low thermal expansion, and adequate crystal size. Unfortunately, only several tens of different phases of roughly 20,000 crystalline phases have ever been applied to practical nonlinear optical frequency conversion.[10] Therefore, the success of a nonlinear optic relies on the existence of a very specific set of physical properties in a single material.

The discovery and study of nonlinear optical (NLO) materials has developed into an active field of materials research since frequency conversion of laser light was first witnessed in a quartz crystal in 1961.[11] Laser light can be converted from one frequency to another by using nonlinear optical materials, thus significantly increasing the range of applications (Figure 1.2). Monochromatic light generated at shorter wavelengths has been widely used in areas of fundamental science, industry, and defense.

The power ($P_{2\omega}$) in second harmonic generation (SHG) from a crystal of length L, may be approximated by Eq. 1.1,[12]

$$P_{2\omega} \propto P_{\omega}^{2} \cdot L^{2} \cdot d_{jm}^{2} \exp\{-L(\alpha_{\omega}+\frac{1}{2}\alpha_{2\omega})\}[\frac{\sin^{2}L \cdot \Delta K/2}{(L \cdot \Delta K/2)^{2}}] \qquad [Eq.\ 1.1]$$

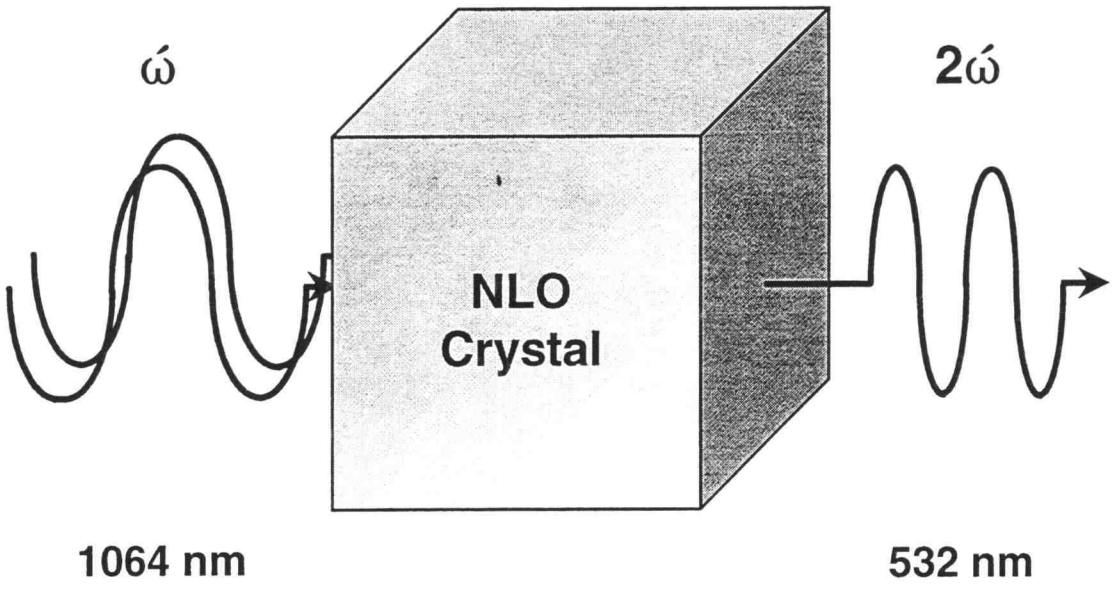

Figure 1.2 Frequency conversion of light via a crystalline medium.

Here P_ω is the power of the incident beam, d_{jm} is the SHG coefficient, α_ω is the absorption coefficient of the crystal at the fundamental wavelength, $\alpha_{2\omega}$ is the absorption coefficient of the crystal at the second harmonic wavelength, and ΔK is the wave vector mismatch between the fundamental and second harmonic waves. The exponential term approximates the absorption characteristics of the NLO crystal and the *sin* term describes the ability to phase-match the incoming and doubled waves. It is evident from Equation 1.1. that high powers can be obtained in the second harmonic wave with a large second harmonic coefficient. If the absorption bands of the crystal overlap either the fundamental or second harmonic wavelength, an exponential decrease in the output power will ensue. The phase mismatch between the fundamental and second harmonic waves also affects the second harmonic output power.

The macroscopic second harmonic coefficient is defined as

$$d_{jm} \Rightarrow \chi^{(2)}_{IJK}(\omega,\omega) = \frac{1}{V}\sum_{ijk} R_{Ii} R_{Jj} R_{Kk} \beta_{ijk}(\omega,\omega) \qquad [Eq.\ 1.2]$$

where V is the volume of the unit cell, the R direction cosines relate molecular coordinates to crystal coordinates, and the coefficients $\beta_{ijk}(\omega,\omega)$ are the microscopic hyperpolarizability tensor components for the relevant anionic groups.

$$\beta_{ijk}(\omega,\omega) = \frac{1}{4}h^2 \sum_{p} \sum_{e,e'} \frac{\langle g|\tilde{\mu}_i|e\rangle\langle e|\tilde{\mu}_j|e'\rangle\langle e'|\tilde{\mu}_k|g\rangle}{(\omega_e-\omega_g-2\omega)(\omega'-\omega_g-\omega)} \qquad [Eq.\ 1.3]$$

In Eq. 1.3 $|g\rangle$ represents a ground electronic state, and $|e\rangle$ and $|e'\rangle$ represent excited electronic states.

An explanation of Equation 1.3 may be gained by considering the *ijk* subscripts for β; here, *ijk* can be 1, 2, or 3 (≡ *x*, *y*, or *z*). The subscript *I* indicates the direction of polarization induced by the incoming photons and the subscripts *j* and *k* signify the directions of electric polarization for the incoming photons. The quantity β_{333} describes the magnitude of polarization induced in the *z* direction when two photons also polarized along *z* are incident on a molecule. By permuting over all possible *ijk* values, every possible interaction is described.

For a material to qualify for efficient second harmonic conversion, it should possess a large second harmonic coefficient and the hyperpolarizability tensors must sum constructively. It should be noncentrosymmetric, since in a centrosymmetric crystal each positive β_{ijk} will have a negative partner $-\beta_{ijk}$ that will lead to Equation 1.2 summing to zero. The integral specified in the numerator of Equation 1.3 represents the transition moments associated with the ground and excited states in the three-photon process. The denominator represents the differences in energies between the energy gaps and the fundamental and second harmonics.

There is only one type of BO3 group in the materials, $SrAl_2(BO_3)_2O$ (SABO) (space group R32) and $BaAl_2(BO_3)_2O$ (BABO) (space group R32) and two crystallographically nonequivalent borate groups in the material, $Na_2Al_2(BO_3)_2O$ (NABO) (space group P31c) that lie in planes orthogonal to the c axis like $YAl_3(BO_3)_4$ (YAB) (space group R32).[13] The compound YAB has been discovered as a common NLO material. The borate framework of YAB is constructed from isolated BO_3 triangles with a high second-order coefficient 1.48 pm/V and 48% of

optical maximum. There are two sets of B atoms labeled as 1 and 2 about the C_3 axis; set 1 is below the plane containing the Sr atom of SABO, the Ba atom of BABO, or the Na atom of NABO and set 2 is above. Since the nonlinear susceptibility is proportional to $\cos 3\theta$ (θ = misalignment angle), the calculated second-order nonlinear coefficients with YAB are described in Chapters 3, 4, and 5, respectively.

The Czochralski process, by far, is the most efficient and common technique for crystal growth from a melt. A congruent material, however, is essential for application of the technique. Unfortunately, only a few crystalline phases come close to melting congruently. Therefore, congruence is one of the desirable characteristics for a new nonlinear material.

All of the above mentioned characteristics play an important role in dictating the utility of a new material. The aforementioned characteristics are only a few of the necessary chemical and mechanical characteristics for a useful frequency doubler.[14]

Other conditions that are desirable for applications:

1. Low melting point
2. Melt congruently
3. Noncentrosymmetric structure
4. Chemical stability and mechanical strength
5. High optical quality
6. High damage threshold
7. Wide transparency range
8. Large birefringence to allow easy phase matching
9. Large nonlinear coefficients

Two borates, BBO and LBO, have been used commercially as frequency converters in the UV region.[15] BBO has large nonlinear coefficients (see Table 1.1), 3 to 6 times that of the well-known converter KDP.[11] The fifth harmonic generation of 1.06 μm Nd:YAG to 213 nm has been demonstrated in BBO with 11% overall efficiency.[16] LBO exhibits a lower threshold power than BBO, and it has capabilities as an efficient frequency converter at high powers. LBO can achieve higher second harmonic efficiencies for mode-locked Nd:YAG lasers than KTP because of damage limitations in the latter crystals. $CsLiB_6O_{10}$ (CLBO) has the highest reported damage threshold of any commercially available solid-state frequency converter.[17] Also, it has been shown to exhibit a threshold power for 50% conversion efficiency that is two orders of magnitude lower than that of KDP; it is optically transparent in the range 160 nm to 2.6 μm, making it useful for applications in the UV region.

Table 1.1 Common Nonlinear Optical Materials

	Transmission Range (μm)	Damage Threshold (GW/cm^2)	Nonlinear Coefficient*	Threshold Power (MW)
KDP	0.20 - 1.5	6	$d_{36} = 0.76$	75
KTP	0.35 - 4.5	3	$d_{31} = 13.5$	0.1
			$d_{32} = 10.4$	
			$d_{33} = 28.4$	
YAB	0.16 - 4.5	-	$d_{11} = 5.7$	-
BBO	0.19 - 3.5	13.5	$d_{11} = 4.1$	90
LBO	0.16 - 2.6	25	$d_{31} = 0.15$	0.1
			$d_{32} = 2.97$	
			$d_{33} = 2.75$	

* $d_{mm} \times 10^9$ esu cm^{-3}

The favorable nonlinear properties of YAB, $KBe_2BO_3F_2$ (KBBF), and $Sr_2Be_2(BO_3)_2O$ (SBBO) are derived from the borate matrix of isolated BO_3 triangles. As one of my projects to identify new nonlinear materials, I discovered three new structures possessing matrices similar to that of YAB and SBBO. The SABO, BABO, and NABO structures and characteristics are described in Chapters 3 - 5. Among these materials, the compounds SABO and BABO are particularly important; both from powder SHG measurements and computations, we have

predicted that SABO and BABO are promising NLO materials. The new crystals will have diverse applications in the future, though some of the obstacles, such as growing these crystals to commercially usable sizes remain to be surmounted. They could lower the cost of lasers used in eye surgeries such as radical keratotomy and improve the performance of lasers used to monitor toxic pollutants in the environment.

In these materials the nonlinear effects derive from the natural orientation of the molecular-like borate groups rather than any small displacements of individual atoms as in ferroelectrics. The efficiency of the frequency-conversion process is directly related to the nature and arrangement of the borate groups in the crystal. In fact, a diminution in NLO effects is expected for most materials on heating. Ferroelectrics, such as $KNbO_3$, and NLO polymers depole as they are heated. In temperature tunning for phase matching with $KNbO_3$, a 12-V field must be applied to the crystal at temperatures as low as 50°C to maintain the poled state. In this work, the new structure SABO has been determined where the conversion efficiency may be considerably enhanced through reorientation of the BO_3 groups by simple heating. The thermal contraction of SABO and related NLO properties are detailed in Chapter 3.

Section IV. Luminescent materials

A luminescent material (phosphor) is also an inorganic material that absorbs some form of energy and then emits part of this energy as light. The absorbed energy can be derived from IR, UV, or visible light, high energy electrons, a

mechanical stress, or simple heat, to name just a few.[18] Phosphors are used in fluorescent lamps, lasers, digital radiography, high definition television screens, fiber optics, solar concentrators, X-ray photography, and packets of washing powder.[19, 20, 21, 22] Reduction of cost, high efficiency (usually > 90%), stability under high energy illumination, absorption and emission in well-defined regions, ease of manufacture, and environmental requirements are to be only considered in the search for and development of phosphors having desirable characteristics.

A luminescent material (phosphor) may be defined as a solid that converts certain types of energy into electromagnetic radiation over and above thermal radiation.[23] Luminescence can be excited by many types of energy. Photoluminescence is excited by electromagnetic (often ultraviolet) radiation, cathodoluminescence by a beam of energetic electrons, electroluminescence by an electric voltage, triboluminescence by mechanical energy; --e.g., grinding, X-ray luminescence by X rays, chemiluminescence by the energy of a chemical reaction, and so on.

Minimization of radiative energy losses and efficiency and color rendition are important considerations for phosphor materials. For some applications, phosphors must have robust UV and thermal stabilities. Another consideration is phosphor efficiency which is intimately connected to the quantum yield of the material. Loss of efficiency through nonradiative pathways can be reduced by isolating the active ions in the structure and by reducing the number of ions in the framework that would lead to quenching. Today's researchers have concluded that a three-color lamp is more efficient and has a better rendition than those produced

by older two-color phosphors. A number of borates are also known to be useful luminescent hosts. The luminescence of these hosts is associated with dilute concentrations of transition, lanthanide, or heavy ions (Tl^{+}, Pb^{2+}, Bi^{3+}, Mn^{2+}, Sb^{3+}) isolated in the matrices; these ions are referred to as "activators." Their energy states are treated through basic atomic theory with modification of their energy levels through crystal-field effects. Among the known activators, Ce^{3+} (sensitizer or UV emission), Eu^{2+} (blue emission), Eu^{3+}(red emission), Tb^{3+} (green emission) and Ga^{3+} (bluish white emission) are particularly important in producing efficient visible emission in a variety of hosts.

In the spectroscopy involving rare-earth ions, blue-emitting phosphors based on Eu^{2+} ions are commercially important. Depending on the host lattice, broad-band emission from $4f^{6}5d \rightarrow 4f^{7}$ transitions or sharp line emission spectra from transitions within the $4f^{7}$ configuration may be observed. The emission properties (Stokes shift, wavelength of emission peak, and efficiency) of a luminescent center are affected by crystal field, size and symmetry of the substitutional site, and the nature of the neighboring atoms. The luminescence of the new compounds of $SrAl(BO_3)O$, SABO, and BABO doped with Eu^{2+} are described in Chapters 2-4.

The red luminescence of the Eu^{3+} ion doped into inorganic solids has been extensively studied.[24, 25, 26] The sharp emission feature near 612 nm has found important applications in fluorescent lighting and display technologies such as color television and plasma displays. The transition of these lines occurs from the excited $^{5}D_0$ level to the $^{7}F_J$ levels (J=0,1,2,3,4,5,6) of the 4f configuration. Because f→f type transitions of the 4f orbitals are well shielded by the filled $5s^2$ and $5p^6$

levels, these transitions are only weakly influenced by the host lattice. Furthermore, since the transitions are not spin allowed, long excited state lifetimes on the order of 10^{-3} seconds are observed.

Optical absorption transitions such as those for Eu^{3+} are strongly forbidden as electric-dipole transitions by the parity selection rule. Transitions can only occur, therefore, as weak magnetic-dipole transitions which obey the selection rule $\Delta J = 0, \pm 1$. However, the parity selection rule can be relaxed when odd components of the crystal field mix a small amount of opposite-parity wave functions (e.g., 5d) into the 4f wave functions. Such a case arises when the luminescent ion occupies a site that lacks or deviates from inversion symmetry to bring about the so-called forced electric-dipole transition. Transitions for $\Delta J = 0, \pm 2$ are hypersensitive to this effect.

For a luminescent center on a site of inversion, the most intense transition is $^5D_0 \rightarrow {}^7F_1$, which occurs near 590 nm. The orange color of this line is inadequate for display and lighting purposes. However, once the symmetry constraint is lifted, the $^5D_0 \rightarrow {}^7F_2$ transition can dominate, thereby, generating a saturated red line near 612 nm. Some of the characteristics of orange and red emissions are described in Appendix.

Since the Ga^{3+} ion has a d^{10} configuration in the crystal ion and a d^{10} activator ion as a unusual example of luminescent complexes with a very broad emission band, the luminescence of Ga^{3+} in the host $SrGa_2(B_2O_5)O_2$ is discussed in Chapter 7 as a intrinsic luminescence material.

V. Synthesis and Characterization

New phases were identified by powder X-ray diffraction, and single crystals were grown either from the melt or by adding a flux, depending on whether the material melted congruently or incongruently. The structures of the compounds were determined by using data from an automated Rigaku AFC6R single crystal X-ray diffractometer. The optical properties were investigated if the material exhibited suitable structural and melting characteristics. For noncentrosymmetric structures, a powder second harmonic experiment was performed to determine its approximate efficiency as a frequency converter. The observed conversion efficiency for each material was then compared with a calculated susceptibility obtained from a set of computer programs written in this laboratory. The computations provided a means for comparison and allowed for a better understanding of the origin of the observed nonlinear effects. For potential luminescent materials, the suitable optical activator was chosen for substituting the host ions. Excitation and emission spectra were recorded with a spectrometer assembled in this laboratory

References

1. Chen, C.; Wu, B.; Jiang, A.; You, G. *Sci. Sin., Ser B,* **1985**, *28*, 235.

2. Welker, T., *J. Luminescence*, **1991**, *48*, 49.

3. Blasse, G., Chem. Phys. Letters, 175(3), **1990**, 237.

4. Chen, C., Wang, Y., Xia, Y., Wu, B., Tang, D., Wu, K., Wenrong, Z., Yu, L., and Mei, L., J. Appl. Phys., **1995**, 77, 2268.

5. Chen, C., Wang, Y., Wu, B., Wu, W., Zeng, W., and Linhua, Y., Nature, **1995**, 373, 322.

6. Schaffers, K. I. Ph.D. Thesis, Oregon State University, **1992**.

7. Y. Xia, C. Chen, D. Tang, and B. Wu, *Adv. Mater.*, **1995**, 7, 79.

8. Wu, K. C. and Chen, C. T. Appl. Phys., A54, **1992**, 209-220.

9. Pelley, B. and Ellis, D. E., J. Chem. Phys., **1982**, 76, 1949-1960.

10. P. F. Bordui, *Annu. Rev. Mater. Sci.*, **1993**,23, 321.

11. Franken, P.; Hill, A.; Peters, C.; Weinreich, G. *Phys. Rev. Lett.* **1961**, *7*, 118.

12. Weber, M. J. *CRC Handbook of Laser Science and Technology*, "Section 1: Nonlinear Optical Materials", Boca Raton, Fla.: CRC Press, **1986**.

13. Ballman, A. A., Amer. Mineral., **1962**, 47, 1380.

14. Akella, A. Ph.D. Thesis, Oregon State University, **1994**.

15. Eckardt, R. C.; Masuda, H.; Fan, Y. X.; Byer, R. L. *IEEE J. Quantum Electron.* **1990**, *26*, 922.

16. Eimerl, D.; Davis, L.; Velsko, S.; Graham, E. K.; Zalkin, A. *J. Appl. Phys.* **1987**, *62*, 1968.

17. Tu, T.; Keszler, D. A. *Mat. Res. Bull.*, **1995**, *30*, 209.

18. G. R. Fonda and E. F. Apple, *Luminescent Materials*, Encyclopedia of Chemical Technology, **1981**, 14, 527.

19. L. J. Andrews, G. H. Beall and A. Lanpick, *J. Luminescence*, **1986**, 36, 65.

20. K. Takahashi, J. Miyahara and Y. Shibajara, *J. Electrochem. Soc.*, **1985**, 132, 1492.

21. G. Blasse, *Mat. Chem. Phys.*, **1987**, 16, 201.

22. Blasse, G.; Grabmaier, B. C., *Luminescent Materials*, **1994**, 1.

23. Blasse, G.; Grabmaier, B. C., *Luminescent Materials,* Springer-Verlag, **1994**.

24. Judd, B. R., *Phys. Rev.*, **1966**, 127, 750; Ofelt, G. S., *J. Chem. Phys.*, **1962**, 37, 511.

25. Maestro, P., et al., *Journal of the Electrochemical Society*, **1992**, 139, No. 5, 1479.

26. West, P. and Clements, N. S., *Journal of Luminescence*, **1992**, 54, 245.

CHAPTER 2

SYNTHESIS, STRUCTURE, AND LUMINESCENCE OF $SrAlBO_4$

Ki-Seog Chang and Douglas A. Keszler

To be submitted to Acta Crystallographica C., **1997**

Abstract

The structure of the borate $SrAlBO_4$ has been established by single-crystal X-ray diffraction methods. It crystallizes in the orthorhombic space group Pccn (Z = 4) with unit-cell parameters a = 8.853 Å, b = 15.150 Å, c = 5.708 Å, and V = 765.65 $Å^3$. The structure was refined from 600 total reflections to the final residuals R = 0.059 and wR = 0.0665. It is characterized by an association of BO_3 triangles, AlO_4 tetrahedra, SrO_8 polyhedra.

In my research, I found green emission at 529 nm for Eu^{2+}:$SrAlBO_4$ with Stokes shift = 8000 cm^{-1}; such green emission of Eu^{2+} has long been known. The large Stokes shift has been suggested to result from the high coordination number of the O atoms by Sr. The Sr-O distance of $SrAlBO_4$ is 2.675 Å. The UV excited luminescence of the Eu^{2+} ion in the borate $SrAlBO_4$ yields a visible emission.

Materials index: Strontium, Aluminum, Borate.

Introduction

Borates have long been important for the production of a variety of glasses. The glass-forming regions of alkaline-earth (Ca, Sr, Ba) aluminum borate systems were recently examined by MacDowell.[1] The materials of primary interest center near the 1 : 1 : 1 molar ratio of MO (M = Sr, Ba, or Ca) : Al_2O_3 : B_2O_3 where the glass - ceramics were highly crystalline. Crystals of composition 2CaO: Al_2O_3: B_2O_3, melting incongruently at 1098 ± 10°C were obtained from a 2CaO: Al_2O_3: B_2O_3 melt in the three ternary aluminum borate system.[2] The melt was cooled from 1130 to 1080°C at 10°C/h. This compound forms in the space group Ccc2 with the following cell constants: a = 8.269(2) Å, b = 15.227(3) Å, c = 5.733(3) Å, and Z = 8.[3] The crystal structure of di-strontium aluminum borate $SrAlBO_4$ with R = 0.163 was reported by Nagai, T. and Ihara, M.[4] The mixture, SrO 44.6 wt%, Al_2O_3 25.4 wt%, and B_2O_3 wt% was melted in the 3 cc Pt crucible at 1423°K, to make a metastable compound, glass. The crystallization occurred at 1173°K for 48 hours. We have also recently synthesized the compound $SrAlBO_4$ by using the flux method, which is different from Nagai and Ihara group's annealing techniques, and identified the compound $SrAlBO_4$ with R = 0.059 as a new luminescent material. The structure consists of an 8-coordinated Sr atom, an AlO_4 tetrahedron, and a BO_3 triangle.

We also describe the luminescence of the Eu^{2+} ion at a 8 coordinated Sr atom cite in the $SrAlBO_4$.

Experimental Section

Synthesis and Crystal Growth

A powdered sample of $SrAlBO_4$ was prepared by heating a stoichiometric mixture of the reagents $SrCO_3$ (Alfa, 99.99%), Al_2O_3 (Alfa, 99.999%), and B_2O_3 (Alfa, 99.98%). The mixture was heated in a Pt crucible at 893 K for 1 h, cooled, ground, and again heated at 1153 K for 12 h. An X-ray powder diffraction pattern of the product, obtained with a Philips diffractometer, matched that generated with the computer program LAZY-PULVERIX[5] and the results of the single-crystal study (vide infra). Since the compound decomposes at 1273 K, crystals were grown in a Pt crucible from a melt containing 80 mol% $SrAlBO_4$ and 20 mol% $LiBO_2$. The melt was cooled at 0.07 K/min from 1190 to 800 K, and then 5 K/min to room temperature. A clear, colorless crystal was physically separated from the matrix for X-ray measurements.

Crystallographic Study

The crystal was mounted on a glass fiber and analyzed on a Rigaku AFC6R X-ray diffractometer. Unit-cell parameters were derived from least-squares refinements with the setting angles of 20 automatically-centered reflections in the range of $30.0 < 2\theta < 36.0°$. Intensity data were collected at room temperature by using the ω-scan technique with a rate = 16.0°(ω)/min and peak widths = 1.50 + 0.30 tanθ. The cell constants and Laue symmetry *mmm* correspond to the orthorhombic crystal system. The intensity data were collected over the range of

indices $0 \leq h \leq 12$, $0 \leq k \leq 21$, $0 \leq l \leq 8$. From 1337 measured reflections, a total of 600 were observed [$F_0^2 > 3\sigma(F^2)$]. The intensities of three standard reflections were monitored throughout data collection; average fluctuations were 3.0%.

The structure was solved and refined by using programs from the TEXSAN crystallographic software package[6] on a μ-VAX-II computer. The crystals exhibit the systematic absences **0kl**: $l \neq 2n$; **h0l**: $l \neq 2n$; **hk0**: $h + k \neq 2n$. This condition, the Laue symmetry mmm, and the distribution of intensities are consistent with space group Pccn. The space group Pccn has been chosen on the basis of a successful solution and refinement. The atoms Sr and Al were located by using the direct methods program SHELXS.[7] The remaining atoms were placed following analysis of difference electron density maps. After full-matrix, least-squares refinement of the model with isotropic displacement coefficients on each atom, an absorption correction was applied by using the program DIFABS.[8] The data were then averaged: Final refinement with anisotropic displacement coefficients on each atom resulted in the residuals R = 0.059 and Rw = 0.065. The largest peak in the final difference electron density map corresponds to 4.08 % of the Sr atom. Relevant crystallographic data and atomic parameters and anisotropic displacement coefficients are listed in Table 2.1 and Table 2.2, respectively.

Table 2.1 Crystallographic Data and Atomic Parameters for $SrAlBO_4$

a = 8.853(2) Å, b = 15.150(2) Å, c = 5.708(2) Å, space group Pccn (no.56),

Z = 8, formula wt. = 189.41 u, $\mu = 137.5\ cm^{-1}$, $\rho_{calcd} = 3.286\ g\ cm^{-3}$,

600 averaged reflections, 64 variables, R =0.059, wR = 0.065

atom	x	y	z	β_{eq}*
Sr	0.8857(1)	0.64819(8)	0.1058(2)	0.77(4)
Al	0.7418(5)	0.4486(2)	0.1381(8)	0.6(1)
O1	0.889(1)	0.8148(5)	0.130(2)	0.9(1)
O2	0.727(1)	0.5133(6)	0.392(2)	1.0(4)
O3	0.080(1)	0.6162(6)	0.407(2)	1.0(4)
O4	0.902(1)	0.3795(6)	0.178(2)	1.0(4)
B	0.478(2)	0.641(1)	0.118(3)	0.9(2)

$$*\beta_{eq} = 8\frac{\Pi^2}{3}\sum_i \sum_j U_{ij} a_i^* a_j^* a_i a_j$$

Table 2.2 Anisotropic Displacement Coefficients for $SrAl(BO_3)O$

ATOM	U_{11}	U_{22}	U_{33}	U_{12}	U_{13}	U_{23}
Sr	0.0030(5)	0.0159(5)	0.0102(5)	0.0001(6)	-0.0008(7)	-0.0023(7)
Al	0.002(2)	0.014(2)	0.008(2)	0.001(2)	-0.001(1)	-0.001(2)
O1	0.012(2)					
O2	0.011(5)	0.021(4)	0.006(4)	0.005(4)	-0.002(5)	-0.002(5)
O3	0.005(5)	0.021(5)	0.014(5)	0.003(4)	-0.001(5)	-0.009(5)
O4	0.009(5)	0.021(5)	0.007(4)	0.006(4)	0.003(4)	-0.004(4)
B	0.012(3)					

Results and Discussion

Crystal Structure

The structure of the title compound $SrAlBO_4$ (Figure 2.1) has layers of isolated flat orthoborate BO_3 groups along the c-axis (Figure 2.2) and tetrahedron chains of Al_2O_7 groups. The common features of unit cell and simple borate structures are shown in Figures 2.1 and 2.2, respectively. The structure contains one type of B atom, an 8 - coordinate Sr atom, and a 4 - coordinate Al atom. A isolated orthoborate BO_3 groups with 8e connected to Al - centered oxygen tetrahedron chains. The isolated BO_3 groups are also bridged to Sr - centered 8 coordinated oxygen.

Selected interatomic distances and angles are listed in Table 2.3. The Sr atom is surrounded by four O1 atoms, two O2 atoms, an O3 atom, and an O4 atom in a 8e site with a total of 8 oxygen atoms. The interatomic Sr-O distance is 2.675 ± 0.133 Å. The Sr atom is coordinated by 8 oxygen atoms. The strontium atoms serve to hold the chains together through coordination with oxygen atoms. The eight O atoms around the Sr atom are slightly distorted from an ideal angle. The O-Sr-O angles are 81.4(2), 80.0(1), 98.6(3), 101.0(3), 62.1(2), 79.2(3), 81.6(3), and 84.0(3)° for O1-Sr-O1, O1-Sr-O2, O1-Sr-O3, O1-Sr-O4, O2-Sr-O2, O2-Sr-O3, O2-Sr-O4, and O3-Sr-O4 angles, respectively (Figure 2.3). The AlO_4 anion has distorted tetrahedron symmetry and the Al-O distance is normal. The Al-O distances are 1.75(1), 1.74(1), 1.76(1), and 1.78(1) Å for two Al-O2, one Al-O3, and one Al-O4 distance, respectively. The O-Al-O angles are 111.4(5) ° for O2-Al-O2, 109.0(5) ° for O2-Al-O3, 108.1(5)° for O2-Al-O4, 110.6(5) ° for O3-Al-O3 and

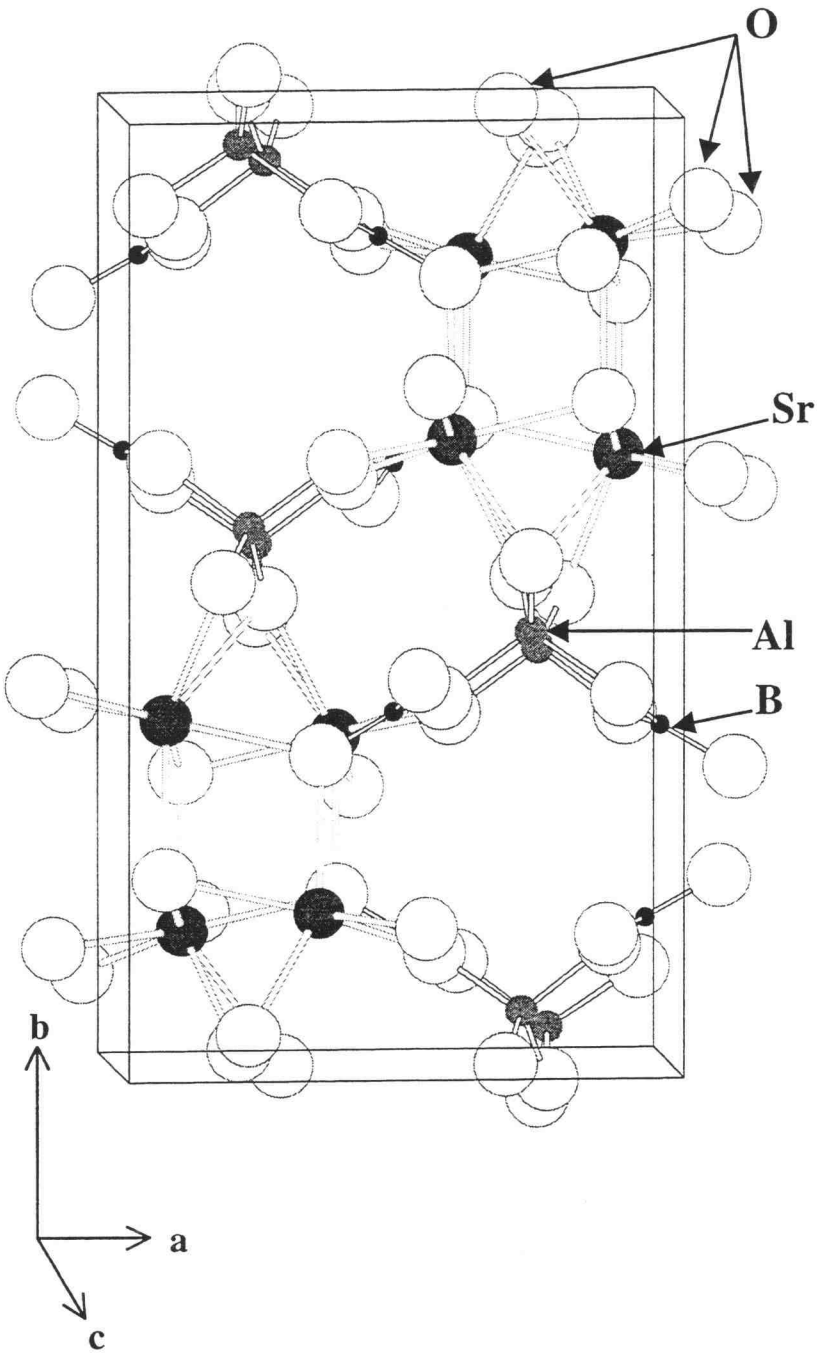

Figure 2.1 Drawing of the unit cell of $SrAlBO_4$.

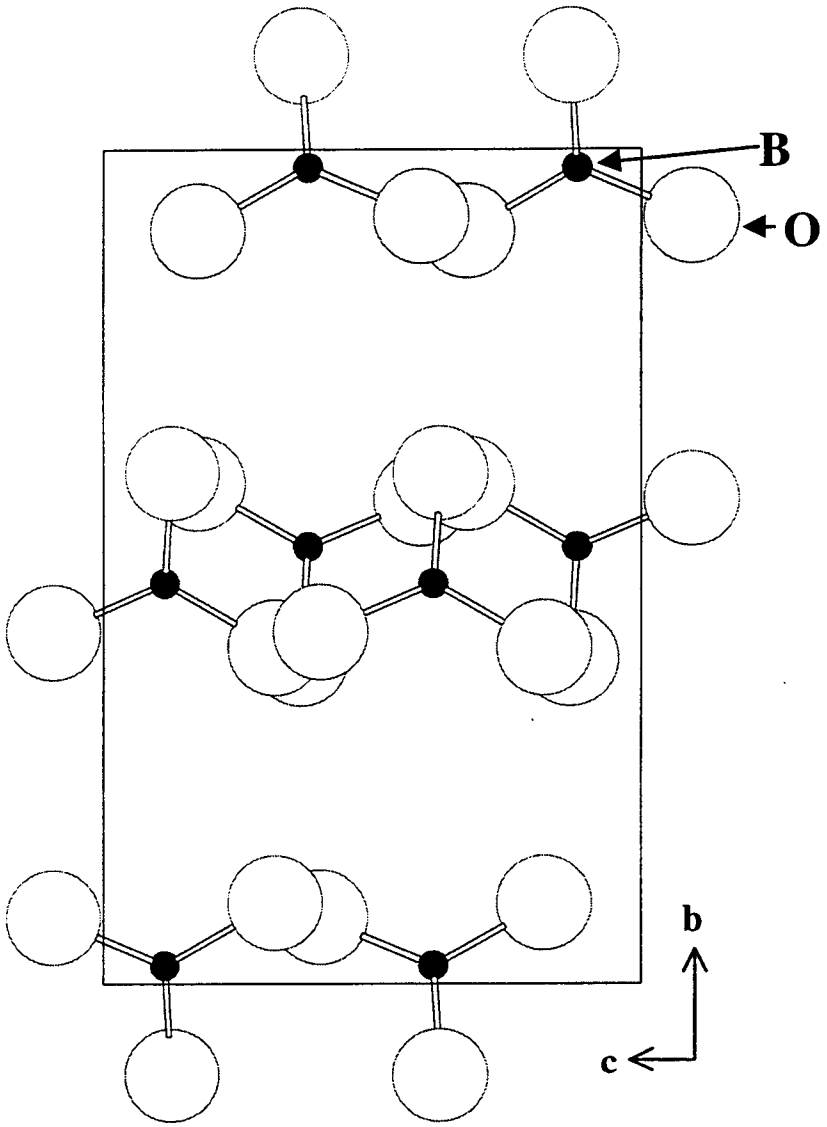

Figure 2.2 Drawing of BO_3 group (100) projection of the unit cell in the $SrAlBO_4$.

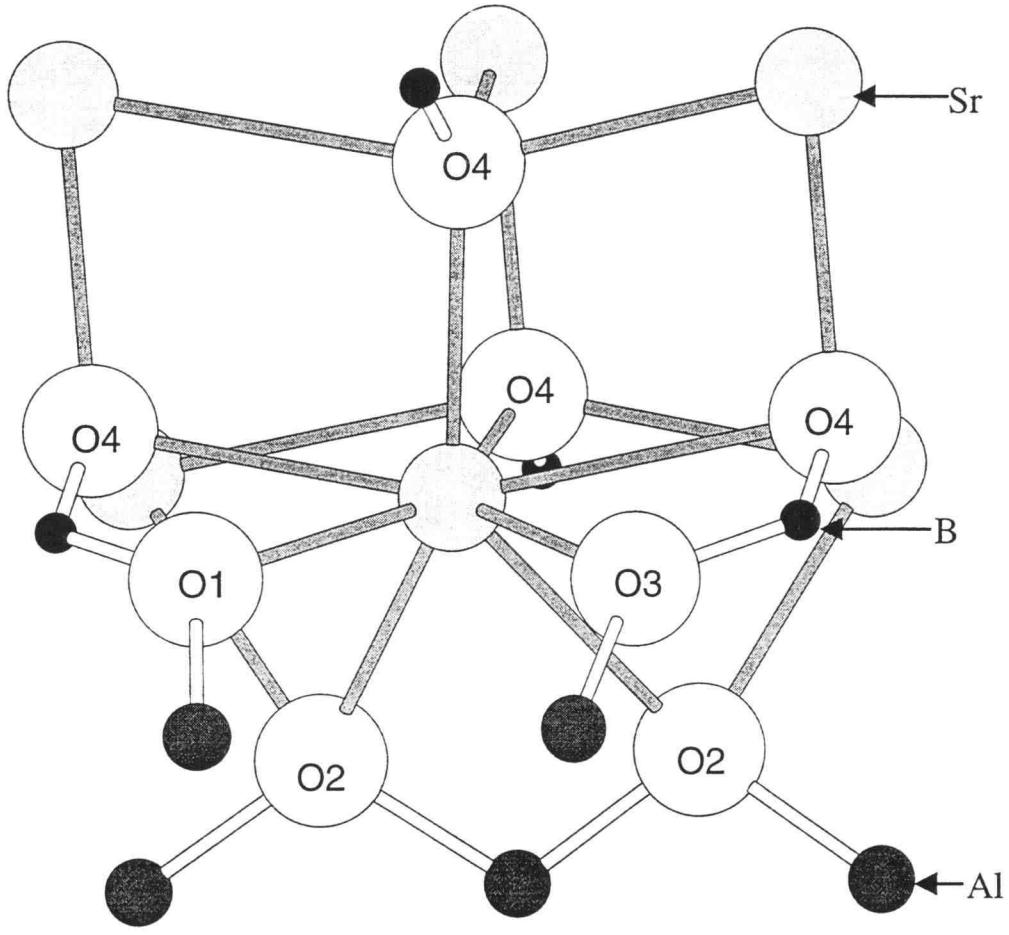

Figure 2.3 Drawing of the 8 oxygen coordinated Sr atom.

109.8(4) ° for O3-Al-O4 angle. The BO_3 anion has triangular symmetry, and B-O distance is also normal. The B-O distances are 1.35(2) Å for B-O1, 1.36(2) Å for B-O3, and 1.38(2) Å for B-O4 distance. The O-B-O angles are 121(1) ° for O1-B-O3, 119(1) ° for O1-B-O4, 120(1) ° for O3-B-O4 angle. The basic unit of these chains consists of tetrahedral AlO_4 anions and triangular BO_3 anions. The crystal chemistry of anhydrous borates extends from the simple orthoanions to their condensation into complex rings, chains, networks, and frameworks. The compound $SrAlBO_4$ has the unique structure of alternately isolated orthoanions, $(BO_3)^{3-}$ group (Figure 2.4).

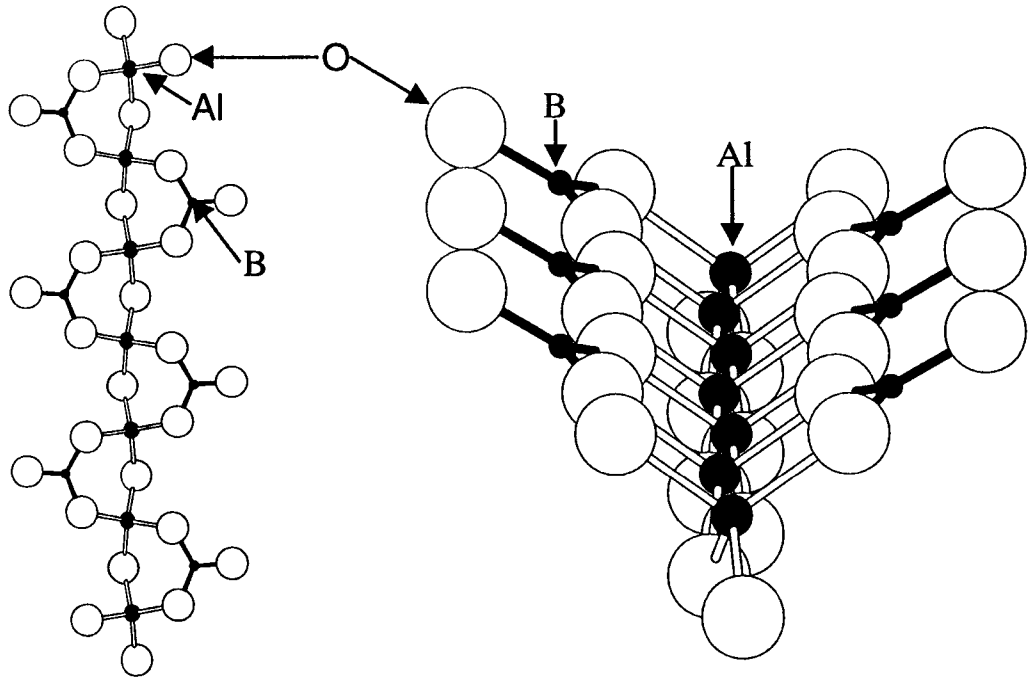

Figure 2.4 The unique structure of $(BO_3)^{3-}$ group in the compound $SrAlBO_4$.

Table2.3 Selected Interatomic Distances (Å) and Angles (°) for $SrAlBO_4$

Interatomic	Distances (Å)	Interatomic Angles (°)	
Sr-O1(×4)	2.528(9)	O1-Sr-O1	81.4(2)
	2.78(1)	O1-Sr-O2	80.0(1)
	3.04(1)	O1-Sr-O3	98.6(3)
	2.503(9)	O1-Sr-O4	101.0(3)
Sr-O2(×2)	2.968(9)	O2-Sr-O2	62.1(2)
	2.583(9)	O2-Sr-O3	79.2(3)
Sr-O3(×1)	2.478(9)	O2-Sr-O4	81.6(3)
Sr-O4(×1)	2.521(9)	O3-Sr-O4	84.0(3)
Al-O2(×2)	1.75(1)	O2-Al-O2	111.4(5)
	1.74(1)	O2-Al-O3	109.0(5)
Al-O3(×1)	1.76(1)	O2-Al-O4	108.1(5)
Al-O4(×1)	1.78(1)	O3-Al-O3	110.6(5)
		O3-Al-O4	109.8(4)
B-O1(×1)	1.35(2)	O1-B-O3	121(1)
B-O3(×1)	1.36(2)	O1-B-O4	119(1)
B-O4(×1)	1.38(2)	O3-B-O4	120(1)

Luminescence

It has been demonstrated that correlations exist among Eu^{2+} excitation energies, Stokes shifts, and the coordination environments of the O atoms in the crystal structures of borates.[9] The Eu^{2+} ion substitutes on 8-coordinate Sr site shown in Figure 2.3. A large Stokes shift is expected on the basis of the coordination numbers of atom O1-bound angles also contribute to the relatively high excitation energy of 26,500 cm^{-1}.[9] Following a relatively large Stokes shift of 8,000cm^{-1}, a green emission at 529 nm is observed (Figure 2.5).

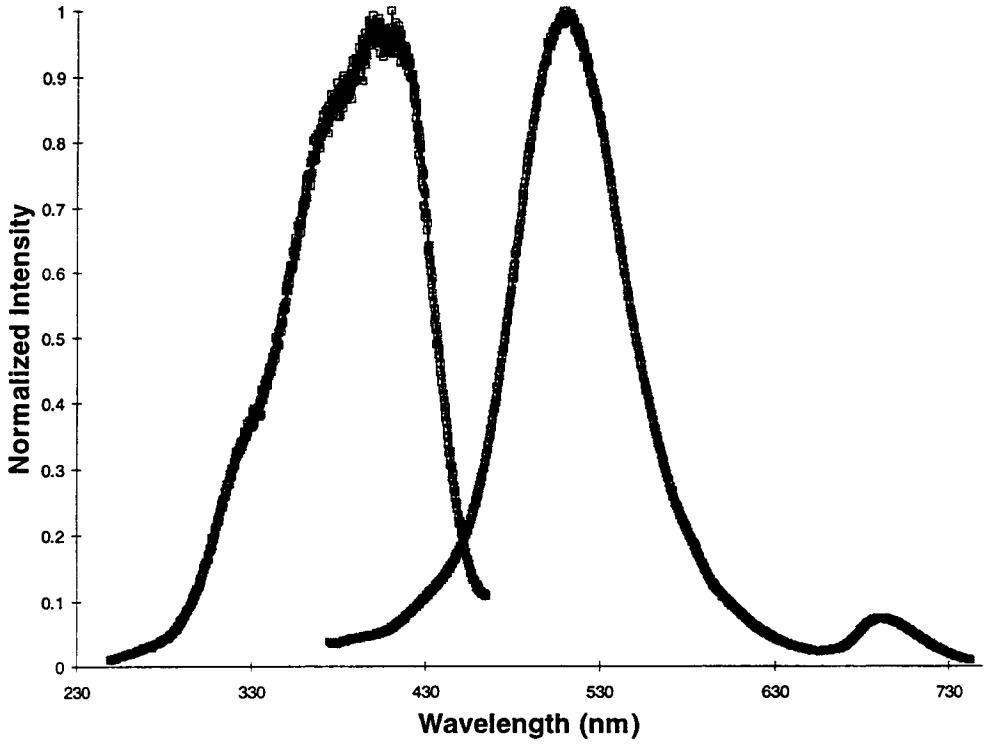

Figure 2.5 Excitation and emission spectra of the luminescence of 1% Eu^{2+}: $SrAlBO_4$.

Acknowledgments

This work was supported by the National Science Foundation, Solid State Chemistry Program.

References

1. MacDowell, J. F. *J. Am. Ceram. Soc.*, **1990**, 73(8) 2287.

2. Schafer, V., *Neues Jb. Miner. Mh.*, **1967**, 4-5, 131-136.

3. Schuckman, W., *Neues Jb. Miner. Mh.*, **1968**, 80-86.

4. Nagai, T.; Ihara, M. *Yogyo - Kyokai - Shi*, **1972**, 80(11), 14.

5. Yvon, K.; Jeitschko, W.; Parthe, E. *J. Appl. Cryst.* **1977**, *10*, 73.

6. ***TEXSAN***, Structure Analysis Package, Molecular Structure Corp., MSC 3200A, Research Forest Drive, the Woodlands, TX 77381.

7. Sheldrick, G. M. In *Crystallographic Computing 3*; Sheldrick, G.M.; Krüger, C.; Goddard, R.; Eds.; Oxford Univ. Press, Oxford, U. K., **1985**, p 175.

8. Walker and Stuart, *Acta Cryst.*, A39, **1983**, 158-166.

9. Diaz, A. and Keszler D. A., *Mat. Res. Bul.*, **1996**, 31, 2, 147-151.; Diaz, A., Ph.D. Dissertation, Oregon State Univ., **1996**.; Diaz, A. and Keszler D. A., *Chem. Mater.* in press.

10. Blasse, G., Wanmaker, W. L., Vruget, J. W., and Bril, A., *Philips Res. Repts.*, **1968**, 23, 189.

CHAPTER 3

SYNTHESIS, STRUCTURE, NONLINEARITY, AND THERMAL EXPANSION OF $SrAl_2(BO_3)_2O$

Ki-Seog Chang and Douglas A. Keszler

In preparation for submission to J.Solid State Chem., **1998**

Abstract

The structure of the borate oxide $SrAl_2(BO_3)_2O$ has been established by single-crystal X-ray diffraction methods. It crystallizes in the trigonal space group R32 (Z = 3) with unit-cell parameters a = 4.891(2) Å, c = 23.923(4) Å, and V = 495.6(2) Å^3. The structure was determined from 414 unique reflections and refined to the final residuals R = 0.054 and R_w = 0.058. It is characterized by an association of BO_3 triangles, distorted SrO_6 trigonal prisms, distorted AlO_4 tetrahedra, and a unique two-coordinate O atom. From consideration of the BO_3-group alignment, a second-order optical susceptibility of $d_{11} \approx 2.02$ pm/V is predicted. A thermal contraction is observed with a coefficient -1.64×10^{-4} Å/°C on the c axis for the temperature range 23-215°C.

Materials index: Strontium, Aluminum, Borate.

Introduction

Borates have long been important for the production of a variety of glasses. The crystal structure of di-strontium aluminum borate $SrAlBO_4$ with R = 0.163 was reported by Nagai, T. And Ihara, M.[1] We have also recently synthesized and identified the compound $SrAlBO_4$ with R = 0.059 as a new luminescent material. The structure consists of 8-coordinated Sr atoms, AlO_4 tetrahedra, and BO_3 triangles. The strontium boratoberyllate $Sr_2Be_2(BO_3)_2O$ has been grown by using the top-seeding high-temperature flux method with the growth temperature about 1373 K. The strontium boratoberyllate has been discovered as a new ultraviolet nonlinear optical crystal.[2, 3, 4] The glass-forming regions of alkaline-earth (Ca, Sr, Ba) aluminum borate systems were recently examined by MacDowell.[5] The materials of primary interest center near the 1 : 1 : 1 molar ratio of MO (M = Sr, Ba, or Ca) : Al_2O_3 : B_2O_3, where the glass - ceramics were highly crystalline. The thermal expansion coefficient as low as $6\times10^{-7}/°C$, was measured on $SrAl_2(BO_3)_2O$ glass - ceramics. Since a simple orthoborate $(BO_3)^{3-}$ of $SrAl_2(BO_3)_2O$ can have absorption edges 150 - 160 nm, efforts have been directed to the new structures for a second-harmonic generation of wavelengths shorter than 190 nm.[6]

We also describe the thermal expansion coefficient on the c axis between 23°C and 215°C and the linear and nonlinear optical properties of $SrAl_2(BO_3)_2O$.

Experimental Section

Synthesis and Crystal Growth

A powdered sample of $SrAl_2(BO_3)_2O$ was prepared by heating a stoichiometric mixture of the reagents $SrCO_3$ (Alfa, 99.99%), Al_2O_3 (Alfa, 99.999%), and B_2O_3 (Alfa, 99.98%). The mixture was heated in a Pt crucible at 893 K for 1 h, cooled, ground, and again heated at 1073 K for 12 h. An X-ray powder diffraction pattern of the product, obtained with a Philips diffractometer, matched that from the computer program LAZY-PULVERIX[7] and the results of the single-crystal study (vide infra). Since the compound decomposes at 1273 K, crystals were grown in a Pt crucible from a melt containing 70 mol% $SrAl_2(BO_3)_2O$ and 30 mol% $LiBO_2$. The melt was cooled at 0.07 K/min from 1190 to 800 K, and then 5 K/min to room temperature. A clear, colorless crystal was physically separated from the matrix for X-ray measurements.

Crystallographic Study

The crystal was mounted on a glass fiber and analyzed on a Rigaku AFC6R X-ray diffractometer. Unit-cell parameters were derived from least-squares refinements with the setting angles of 20 automatically-centered reflections in the range of $26 < 2\theta < 31°$. Intensity data were collected at room temperature by using the ω-scan technique with a rate = 16.0°(ω)/min and peak widths = 1.50 + 0.30 tanθ. The cell constants and Laue symmetry *3m1* correspond to the rhombohedral system with a hexagonal setting. The intensity data were collected over a range

of indices $-7 \leq h \leq 7$, $0 \leq k \leq 7$, $-36 \leq l \leq 36$. From 1341 measured reflections, a total of 263 unique reflections were observed [$F_0^2 > 3\sigma(F^2)$]. The intensities of three standard reflections were monitored throughout data collection; the average fluctuations was 3.0%.

The structure was solved and refined by using programs from the TEXSAN crystallographic software package[8] on a μ-VAX-II computer. The crystal exhibits the systematic condition **hkl**: -h+k+l = 3n. This condition, the Laue symmetry, and the distribution of intensities are consistent with space groups R32 and R3m. The space group R32 has been chosen on the basis of a successful solution and refinement. The atoms, Sr and Al, were located by using the direct methods program SHELXS.[9] The remaining atoms were placed following analysis of difference electron density maps. After full-matrix, least-squares refinement of the model with isotropic displacement coefficients on each atom, an absorption correction was applied by using the program DIFABS.[10] The data were then averaged. Final refinement with anisotropic displacement coefficients on each atom resulted in the residuals R = 0.054 and R_w = 0.058. The largest peak in the final difference electron density map corresponds to 2.76% of the Sr atom. Relevant crystallographic data and atomic parameters and anisotropic displacement coefficients for $SrAl_2(BO_3)_2O$ are listed in Tables 3.1 and 3.2, respectively.

Powder X-ray diffraction data over the temperature range 25-250°C were obtained on a Siemens D5000 diffractometer by using Cu Kα radiation and a locally constructed heating unit.

Liquidus curves for the system $SrAl_2(BO_3)_2O$-$LiBO_2$ were generated by

measuring its melting points. A sample of the binary systems was prepared by mol% mixture of $SrAl_2(BO_3)_2O$ and $LiBO_2$. The mixture was heated in a Pt crucible at a constant temperature for 1h. Melting point measurements were made on a Thermolyne Type 1300 furnace and a thermal control system, Temp Control O-20ma Type R.

Table 3.1 Crystallographic Data and Atomic Parameters for $SrAl_2(BO_3)_2O$

a = 4.891(2) Å, c = 23.923(4) Å, space group R32 (no. 155), Z = 3

formula wt. = 275.20 u, $\mu = 81.63\ cm^{-1}$, $\rho_{calcd} = 2.766\ gcm^{-3}$

263 averaged reflections, 20 variables, R =0.054, $R_w = 0.058$

atom	site symmetry	x	y	z	B_{eq}*
Sr	D_3	0	0	0	1.11(5)
Al	C_3	0	0	0.5698(2)	1.1(1)
O1	D_3	0	0	½	3.0(4)
O2	C_1	0.424(2)	0.393(2)	0.0661(3)	1.8(2)
B	C_3	0	0	0.7344(6)	0.9(3)

$$*B_{eq} = \left(\frac{8\pi^2}{3}\right) \sum_i \sum_j U_{ij} a_i^* a_j^* a_i a_j$$

Table 3.2 Anisotropic displacement coefficients for $SrAl_2(BO_3)_2O$

Atom	U_{11}	U_{22}	U_{33}	U_{12}	U_{13}	U_{23}
Sr	0.014	0.014	0.014	0.007	0	0
Al	0.014	0.014	0.013	0.007	0	0
O1	0.042	0.042	0.028	0.021	0	0
O2	0.024	0.025	0.023	0.016	0	0
B	0.012	0.012	0.013	0.006	0	0

Results and Discussion

Crystal Structure

The contents of the unit cell are depicted in Figure 3.1. The structure is built from distorted SrO_6 trigonal prisms, distorted AlO_4 tetrahedra, and BO_3 triangles. The BO_3 groups adopt prototypical layers that extend in the ab plane. The BO_3 groups are bridged by the Sr atoms and the Al atoms through a linear Al-O-Al interaction that parallels the c axis. As such, simple Al_2O_7 groups may be identified in the structure (cf., Figure 3.1)

An alternative description of the structure emphasizes the complex, thick slabs $[Al_2B_2O_7]^{2-}$. In this description, these slabs pack in an ABCAB··· pattern with the Sr atoms serving to connect the layers.

Selected interatomic distances and angles are listed in Table 3.3. The Sr atom is surrounded by six O2 atoms at the vertices of a slightly distorted trigonal prism. The interatomic Sr-O distance, 2.552(7) Å, is comparable to the value, 2.54Å, calculated from crystal radii.[11] The O-Sr-O angles reflect the relative 20° displacement of the trigonal planes of the prism. The AlO_4 anion has distorted tetrahedral symmetry, point group C_3. The Al-O distances are consistent with the coordination numbers of the O atoms; 1.670(4) Å for interaction with the two-coordinate O1 atom and 1.770(7) Å for interaction with the three-coordinate O2 atom. The O-Al-O angles (cf., Table 3.3) are also consistent with the coordination numbers of the O atoms. Material details of the BO_3 triangles, point group D_{3h} are normal.

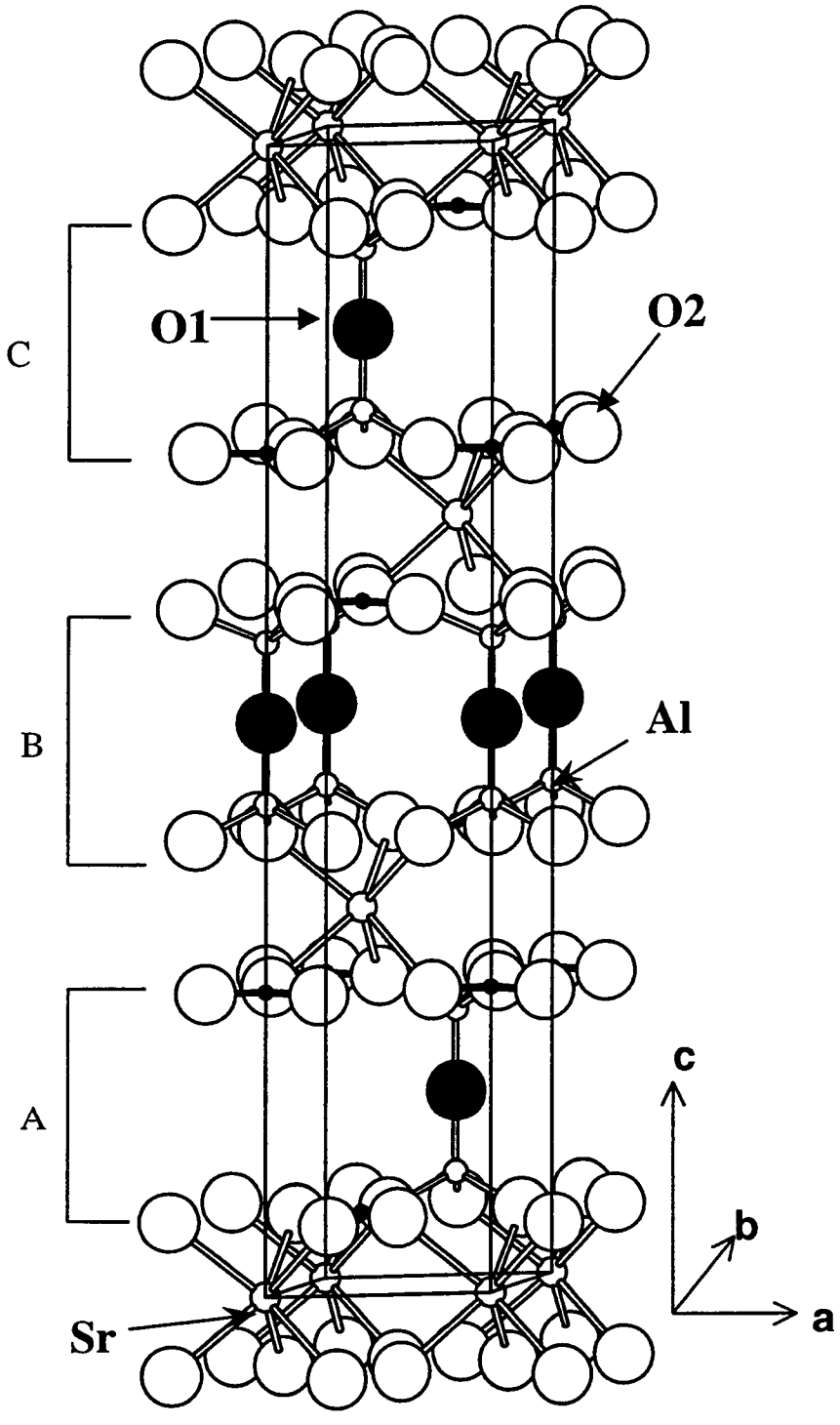

Figure 3.1 Drawing of the unit cell of $SrAl_2(BO_3)_2O$.

Table 3.3 Selected Interatomic Distances (Å) and Angles (°) for $SrAl_2(BO_3)_2O$

Interatomic	Distances (Å)		Interatomic Angles (°)
Sr-O2(X6)	2.552(7)	O2-Sr-O2	76.9(3)
			85.6(2)
			128.2(3)
			139.5(3
Al-O1	1.670(4)	O1-Al-O2	114.5(2)
Al-O2(x3)	1.770(7)	O2-Al-O2	104.0(3)
B-O2(x3)	1.354(7)	O2-B-O2	120

Selected interatomic distances and angles of Na β-alumina are listed in Table 3.4. The complex, thick slabs $[Al_2B_2O_7]^{2-}$ of $SrAl_2(BO_3)_2O$ is very similar to those of β-alumina packing in an ABAB··· pattern with spinel blocks.[12] The unit cell of β-alumina is composed of two spinel blocks separated by a mirror. These blocks result from the stacking of four layers of oxygen ions in the c direction. The layers are separated by the Al^{3+} cations distributed in the octahedral and tetrahedral sites. The not-compact plane separating both spinel blocks contains a sodium ion in a interstitial site and oxygen ion. Spinel-type blocks are joined through linear Al-O-Al sticks. Planes of the linearly bound O atoms are spaced by approximately 11Å along the c axis through the spinel blocks. In $SrAl_2(BO_3)_2O$, spacing of these O planes along the c axis is only 7.97Å.

Table 3.4 Selected Interatomic Distances (Å) and Angles (°) for β-alumina

Interatomic	Distances (Å)	Interatomic Angles (°)	
Octahedra			
Al1-O1(x2)	2.022	O1-Al1-O1	85.72
Al1-O2(x2)	1.837	O2-Al1-O1	87.75
Al1-O3	1.970	O2-Al1-O2	98.04
Al1-O4	1.819	O3-Al1-O2	119.34
		O3-Al1-O4	116.72
		O4-Al1-O1	85.84
		O4-Al1-O2	99.73
Al4-O1(x6)	1.895	O1-Al4-O1	89.09, 90.91, 180.0
Tetrahedra			
Al2-O1(x3)	1.801	O1-Al2-O1	109.92, 109.94
Al2-O3	1.809	O1-Al2-O3	108.40
Al3-O2(x3)	1.768	O2-Al3-O2	106.43, 106.45
Al3-O5	1.677	O2-Al3-O5	112.36

Dicussion

Considering the structure of the title compound, it is worthwhile to consider its nonlinear optical properties, luminescent characteristics, and thermal-expansion behavior.

Frequency conversion

As a noncentrosymmetric material, it is capable of exhibiting second-harmonic optical frequency conversion. Reliable second-order susceptibility coefficients can generally be derived from application of the anionic group theory[12] In this model, the susceptibility derives predominately from the virtual, electronic charge-transfer characteristics of the individual BO_3 groups. The macroscopic nonlinear coefficients, d_{ij}, for the crystal derive from the relative orientations and number density of the BO_3 groups. As noted above, the BO_3 groups peak in layers that extend in the ab plane. As seen in Figure 3.2 pairs of BO_3 groups may be superimposed one on the other by a rotation of 20° about the c axis. Without this misalignment, BO_3 groups would be optimally oriented for second-harmonic generation. In previous work, we derived the analytical expressions governing the orientation dependence of the hyperporizability coefficients for individual BO_3 groups For the present compound, we need to consider only rotations about the c axis which follow the from cos3θ, where θ is the angle of projection onto the a axis. This result leads to a macroscopic coefficient d_{11} = cos3(10°) = 0.87. In other words, the 20° relative rotation affords an orientation that is 87% of optimum. To derive a numerical value for d_{11}, we must consider the number density of the BO_3 groups and the value of microscopic hyperpolarizability coefficient. The

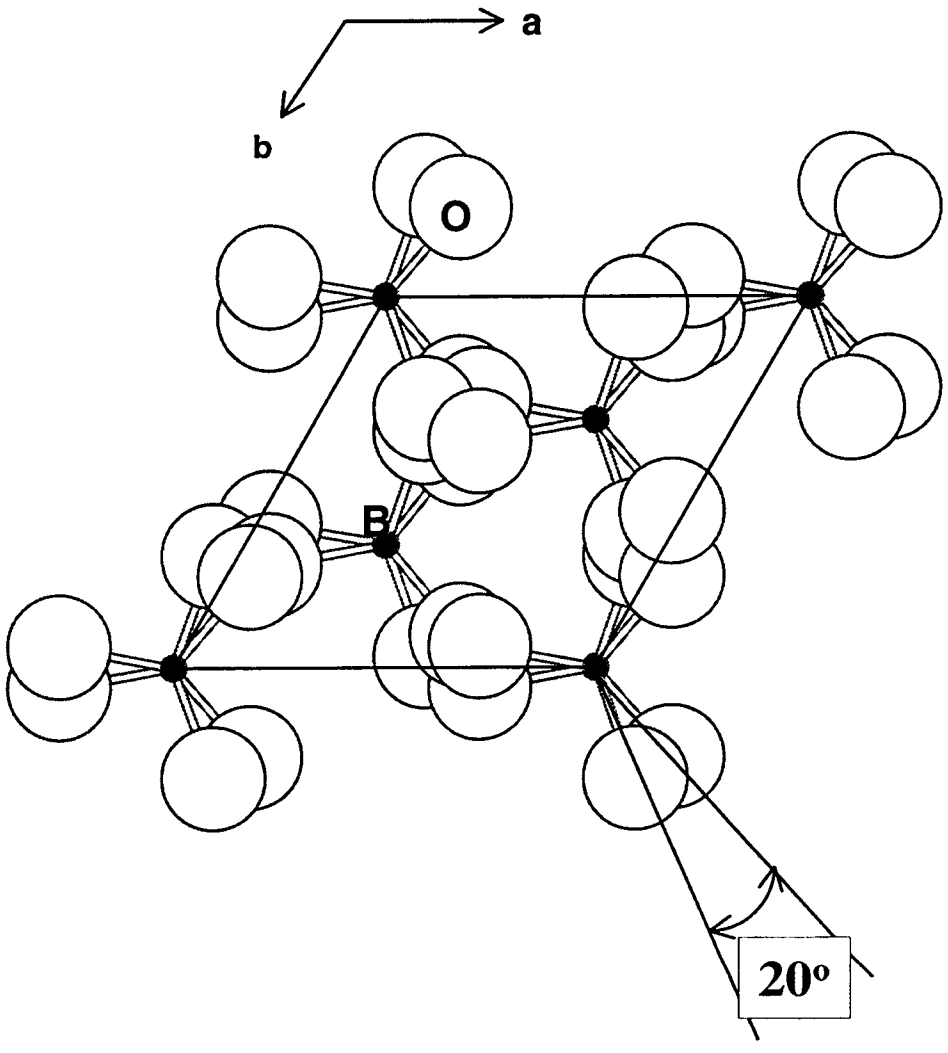

Figure 3.2 Drawing of the rotation of the isolated planar BO_3 group by 20° as viewed perpendicular to the c axis.

hyperpolarizability coefficient is derived from d_{11} = 1.48 pm/V for YAB [$YAl_3(BO_3)_4$]. The alignment of BO_3 groups in this material is 49% of optimum[13] and the number density = 0.0166 BO_3 groups/Å^3. For $SrAl_2(BO_3)_2O$, the number density = 0.0166 BO_3 groups/Å^3. Coupling this value and the orientation factor, a macroscopic coefficient, d_{11} = 1.48 pm/V, is derived. This value may be compared to the maximum coefficients of BBO (1.60 pm/V), LBO (0.69 pm/V), CLBO (0.95 pm/V), and YCOM (1.3 pm/V). Clearly we anticipate that $SrAl_2(BO_3)_2O$ will be observed to have the highest nonlinearity among all known borates.

The general applicability of the material will be largely determined by its mechanical and thermal properties as well as the ability to grow large, optical quality crystals. The compounds decomposes at 1010°C, so crystals must be grown from a solution. $LiBO_2$ is a suitable solvent for crystal growth. As seen from the liquids curves of Figure 3.3, this solvent will provide precipitation of $SrAl_2(BO_3)_2O$ up to 80 mol%.

Luminescence

The room-temperature excitation and emission spectra of Eu^{2+}:$SrAl_2(BO_3)_2O$ shown in Figure 3.4. A typical broad-band emission associated with the $4f^65d^1 \rightarrow 4f^7$ transition of Eu^{2+} is observed; the Stokes shift is 7600cm^{-1}. A model correlating Eu^{2+} emission color and the coordination environments of the O atoms has recently been proposed by Diaz and Keszler.[13] According to this model, short wavelength blue or UV emission with small Stokes shifts are to be observed in those borates containing O atoms that are lightly coordinated by heavy atoms such as Sr or Ba.

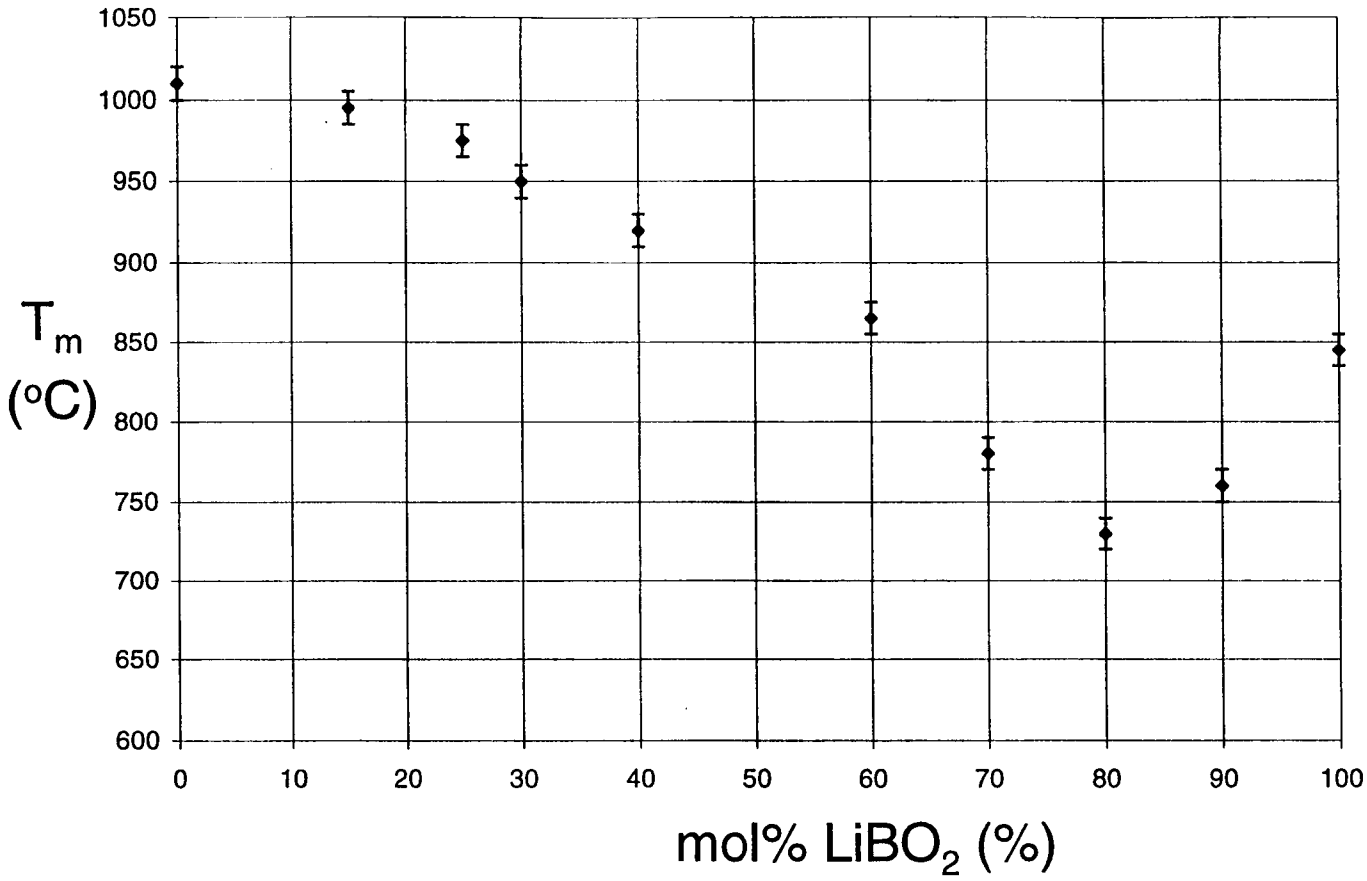

Figure 3.3 Melting point diagram of $SrAl_2(BO_3)_2O$ with $LiBO_2$.

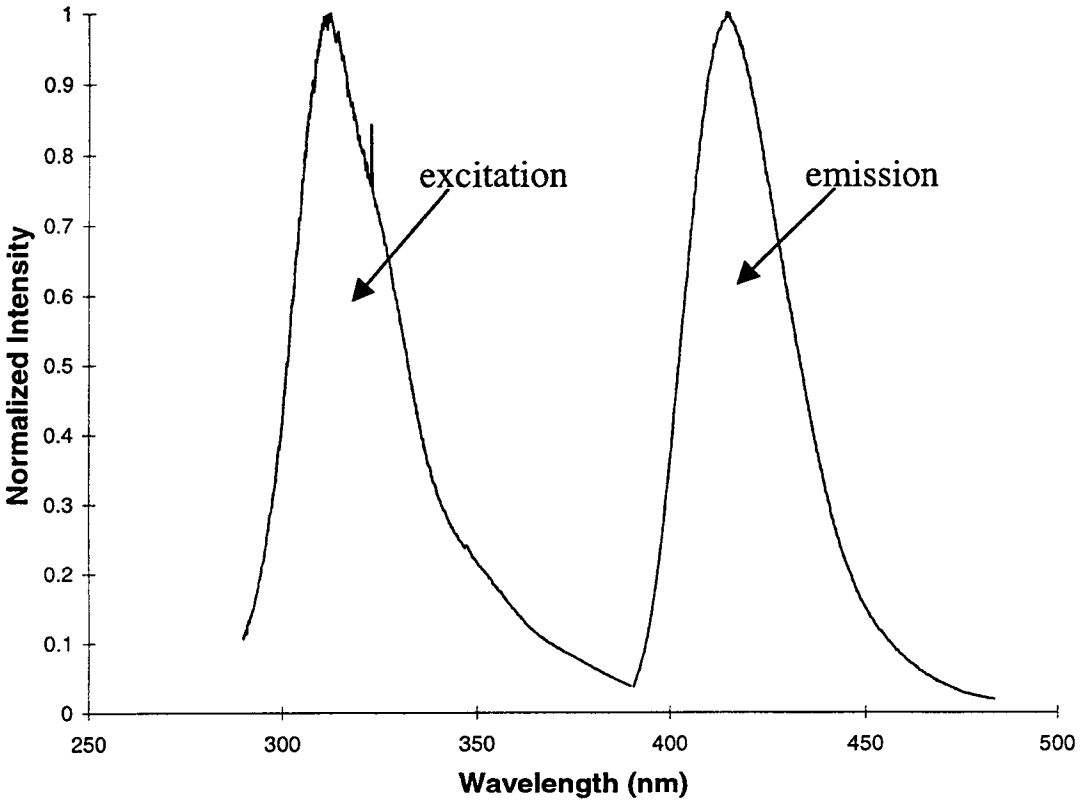

Figure 3.4 Excitation and Emission spectra of the luminescence of 1% Eu^{2+}: $SrAl_2(BO_3)_2O$ at 298°K.

In $SrAl_2(BO_3)_2O$, the pertinent O atom, O2, is bound by one atom each of Sr, Al, and B. As a result, the O atoms are held firmly in place - the host is classified as rigid - and a small Stokes shift with short wavelength emission is observed.

Thermal Expansion

On the basis of dilatometric measurements, a thermal expansion coefficient of $6.60 \times 10^{-6}/°C$ has been reported[5] for the title compound. We have measured thermal expansion over the limited temperature range 25 - 215°C by using X-ray diffraction. As seen in Figure 3.5, both the c and a cell parameters decrease sharply for temperatures up to approximately 150°C. Over this temperature range, the expansion coefficients for the c and a axes are -1.957×10^{-4} Å/°C and -1.77×10^{-5} Å/°C, respectively. Above 150°C the slope of the line for a axis flattens and begins to increase. Overall a volume contraction is observed over the temperature range 23 - 215 °C.

Two mechanisms may be identified to account for the negative thermal expansion. Transverse thermal motion of the two-coordinate O atom (Figure 3.5) can lead to a decrease in Al···Al distance and a decrease in the c cell parameter with increasing temperature. Similarly, the trigonal planes about the Sr atom may counterrotate to a trigonal antiprismatic geometry, point group D_{3d}. (Figure 3.7) As this rotation occurs, a compression along the three-fold c to a more axis regular octahedral geometry would be expected to occur. (cf., Figure 3.6) The former mechanism involves activation of a high energy Al-O-Al bending mode, while the

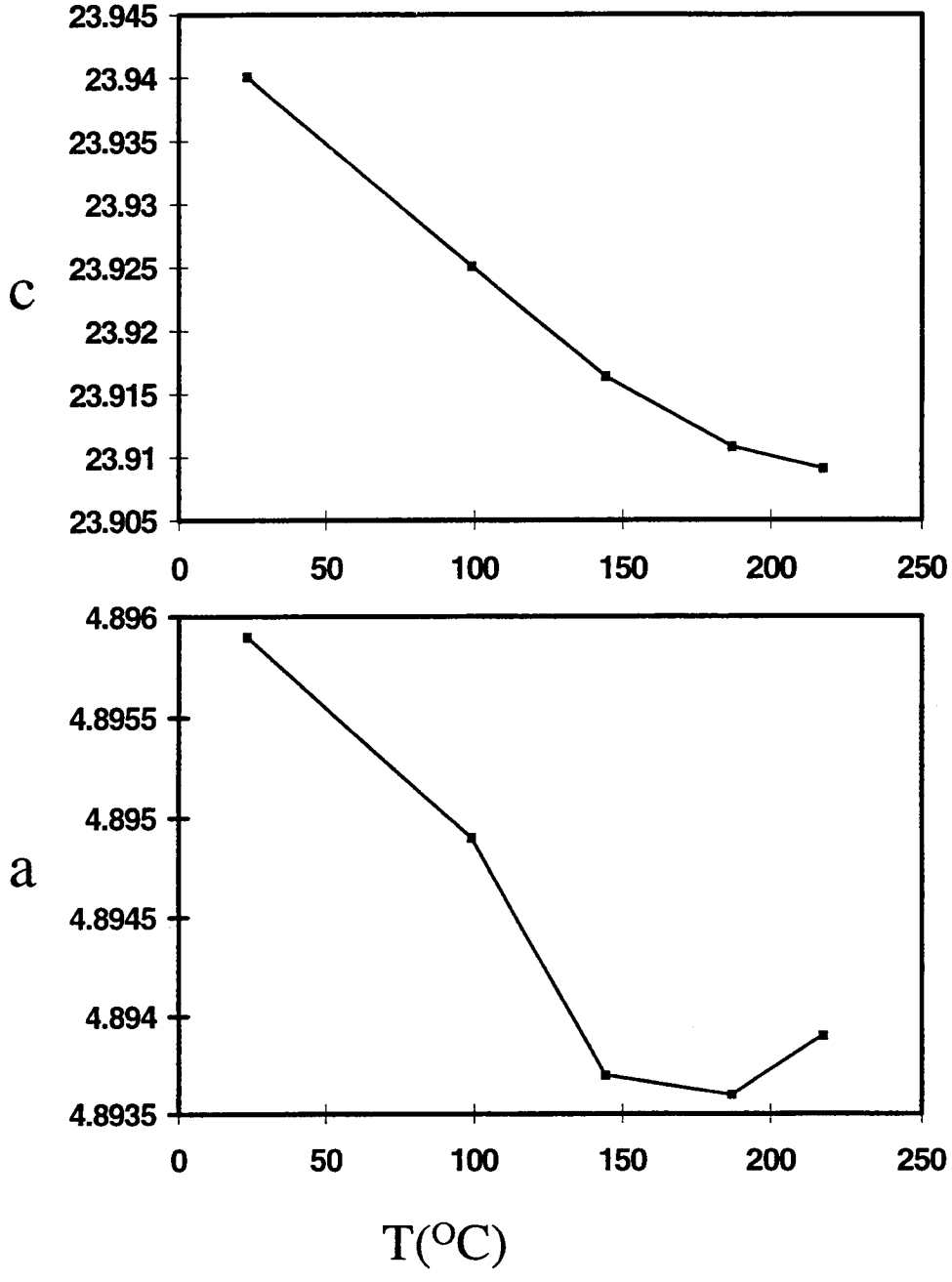

Figure 3.5 Unit-cell parameters vs. temperature

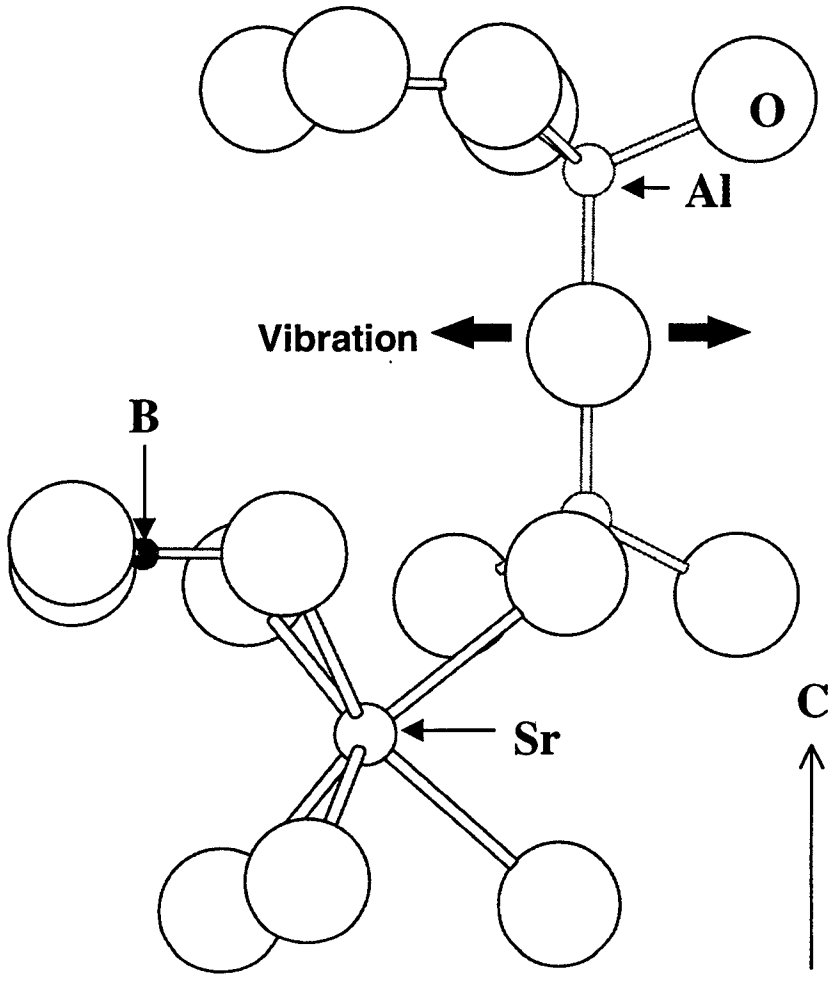

Figure 3.6 Drawing of the structure of unique 2 coordinated O atom, AlO_4 tetrahedrons, BO_3 triangles, and SrO_6 trigonal prism as viewed along the c axis.

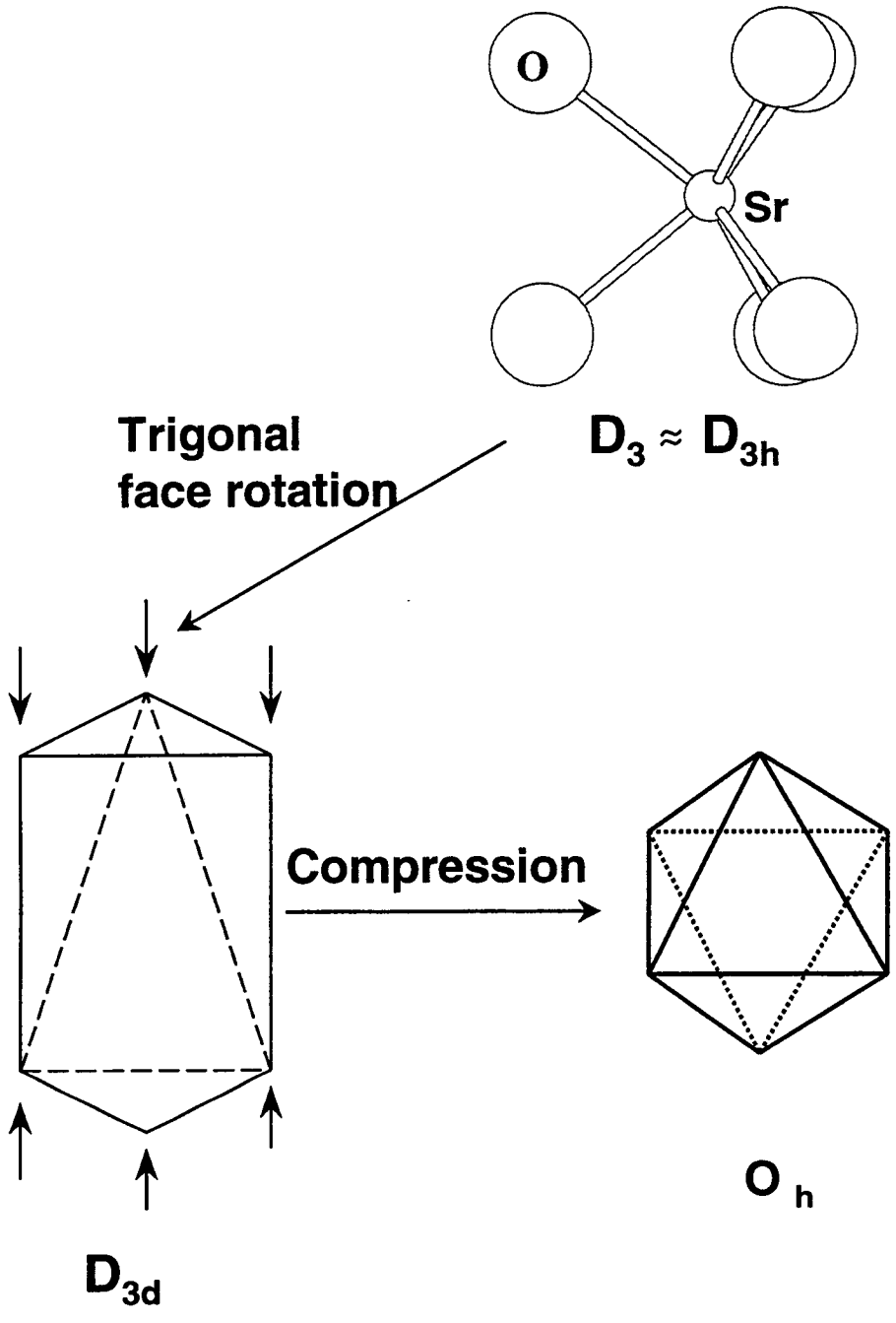

Figure 3.7 Drawing of the Sr-centered trigonal prism distort toward an octahedron at high temperature.

latter involves activation of lower energy librational phonon modes. For this reason, we favor the latter model over the described temperature range.

The polyhedral compression model also correlates to the thermal expansion behavior of the material $LiSrAlF_6$. Like the title compound, this fluoride is trigonal, contains a distorted trigonal prismatic SrF_6 site, and undergoes a thermal contraction along the c axis when heated.[13] Unlike the title compound, the fluoride contains no two coordinate F atoms. The thermal contraction in the distorted trigonal prismatic SrF_6 is to a more regular octahedron having a smaller aspect ratio.

If the polyhedral compression model is correct, the thermal contraction will derive from concerted rotations of the BO_3 groups. As noted above, the nonlinearity of the material is highly sensitive to the BO_3-group rotations. ($d_{11} \equiv \cos 3\theta$) In ongoing experiments, we are now seeking to establish relationships between the structure of the material and its physical properties over a broad temperature range, 77 - 1000K.

Acknowledgments

This work was supported by the National Science Foundation (DMR92-21372). We want to thank Dr. John Evans for assistance with the thermal expansion measurements.

References

1. Nagai, T.; Ihara, M. *Yogyo - Kyokai - Shi*, **1972**, 80(11), 14.

2. Xia, Y.; Chen, C.; Tang, D.; Wu, B., Adv. Mater., **1995**, 7: 79--81.

3. Chen, C.; Wang, Y.; Xia, Y.; Wu, B.; Tang, D.; Wu, K.; Wenrong, Z.; Yu, L.; Mei, L. J., Appl. Phys., **1995**, 77: 2268--2272.

4. Chen, C.; Wang, Y.; Wu, B.; Wu, K.; Zeng, W.; Linhua, Y., Nature **1995**, 373: 322--324.

5. MacDowell, J. F., *J. Am. Ceram. Soc.*, **1990**, 73(8) 2287.

6. Keszler, D. A., Solid State & Materials Science **1996**, in press.

7. Yvon, K.; Jeitschko, W.; Parthe, E. *J. Appl. Cryst.* **1977**, *10*, 73.

8. ***TEXSAN***, Structure Analysis Package, Molecular Structure Corp., MSC 3200A, Research Forest Drive, the Woodlands, TX 77381.

9. Sheldrick, G. M. In *Crystallographic Computing 3*; Sheldrick, G.M.; Krüger, C.; Goddard, R.; Eds.; Oxford Univ. Press, Oxford, U. K., **1985**, p 175.

10. Walker and Stuart, *Acta Cryst.*, A39, **1983**, 158-166.

11. Peters, C. R.; Bettman, M.; Moore, J. W.; Glick, M. D., , *Acta Cryst.*, B27, **1971**, 1826.

12. Schaffers, K. I., Doctoral Thesis, Oregon State University, **1992**, Chap. 1.

13. Diaz, A. and Keszler, D. A., *Mat. Res. Bul.*, **1996**, 31, 2, 147-151(1996).

CHAPTER 4

SYNTHESIS, STRUCTURE, NONLINEARITY, AND SOLID SOLUTION OF $BaAl_2(BO_3)_2O$

Ki-Seog Chang and Douglas A. Keszler

In Preparation for Publication, **1998**

Abstract

The compound $BaAl_2(BO_3)_2O$ has been shown to continuous substitutional solid solutions with $SrAl_2(BO_3)_2O$ according to Vegard's law. Isotypes, $BaAl_2(BO_3)_2O$ and $SrAl_2(BO_3)_2O$, have been created with cell parameters of (Ba, Sr)$Al_2(BO_3)_2O$ solid solutions: a = 4.891(2) Å, c = 13.923(4) Å, and V = 495.6(2) Å^3, the same space group of $SrAl_2(BO_3)_2O$, R32, and coordinations of $SrAl_2(BO_3)_2O$. The compound $BaAl_2(BO_3)_2O$ has the following cell constants: a = 5.009(3) Å, c = 24.46(1) Å, and V = 531.6(5) Å^3. The structure of the borate oxide $BaAl_2(BO_3)_2O$ has been established by single-crystal X-ray diffraction methods. It crystallizes in the trigonal space group R32 (Z = 3) with unit-cell parameters a = 4.891(2) Å, c = 23.923(4) Å, and V = 495.6(2) Å^3.

The structure of the borate $BaAl_2(BO_3)_2O$ has been also established by single-crystal X-ray diffraction methods. It crystallizes in the trigonal space group R32(h) (Z = 3) with unit-cell parameters: a = 5.006(2) Å, c = 24.411(7) Å, and V = 529.9(4) Å^3. The structure was determined from 514 unique reflections (R_{int} = 0.069) and refined to the final residuals of R = 0.031 and R_w = 0.038. It is characterized by an association of BO_3 triangles, BaO_6 trigonal prisms, AlO_4 tetrahedrons, and a unique two-coordinate O atom. From consideration of the BO_3-group alignment, a second-order optical susceptibility of $d_{11} \approx 1.31$ pm/V is predicted. The magnitude of the second-harmonic signal, produced with a 1064 nm laser beam, is 260 % of that produced by KDP(KH_2PO_4).

Materials index: Barium, Strontium, Aluminum, Borate.

Introduction

Solid solutions are very common in crystalline materials. A solid solution is basically a crystalline phase that can have variable compositions. Often, certain properties of materials are modified by changing the composition in such a way that a solid solution forms and great use may be made of this in designing new materials that have specific properties.[1] We describe solid solutions of (Ba, Sr)$Al(BO_3)_2O$ system for designing new material, $BaAl(BO_3)_2O$ from a known compound of $SrAl(BO_3)_2O$ in my research.

Borates have long been important for the production of a variety of glasses. The crystal structure of di-strontium aluminum borate, $SrAl(BO_3)O$, with R = 0.163 was reported by Nagai, T. And Ihara, M.[2] We have also recently synthesized and identified the compound $SrAl(BO_3)O$ with R = 0.059 as a new luminescent material. The structure consists of an 8-coordinated Sr atom, an AlO_4 tetrahedron, and a BO_3 triangle. The strontium boratoberyllate, $Sr_2Be_2(BO_3)O$, has been grown by using the top-seeding high-temperature flux method with the growth temperature of about 1373 K. The strontium boratoberyllate has been discovered as a new ultraviolet nonlinear optical crystal.[3, 4, 5] The $BaAl_2(BO_3)_2O$ compound in the system BaO-Al_2O_3-B_2O_3 was determined by solid state reactions(Sp.: 910 ± 10°C). This compound melt congruently and has monoclinic symmetry with a = 24.98(4) Å, b = 4.848(4) Å, c = 18.85(3) Å, and β = 120.31(9)° in the space group Pc or P2/c. The glass-forming regions of alkaline-earth (Ca, Sr, Ba) aluminum borate systems were recently examined by MacDowell.[7] The materials of primary interest center near the 1 : 1 : 1 molar ratio of MO (M = Sr, Ba, or Ca) : Al_2O_3 : B_2O_3, where the

glass - ceramics were highly crystalline. The thermal expansion coefficient as low as $6\times10^{-7}/°C$ was measured on $SrAl_2(BO_3)_2O$ glass - ceramics. Since a simple orthoborate $(BO_3)^{3-}$ of $BaAl_2(BO_3)_2O$ can have absorption edges of 150 - 160 nm, efforts have been directed to the new structures for second-harmonic generations of wavelengths shorter than 190 nm.[8]

We also describe computations and powder SHG measurements of $BaAl_2(BO_3)O$, compared with KDP(KH_2PO_4).

Experimental Section

Synthesis and Crystal Growth

A powdered sample of $BaAl_2(BO_3)_2O$ was prepared by heating a stoichiometric mixture of the reagents $BaCO_3$ (Cerac, 99.99%), Al_2O_3 (Alfa, 99.999%), and B_2O_3 (Alfa, 99.98%). The mixture was heated in a Pt crucible at 893 K for 1 h, cooled, ground, and again heated at 1153 K for 12 h. An X-ray powder diffraction pattern of the product, obtained with a Philips diffractometer, matched that generated with the computer program LAZY-PULVERIX[9] and the results of the single-crystal study (*vide infra*). Since the compound decomposes at 1183 ± 5 K, crystals were grown from a melt containing 70 mol% $BaAl_2(BO_3)_2O$ and 30 mol% $LIBO_2$ (Alfa, 99.997%). The melt was cooled in a Pt crucible at 0.05 K/min from 1170 to 800 K, and then 5 K/min to room temperature. A clear, colorless crystal was physically separated from the matrix for X-ray measurements.

Solid Solution

Powders in the solid-solution series $BaAl_2(BO_3)_2O$-$SrAl_2(BO_3)_2O$ system were prepared by heating a stoichiometric mixture of the reagents $BaCO_3$, $SrCO_3$ (Alfa, 99.99%), Al_2O_3, and B_2O_3. The mixtures were heated in Pt crucibles at 893 K for 1 h, cooled, ground, and again heated 1123 K for 22 h. X-ray powder diffraction patterns of the products were collected with a Philips diffractometer. The peak positions were corrected by using an internal silicon powder standard and unit-cell constants were refined by using the least squares computer program ***POLSQ***.[10]

Crystallographic Study

The crystal was mounted on a glass fiber and analyzed on a Rigaku AFC6R X-ray diffractometer. Unit-cell parameters were derived from least-squares refinements with the setting angles of 19 automatically-centered reflections in the range of $30.0 < 2\theta < 36.0°$. Intensity data were collected at room temperature by using the ω-scan technique with a rate = 16.0°(ω)/min and peak widths = 1.50 + 0.30 tanθ. The cell constants and Laue symmetry, *3m1,* correspond to the rhombohedral system with a hexagonal setting. The intensity data were collected over the range of indices $-8 \leq h \leq 8$, $0 \leq k \leq 8$, $-39 \leq l \leq 39$. From 1644 measured reflections, a total of 263 were observed [$F_0^2 > 3\sigma(F^2)$]. The intensities of three standard reflections were monitored throughout data collection; average fluctuations were 3.0%.

The structure was solved and refined by using programs from the TEXSAN crystallographic software package[11] on a μ-VAX-II computer. The crystals exhibit the systematic condition **hkl**: -h+k+l = 3n. This condition, the Laue symmetry, and the distribution of intensities are consistent with space groups R32 and R3m. The space group R32 has been chosen on the basis of a successful solution and refinement. The atoms Ba and Al were located by using the direct methods program SHELXS.[12] The remaining atoms were placed following the analysis of difference electron density maps. After full-matrix, least-squares refinement of the model with isotropic displacement coefficients on each atom, an absorption

correction was applied by using the program DIFABS.[13] The data were then averaged. Final refinement with anisotropic displacement coefficients on each atom resulted in the residuals of R = 0.031 and R_w = 0.038. The largest peak in the final difference electron density map corresponds to 1.61 % of the Ba atom. Relevant crystallographic data and atomic parameters and anisotropic displacement coefficients for $BaAl_2(BO_3)_2O$ are listed in Tables 4.1 and Table 4.2, respectively.

Table 4.1 Crystallographic Data and Atomic Parameters for $BaAl_2(BO_3)_2O$

a = 5.006(2) Å, c = 24.411(7) Å, space group R32(h) (no. 155), Z = 3

formula wt. = 324.91 u, $\mu = 58.536\ cm^{-1}$, $\rho_{calcd} = 3.054\ gcm^{-3}$

504 averaged reflections, 21 variables, R =0.031, wR = 0.038

atom	x	y	z	β_{eq}*
Ba	0	0	0	1.15(1)
Al	0	0	0.56820(7)	1.10(3)
O1	0	0	½	2.3(1)
O2	0.4552(8)	0.4269(8)	0.0668(1)	1.8(1)
B	0	0	0.7370(2)	1.1(1)

$$*\beta_{eq}=8\frac{\Pi^2}{3}\sum_i\sum_j U_{ij}a_i^* a_j^* a_i a_j$$

Table 4.2 Anisotropic displacement coefficients for $BaAl_2(BO_3)_2O$

ATOM	U_{11}	U_{22}	U_{33}	U_{12}	U_{13}	U_{23}
Ba	0.0143(2)	0.0143	0.0153(2)	0.0071	0	0
Al	0.0144(4)	0.0144	0.0129(6)	0.0072	0	0
O1	0.039(2)	0.039	0.010(2)	0.020	0	0
O2	0.023(2)	0.026(2)	0.026(1)	0.017(2)	-0.003(1)	-0.007(1)
B	0.013(1)	0.013	0.016(2)	0.007	0	0

Results and Discussion

Crystal Structure

The structure of the title compound, $BaAl_2(BO_3)_2O$ (Figure 4.1), has layers of isolated, flat orthoborate BO_3 groups that are connected by Al_2O_7 and BaO_6 groups; it is isotypic to $SrAl_2(BO_3)_2O$.

Selected interatomic distances and angles are listed in Table 4.3. The Ba atom is surrounded by six O2 atoms at the vertices of a distorted trigonal prism. The interatomic Ba-O distance, 2.748(3) Å, compares to the value, 2.71Å, computed from crystal radii, [14] A 35° relative rotation of the trigonal planes represents the most significant distortion of the prism. The AlO_4 anion has distorted tetrahedral symmetry, point group C_3. The Al-O distances Al-O1, 1.665(2) Å, Al-O2, 1.772(4) Å, are consistent with the coordination numbers of atoms O1 and O2. The O-Al-O angles are 115.8(1) ° for O1-Al-O2 angle, and 102.4(1) ° for O2-Al-O2 angle. The BO_3 anion has trigonal symmetry, point group D_{3h}, and the B-O distance, 1.358(4) Å, is normal.

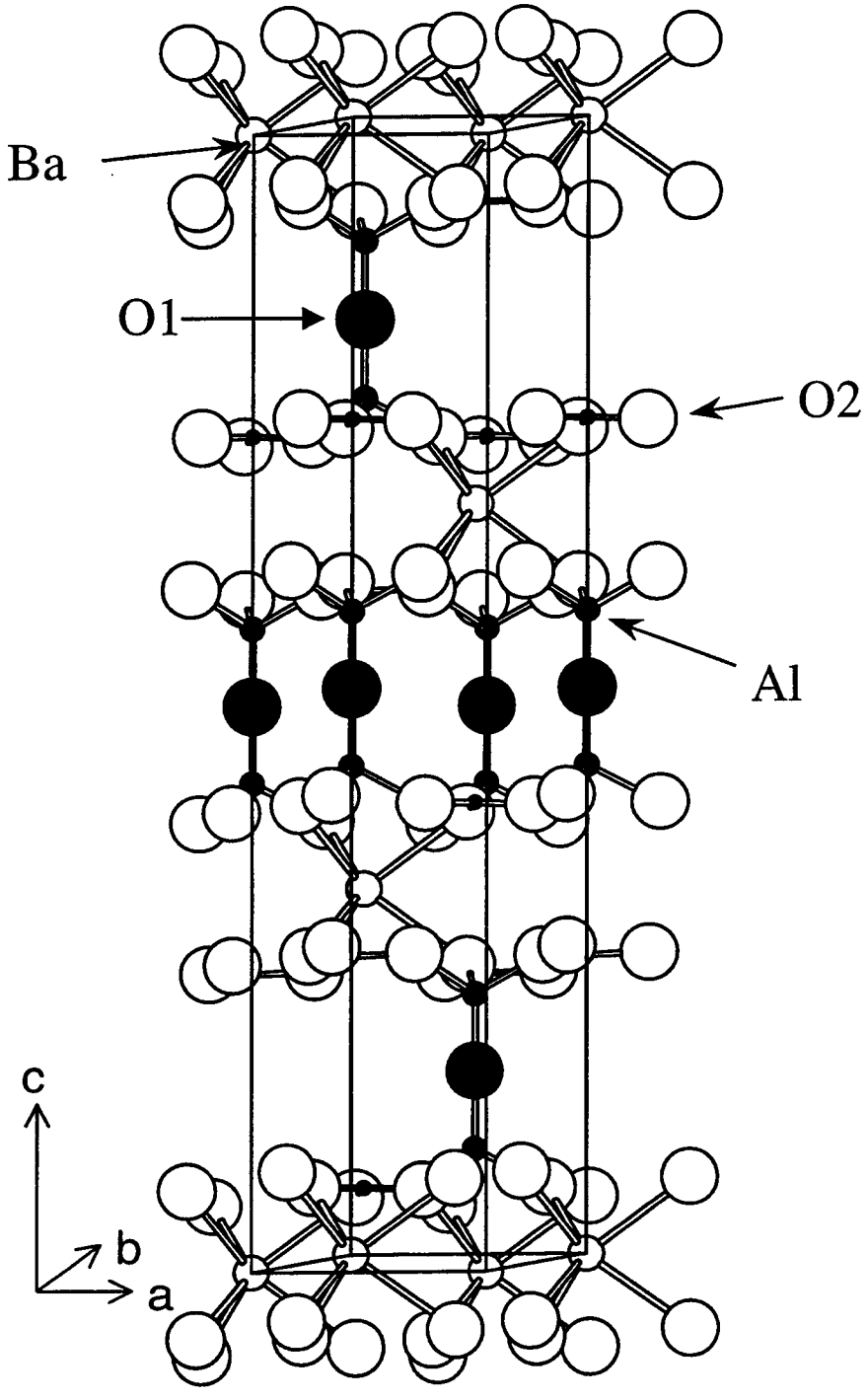

Figure 4.1 Drawing of the unit cell of $BaAl_2(BO_3)_2O$ as a layered structure.

Table 4.3 Selected Interatomic Distances (Å) and Angles (°) for $BaAl_2(BO_3)_2O$

Interatomic	Distances (Å)	Interatomic Angles (°)	
Ba-O2(X6)	2.748(3)	O2-Ba-O2	73.1(1)
			88.3(1)
			115.8(1)
			127.7(1)
			137.4(1)
Al-O1	1.665(2)	O1-Al-O2	115.8(1)
Al-O2(x3)	1.772(4)	O2-Al-O2	102.4(1)
B-O2(x3)	1.358(4)	O2-B-O2	120

Solid Solutions

A solid solution is a crystalline phase that has variable composition. The compound $BaAl_2(BO_3)_2O$ exhibits a continuous substitutional solid solution with $SrAl_2(BO_3)_2O$. Unit-cell volumes in the series $Ba_{1-x}Sr_xAl_2(BO_3)_2O$ continuously decrease for $x<1$ (Figure 4.3), consistent with Vegard's law.

Nonlinearity

The title compound $BaAl_2(BO_3)_2O$ is isotypic to $SrAl_2(BO_3)_2O$ and appears to be structurally related to the NLO material $Sr_2Be_2B_2O_7$.[3, 4, 5] The matrix form of the second-order nonlinear coefficients, d_{ij}, for the point group 32 are listed in Table 4.4. As illustrated in Figure 4.2, there is an important relative rotation of the BO3 groups by 35° about their trigonal axes that affords a nonlinear susceptibility that is 61% of its optimal value. This rotation is directly correlated to the coefficient d_{11} which varies as $\cos 3\theta$, where θ is the projection of the half angle 35°/2. As shown in Chapter 3, we use the reported nonlinearity of $YAl_3(BO_3)_4$ (D_{11} = 1.48pm/V)[15] and calculated number densities of BO_3 groups to derive susceptibility coefficients for new compounds. For the title compound, the relevant values are d_{11} = 1.31pm/V and d_{14} = 0.06pm/V. This susceptibility is sufficient for practical application, so additional studies on the crystal growth of $BaAl_2(BO_3)_2O$ appear to be warranted.

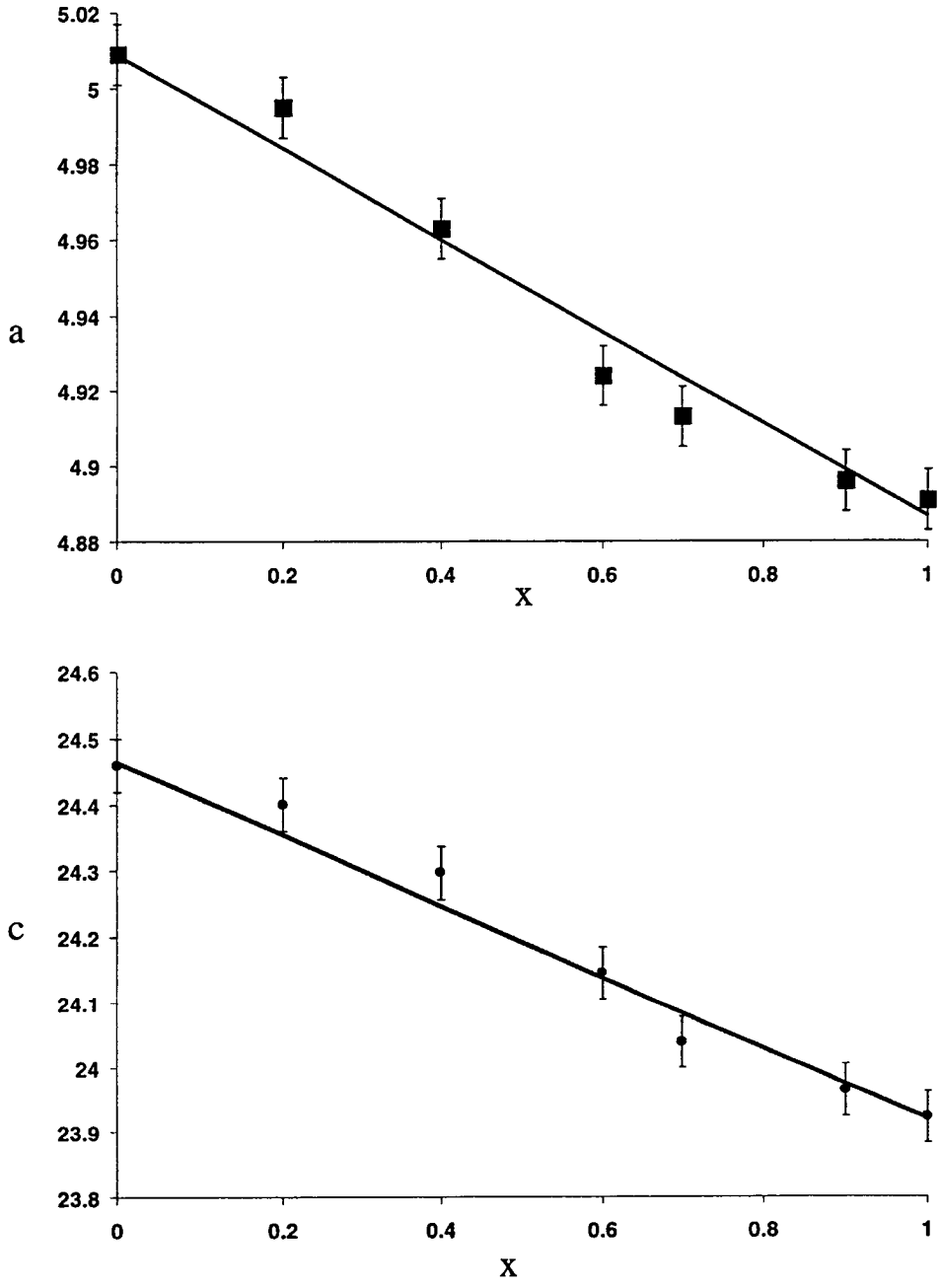

Figure 4.2 Graph of the continuous substitutional solid solutions of the series $Ba_{1-x}Sr_xAl_2(BO_3)_2O$.

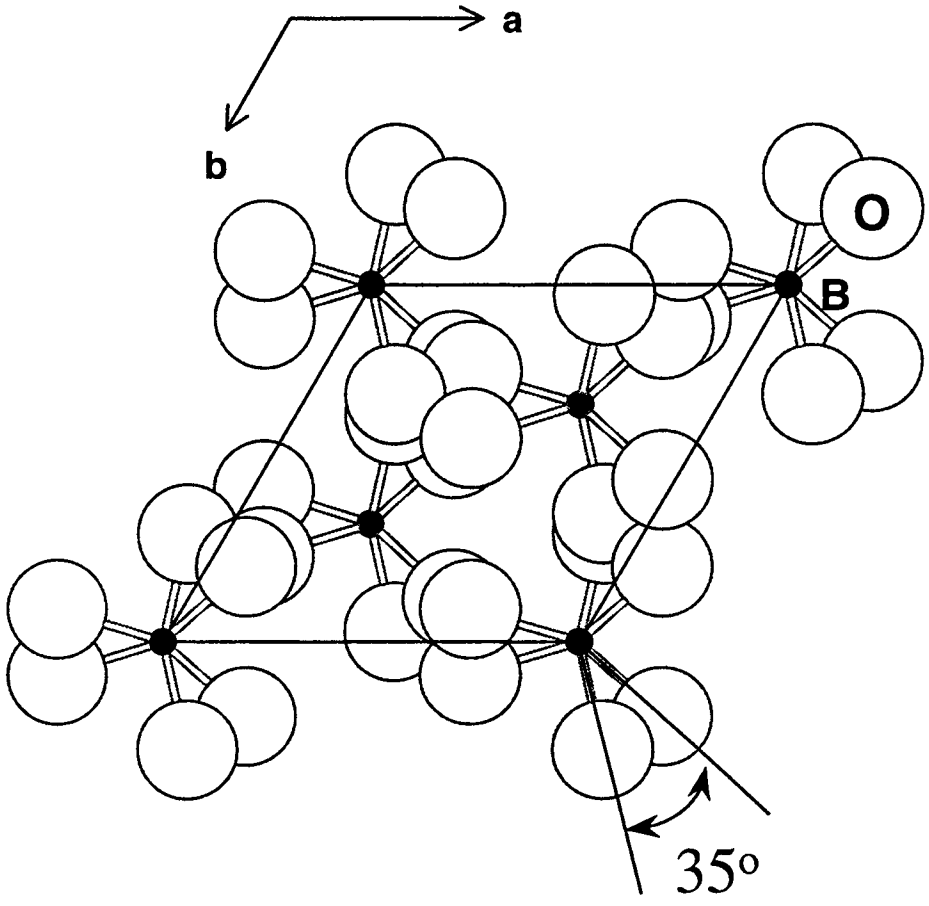

Figure 4.3 Drawing of the rotation of the isolated planar BO_3 group by 35° as viewed perpendicular to the c axis.

Table 4.4 Matrix Form of Second-Order Nonlinear Coefficients, d_{ij}, for point group 32.

d_{11}	$-d_{11}$	0	d_{14}	0	0
0	0	0	0	$-d_{14}$	$-d_{11}$
0	0	0	0	0	0

Table 4.5 Nonlinearity of Aluminum Borates

Compound	Angle of BO3 (°)	% Optimum	Calculated D_{ij} (pm/V)
β-BaB_2O_4			1.6
$SrAl_2(BO_3)_2O$[@]	20	87	2.02
$BaAl_2(BO_3)_2O$	35	61	1.31
$Na_2Al_2(BO_3)_2O$[#]	50	26	0.61
KDP			0.5

[@] Chapter 3

[#] Chapter 5

This result is consistent with the magnitude of the second-harmonic signal from a collection of small single crystals which is 2.6 times that of KDP for 1064 nm fundamental light. The material $BaAl_2(BO_3)_2O$ is a new, noncentrosymmetric compound having optical and crystal-growth characteristics that make it attractive for continued development as a nonlinear optical material.

Frequency Conversion Measurement

The efficiency of the second-harmonic generation from a selection of small crystals of $BaAl_2(BO_3)_2O$, was measured by the method of Kurtz and Pery.[16] Fundamental IR radiation, 1064 nm light, was generated with a Q-switched Molectron MY-34 Nd^{3+}:YAG laser, filtered, and passed through the sample mounted on a silica glass plate. The second harmonic was directed onto a photomultiplier tube through a dichroic mirror and monitored with a Tektronix 2467B oscilloscope (see Figure 4.4 for schematic of experimental set up). A microcrystalline sample of KH_2PO_4 (KDP), served as the standard for the measurements.

Luminescence

In oxide hosts, photoexcitation of the Eu^{2+} ion typically results in broad-band emission arising from the $4f^65d^1 \rightarrow 4f^7$ transition. Characteristics line emission can be observed if the $4f^65d^1$ configuration is higher in energy than the $^6P_{7/2}$ excited state of the $4f^7$ configuration. This type of emission is observed in crystal-field hosts such as the fluorides $SrAlF_5$ and $BaAlF_5$[17, 18] and the mixed fluoride chlorides SrFCl and BaFCl.[19] The stronger crystal fields in oxides make line emission rare, but it has been observed in $SrBe_2Si_2O_7$ and $BaBe_2Si_2O_7$.[20]

Excitation and emission spectra for 1 atom% loading of Eu^{2+} in $BaAl_2(BO_3)_2O$ are shown in Figure 4.5. The emission feature is consistent with predominant emission from $^6P_{7/2}$ state. This result is consistent with the O coordination environment - 1Al, 1B, and $1Eu^{2+}$ - and the expended characteristics of the matrix resulting from the presence of the Ba atom.

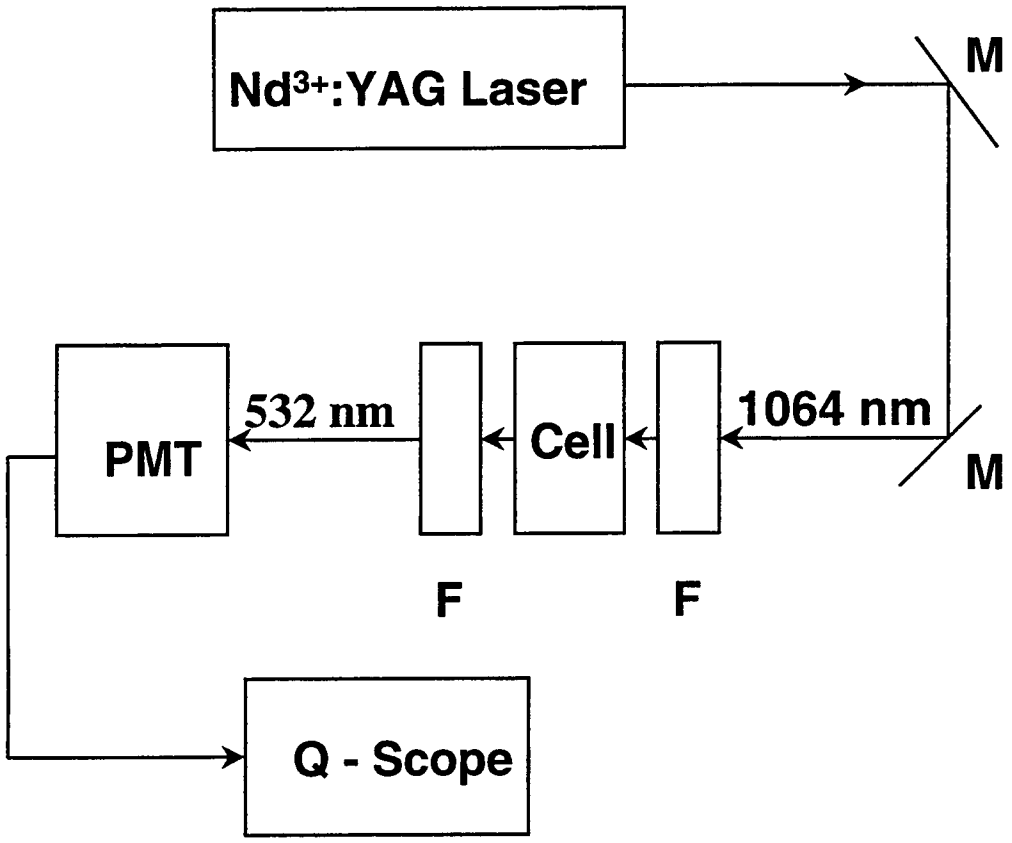

Figure 4.4 Schematic diagram of the apparatus used for SHG measurements.

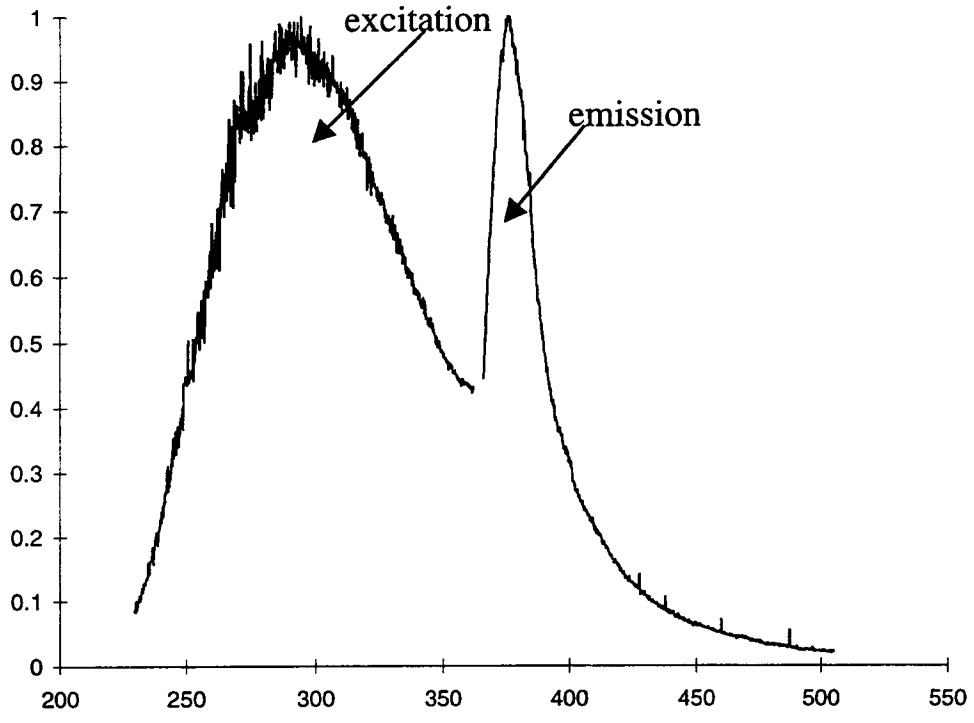

Figure 4.5 Excitation and emission spectra of the luminescence of 1% Eu^{2+}: $BaAl_2(BO_3)_2O$ at 298°K.

Acknowledgments

This work was supported by the National Science Foundation, Solid-State Chemistry Program. We want to thank Dr. Anthony Diaz for assistance with the SHG measurement. KSC thanks the Republic of Korea Air Force for a graduate fellowship.

References

1. West, A.R., *Solid State Chemistry and its Application*, John Wiley & Sons Ltd., **1984**, Chap. 10, 358-373.

2. Nagai, T.; Ihara, M. *Yogyo - Kyokai - Shi*, **1972**, 80(11), 14.

3. Xia, Y.; Chen, C.; Tang, D.; Wu, B., *Adv. Mater.*, **1995**, 7: 79--81.

4. Chen, C.; Wang, Y.; Xia, Y.; Wu, B.; Tang, D.; Wu, K.; Wenrong, Z.; Yu, L.; Mei, L. *J. Appl. Phys.*, **1995**, 77: 2268--2272.

5. Chen, C.; Wang, Y.; Wu, B.; Wu, K.; Zeng, W.; Linhua, Y., *Nature*, **1995**, 373: 322--324

6. Huber, K. H., *N. Jb. Miner. Abh.*, **1970**, 112, 2, 150--160.

7. MacDowell, J. F., *J. Am. Ceram. Soc.*, **1990**, 73(8) 2287.

8. Keszler, D. A., *Current Opinion in Solid State & Materials Science*, **1996**, 1, 204.

9. Yvon, K.; Jeitschko, W.; Parthe, E. *J. Appl. Cryst.* **1977**, *10*, 73.

10. ***POLSQ***: Least Squares Unit Cell Refinement, David Cahen, **1973**.

11. ***TEXSAN***, Structure Analysis Package, Molecular Structure Corp., MSC 3200A, Research Forest Drive, the Woodlands, TX 77381.

12. Sheldrick, G. M., In *Crystallographic Computing 3*; Sheldrick, G.M.; Krüger, C.; Goddard, R.; Eds.; Oxford Univ. Press, Oxford, U. K., **1985**, p 175.

13. Walker, N.; Stuart, D. *Acta Crystallogr.*, Sect. A, **1983**, 39, 158.

15. Schaffers, K. I., Doctoral Thesis, Oregon State University, **1992**, Chap. 1.

16. Krutz, S. W. and Perry, T. T., *J. Appl. Phys.*, **1968**, 39, 3798.

17. Hoffmann, M. V., *J. Electrochem. Soc.*, **1971**, 118, 933.

18. Hoffmann, M. V., *J. Electrochem. Soc.*, **1972**, 119, 905.

19. Sommerdijk, J. L.; Verstegen, J. M. P. J.; Bril, A., *J. Luminescence*, **1974**, 8, 502.

20. Sommerdijk, J. L.; Verstegen, J. M. P. J., *J. Luminescence*, **1974**, 8, 502.

CHAPTER 5

SYNTHESIS, STRUCTURE, NONLINEARITY, AND SOLID SOLUTION OF $Na_2Al_2(BO_3)_2O$

Ki-Seog Chang and Douglas A. Keszler

In Preparation for Publication, **1998**

Abstract

The structure of the borate oxide $Na_2Al_2(BO_3)_2O$ has been established by single-crystal X-ray diffraction methods. It crystallizes in the trigonal space group P31c (Z = 2) with unit-cell parameters a = 4.8087(6) Å, c = 15.2734(6) Å, and V = 305.86(6) $Å^3$. The structure was determined from 1264 unique reflections (R_{int} = 0.096) and refined to the final residuals R = 0.072 and R_w = 0.097. It is characterized by an association of BO_3 triangles, NaO_6 trigonal prisms, and NaO_9 groups, and AlO4 tetrahedra. From consideration of the BO_3-group alignment, a second-order optical susceptibility of $d_{11} \approx 0.61$ pm/V is predicted.

Materials index: Sodium, Aluminum, Borate.

Introduction

The strontium boratoberyllate $Sr_2Be_2B_2O_7$ has been grown by using the top-seeding high-temperature flux method with the growth temperature about 1373 K. The strontium boratoberyllate has been discovered as a new ultraviolet nonlinear optical crystal.[1, 2, 3] The glass-forming regions of alkaline-earth (Ca, Sr, Ba) aluminum borate systems were recently examined by MacDowell.[4] The materials of primary interest center near the 1 : 1 : 1 molar ratio of MO (M = Sr, Ba, or Ca) : Al_2O_3 : B_2O_3 where the glass-ceramics were highly crystalline. The compound $Na_2O{\circ}Al_2O_3{\circ}B_2O_3$ melts congruently at 1010°C. The infrared spectrum of the compound has absorption bands at about 1315, 1230, 1120, 1000, 950, 820, 760, 740, 675, 625, 575, 485, 435, and 420 cm^{-1}. According to Weir and Schroeder,[6] the absorption bands with maximum wavelengths near 1315, 1230, 1120, 760, and 740 cm^{-1} belong to three-coordinated boron atoms. Consequently, the boron atoms in this compound are in oxygen triangles. Since a simple orthoborate $(BO_3)^{3-}$ of $SrAl_2(BO_3)_2O$ can have absorption edges of 150 - 160 nm, efforts have been directed to the new structures for a second-harmonic generation of wavelengths shorter than 190 nm.[7]

We also describe the bond valence method in the $Na_2Al_2(BO_3)_2O$ and the solid solutions of $(Na_2, Sr)Al_2(BO_3)_2O$.

Experimental Section

Synthesis and Crystal Growth

A powder sample of $Na_2Al_2(BO_3)_2O$ was prepared by heating a stoichiometric mixture of the reagents Na_2CO_3 (Mallinkrodt, reagent grade), Al_2O_3 (Alfa, 99.999%), and B_2O_3 (Alfa, 99.98%). The mixture was heated in a Pt crucible at 893 K for 1 h, cooled and ground at room temperature, and again heated in at 1173 K for 12 h. An X-ray powder diffraction pattern of the product, obtained with a Philips diffractometer, matched that generated with the computer program LAZY-PULVERIX[8] and the results of the single-crystal study (*vide infra*). Crystals were grown from a stoichiometric melt that was cooled at 0.07 K/min from 1333 to 900 K, and then 5 K/min to room temperature. A clear, colorless crystal was physically separated from the matrix for X-ray measurements.

Solid Solution

A powdered solid solution sample of $Sr_xNa_{2-2x}Al_2(BO_3)_2O$ system was prepared by heating mixtures of the reagents Na_2CO_3, $SrCO_3$(Alfa, 99.99%), Al_2O_3, and B_2O_3. The mixtures were heated in a Pt at 893 K for 1 h, cooled and ground at room temperature, and again heated at 1173 K for 22 h. X-ray powder diffraction patterns of the products were obtained with a Philips diffractometer. The peak positions were corrected by using an internal silicon powder standard, and unit-cell constants were calculated by using the least-squares computer program ***POLSQ***.[9]

Crystallographic Study

The crystal was mounted on a glass fiber and analyzed on a Rigaku AFC6R X-ray diffractometer. Unit-cell parameters were derived from least-squares refinements with the setting angles of 18 automatically-centered reflections in the range of $31.0 < 2\theta < 36.0°$. Intensity data were collected at room temperature by using the ω-scan technique with a rate = 16.0°(ω)/min and peak widths = 1.40 + 0.30 tanθ. The cell constants and Laue symmetry *31m* correspond to the trigonal system. The intensity data were collected over the range of indices $0 \leq h \leq 8$, $-8 \leq k \leq 8$, $-26 \leq l \leq 26$. From 1264 measured reflections, a total of 809 were observed [$F_0^2 > 3\sigma(F^2)$]. The intensities of three standard reflections were monitored throughout data collection; average fluctuations were 3.0%.

The structure was solved and refined by using programs from the TEXSAN crystallographic software package[10] on a μ-VAX-II computer. The crystals exhibit the systematic absence condition **hkl**: l = 2n+1. This systematic absence, the Laue symmetry $\bar{3}$1m, and the distribution of intensities are consistent with space groups P31c and P31m. The space group P31c has been chosen on the basis of a successful solution and refinement. The atom Al was located by using the direct methods program SHELXS.[11] The remaining atoms were placed following analysis of difference electron density maps. After full-matrix, least-squares refinement of the model with isotropic displacement coefficients on each atom, an absorption correction was applied by using the program DIFABS.[12] The data were then averaged: Final refinement with anisotropic displacement coefficients on each atom

resulted in the residuals R= 0.072 and R_w = 0.097. The largest peak in the final difference electron density map corresponds to 5.08% of the Al atom. Relevant crystallographic data and atomic parameters and anisotropic displacement coefficients are listed in Tables 5.1 and Table 5.2, respectively.

Table 5.1 Crystallographic Data and Atomic Parameters for $Na_2Al_2(BO_3)_2O$

a = 4.8087(6) Å, c = 15.273(4) Å, space group P31c (no. 159), Z = 2

formula wt. = 223.56 u, $\mu = 5.9\ cm^{-1}$, $\rho_{calcd} = 2.536\ gcm^{-3}$

809 averaged reflections, 44 variables, R =0.072, $R_w = 0.097$

atom	x	y	z	β_{eq}^*
Al1	0.3333	0.6667	0.2926	1.35(7)
Al2	0.3333	0.6667	0.5130(1)	1.35(6)
Na1	0	0	0.1513(4)	1.72(5)
Na2	0	0	0.4047(8)	3.5(1)
O1	0.0363(8)	1.3935(8)	0.0500(4)	2.2(1)
O2	-0.039(1)	0.598(1)	0.2601(5)	4.4(2)
O3	0.3333	0.6667	0.4085(8)	7.9(3)
B1	0.3333	0.6667	0.7572(7)	1.0(2)
B2	0.3333	0.6667	0.049(1)	2.8(4)

$$*\beta_{eq}=8\frac{\Pi^2}{3}\sum_i\sum_j U_{ij}a_i^* a_j^* a_i a_j$$

Table 5.2 Anisotropic Displacement Coefficients for $Na_2Al_2(BO_3)_2O$

ATOM	U_{11}	U_{22}	U_{33}	U_{12}	U_{13}	U_{23}
Al1	0.0172(7)	0.0172	0.017(2)	0.009	0	0
Al2	0.0184(7)	0.0184	0.015(1)	0.009	0	0
Na1	0.0228(6)	0.0228	0.020(1)	0.011	0	0
Na2	0.035(1)	0.035	0.063(2)	0.017	0	0
O1	0.010(1)	0.010(1)	0.055(3)	-0.001(1)	-0.006(2)	0.007(2)
O2	0.027(2)	0.031(2)	0.116(6)	0.021(2)	0.004(3)	0.008(3)
O3	0.148(7)	0.148	0.005(4)	0.074	0	0
B1	0.002(1)	0.002	0.034(6)	0.001	0	0
B2	0.034(4)	0.034	0.04(1)	0.02	0	0

Results and Discussion

Crystal Structure

The structure of $Na_2Al_2(BO_3)_2O$ (Figure 5.1) is closely related to the structural type of $SrAl_2(BO_3)_2O$ described in Chapters 3 and 4, respectively. The $Na_2Al_2(BO_3)_2O$ framework of distorted NaO_6 trigonal prisms bridged by Al_2O_7 and BO_3 groups mimics that observed in $MAl_2(BO_3)_2O$ (M = Sr, Ba). In addition, the linear Al-O3-Al interaction is preserved. The present structure differs from the $MAl_2(BO_3)_2O$ type by the inclusion of additional Na atoms in the planes containing the two-coordinate O atoms, producing a 3+6 coordination environment for these Na2 atoms (Figure 5.2).

Selected interatomic distances and angles are listed in Table 5.3. The Na1 atom is surrounded by three O1 and O2 atoms in a trigonal antiprismic site. The interatomic Na1-O distances are 2.382(6) Å for Na1-O1 distance and 2.484(8) Å for Na1-O2 distance. Additional distortions in the trigonal antiprism are represented by the angles 82.4(3)° for O1-Na1-O1, 98.9(2)° for O1-Na1-O2, and 80.2(3)° for O2-Na1-O2 angle. The interatomic Na2-O distances are 2.777(6) Å for Na2-O3, 2.865(9) Å for Na2-O1, and 2.88(1) Å for Na2-O2 (Figure 5-2). Considering the Na1-O distances and the value, 1.38 Å, calculated from crystal radii,[13] the Na2-O distances are abnormally long. We calculated the valence of the Na2 atom by using the bond valence method.[14] The valence v_{ij} of a bond between two atoms I and j is defined so that the sum of all the valences from a given atom I with valence V_i obeys

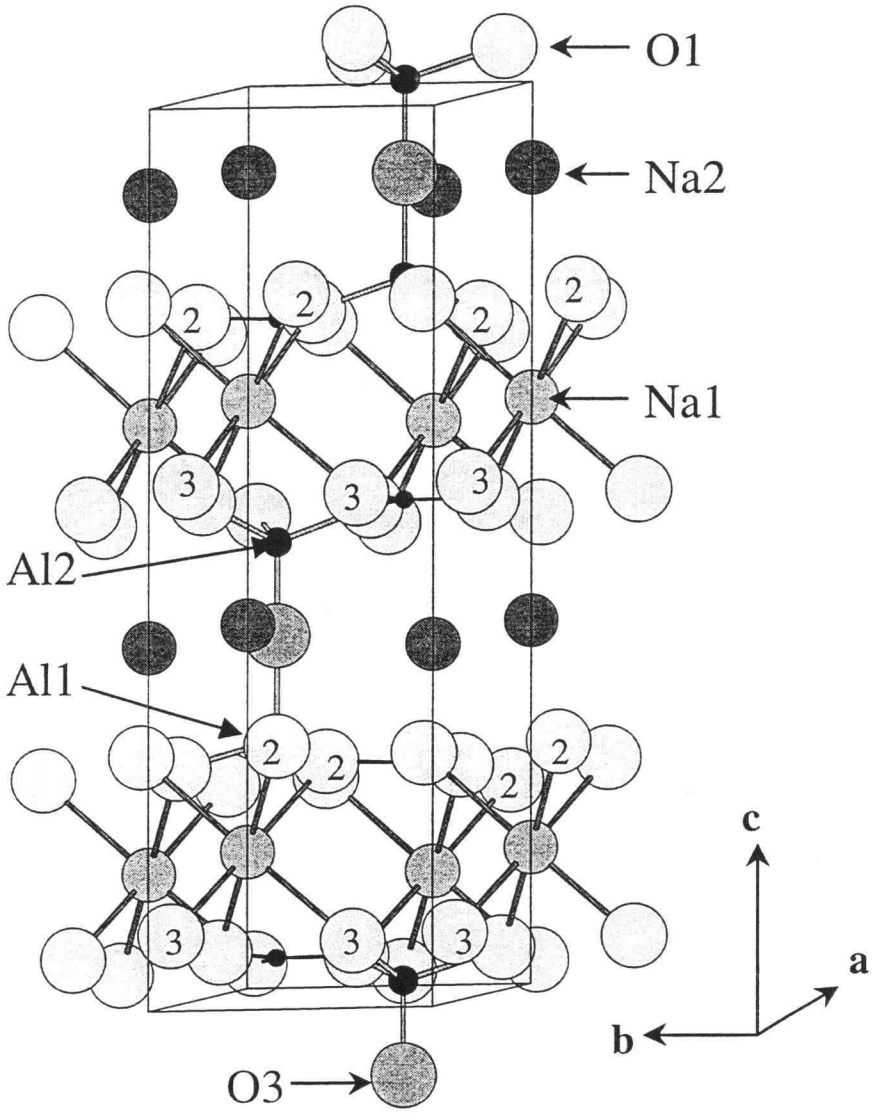

Figure 5.1 Drawing of the unit cell of $Na_2Al_2(BO_3)_2O$ as a open framework.

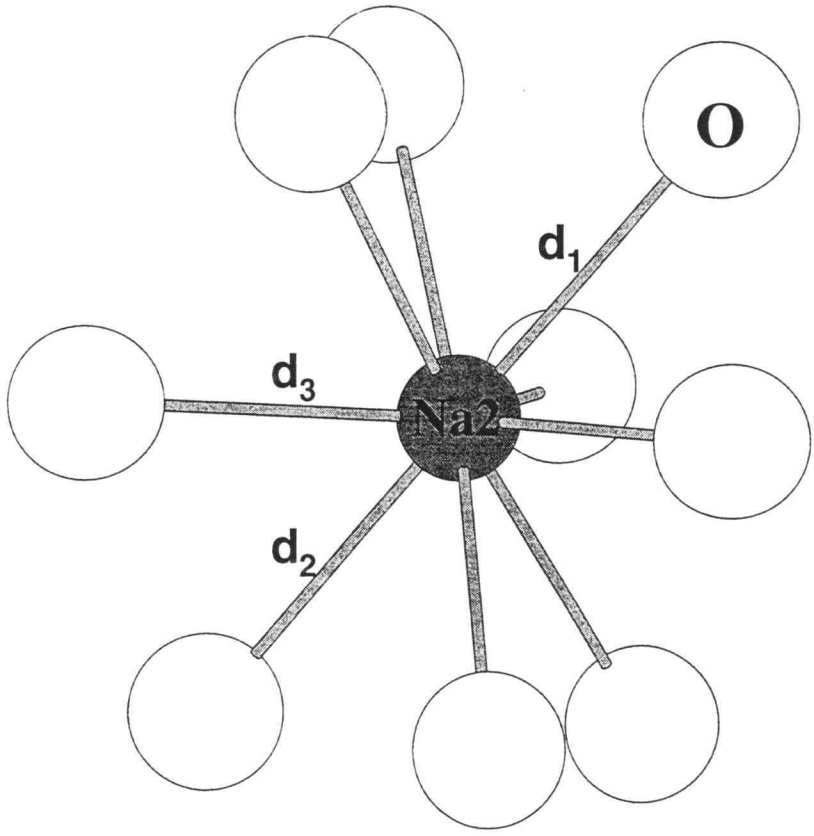

d_1 = 2.865(9) Å
d_2 = 2.88(1)
d_3 = 2.777(6)

Figure 5.2 Diagram of $Na2O_9$ structure for bond valence method.

Table 5.3 Selected Interatomic Distances (Å) and Angles (°) for $Na_2Al_2(BO_3)_2O$

Interatomic	Distances (Å)	Interatomic Angles (°)	
Al1-O2(x3)	1.724(6)	O2-Al1-O2	112.1(2)
Al1-O3(x1)	1.77(1)	O2-Al1-O3	106.8(2)
Al2-O1(x3)	1.746(4)	O1-Al2-O1	110.0(2)
Al2-O3(x1)	1.60(1)	O1-Al2-O3	108.9(2)
Na1-O1(x3)	2.382(6)	O1-Na1-O1	82.4(3)
Na1-O2(x3)	2.484(8)	O1-Na1-O2	98.9(2)
			178.5(3)
		O2-Na1-O2	80.2(3)
Na2-O1(x3)	2.865(9)[@]		
Na2-O2(x3)	2.88(1)[@]		
Na2-O3(x3)	2.7776(6)[@]		
B1-O2(x3)	1.349(6)	O2-B1-O2	120(0)
B2-O1(x3)	1.375(3)	O1-B2-O1	120(0)

[@] Bond Lengths for Bond Valence Method (Figure 5.2)

$$\sum v_{ij} = V_i \qquad (1)$$

Here I corresponds to Na2 and j corresponds to O1, O2, or O3. The most commonly adapted empirical expression for the variation of the length d_{ij} of a bond with valence is

$$v_{ij} = \exp[(R_{ij} - d_{ij})/b] \qquad (2)$$

Here b is commonly taken to be a " universal " constant equal to 0.37 Å.[15] The bond valence parameter R is the length of a single bond, but it is usually determined to fit the bond lengths in compounds that are stable at normal temperatures and pressures. Here $R(Na^+) = 1.80$ Å.[16] According to equations (1) and (2) the bond valence of Na2 is +0.55. The two AlO_4 groups are considerably distorted from tetrahedral symmetry. The Al-O distances are 1.724(6) Å for three Al1-O3 interactions in the trigonal base of the tetrahedra, 1.77(1) Å for Al1-O3, 1.60(1) Å for the three Al2-O1 distances, 1.746(4) Å for the Al2-O1 interaction. The O-Al-O angles are 112.1(2) ° for O2-Al1-O2, 106.8(2) ° for O2-Al1-O3, 110.0(2) ° for O1-Al2-O1, and 108.0.9(2) ° for O1-Al2-O3. The two BO_3 anions have trigonal symmetry; the B-O distances are normal.

As noted above the computed value for atom Na2 is quite abnormal. In addition, the displacement coefficients (Table 5.1) for atoms Na2, O2, and O3 are quite high. It is highly unlikely that these displacement coefficients represent thermal motion of the atoms. Rather, there are likely to be significant local

distortions around the Na2 atoms that are not appropriately modeled with space group P31c. Additional work will be required to unravel some of the detailed complexities of this structure.

Solid Solutions

Because of the structural similarities between the materials $SrAl_2(BO_3)_2O$ and $Na_2Al_2(BO_3)_2O$, we have investigated phase equilibria in the system $Sr_xNa_{2-2x}Al_2(BO_3)_2O$. As shown in Figure 5.3, a steady increase in unit-cell volume is observed with increasing amounts of the larger Sr atom. The data are consistent with complete solid solubility across the entire range of x. There are, however, subtle structural changes that occur across the series. For $x < 0.1$, the trigonal structure of $Na_2Al_2(BO_3)_2O$ is adopted. Across the broad range from approximately $x = 0.1$ to $x = 0.9$ an hexagonal form of the structure, which we designate SNABO, is formed. For $x > 0.9$, the rhombohedral structure of $SrAl_2(BO_3)_2O$ is identified from the X-ray patterns. Some relevant unit-cell data and a summary of the results in Table 5.4.

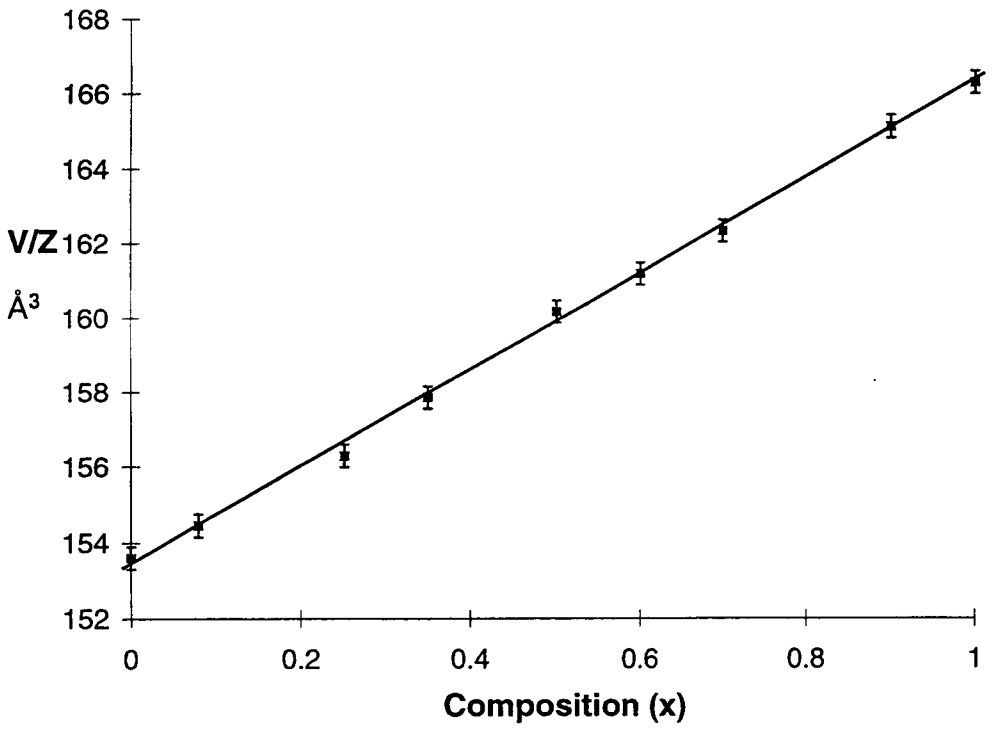

Figure 5.3 Graph of the continuous substitutional solid solutions of the $Sr_xNa_{2-2x}Al_2(BO_3)_2O$ system.

Table 5.4 X-ray Powder Diffraction for Solid Solutions of $Sr_xNa_{2-2x}Al_2(BO_3)_2O$

Composition(x)	a or b (Å)	c (Å)	Asym. Volume (Å^3)	Phase
1	4.902	23.966	166.278	$SrAl_2(BO_3)_2O$
0.9	4.8951	15.912	165.1	SNABO[#]
0.7	4.8732	15.786	162.335	SNABO
0.6	4.8632	15.739	161.185	SNABO
0.5	4.8580	15.674	160.17	SNABO
0.35	4.8405	15.559	157.85	SNABO
0.25	4.8298	15.472	156.28	SNABO
0.08	4.822	15.341	154.45	$Na_2Al_2(BO_3)_2O$
0	4.8179	15.283	153.6	$Na_2Al_2(BO_3)_2O$
1[@]	4.891	23.923	165.003	$SrAl_2(BO_3)_2O$
0.84[@]	4.8834	15.821	163.335	$Sr_xNa_{2-2x}Al_2B_2O_7$
0[@]	4.8087	15.2734	152.93	$Na_2Al_2(BO_3)_2O$

[#] SNABO = $Sr_xNa_{2-2x}Al_2(BO_3)_2O$

[@] Cell Constants of Single Crystals

Nonlinearity

As illustrated in Figure 5.4, there is an important relative rotation of the BO_3 groups by 50° about their trigonal axes. This produces a sencond-order nonlinear susceptibility that is the 26 % of optimal value. The second-order nonlinear coefficient 0.61 pm/V was calculated on the basis of the coefficient d_{11} = 1.48 pm/V the nonlinearity YAB $(YAl_3(BO_3)_4)$[17] and a number density of 1.23×10^{22} BO^3 groups/cm^3 for $Na_2Al_2(BO_3)_2O$.

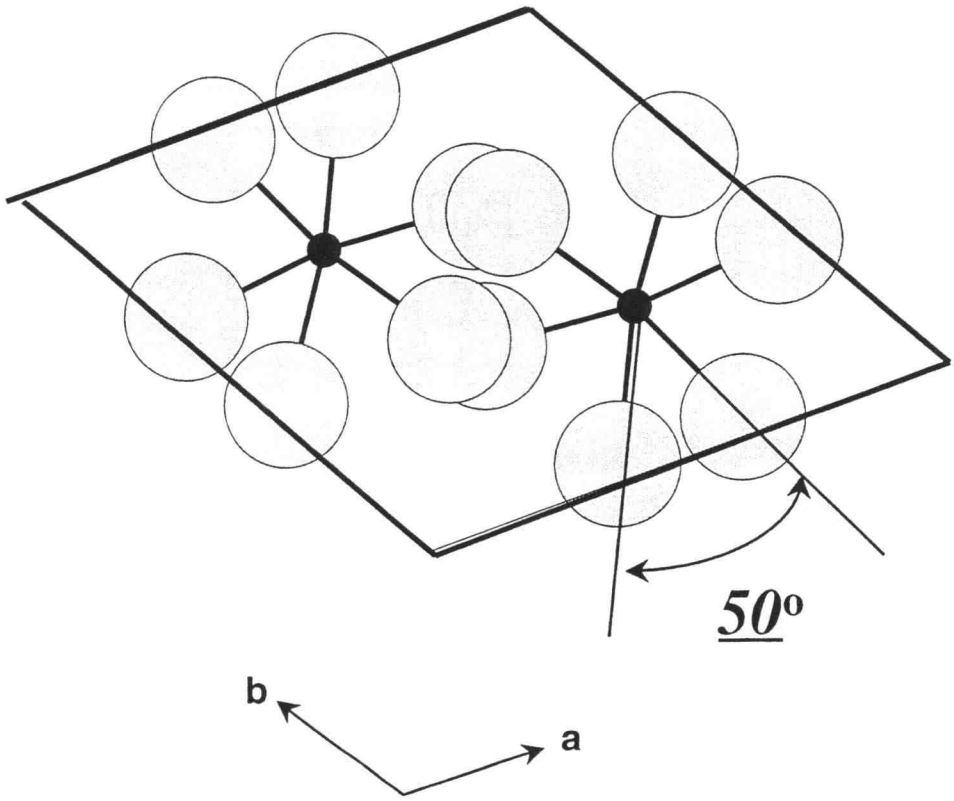

Figure 5.4 Drawing of the rotation of the isolated planar BO_3 group by 50° as viewed perpendicular to the c axis.

Acknowledgments

This work was supported by the National Science Foundation, Solid State Chemistry Program. KSC gratefully acknowledges the Republic of Korea Air Force for a graduate fellowship.

References

1. Xia, Y.; Chen, C.; Tang, D.; Wu, B., *Adv. Mater.*, **1995**, 7: 79--81.

2. Chen, C.; Wang, Y.; Xia, Y.; Wu, B.; Tang, D.; Wu, K.; Wenrong, Z.; Yu, L.; Mei, L., *J. Appl. Phys.*, **1995**, 77: 2268--2272.

3. Chen, C.; Wang, Y.; Wu, B.; Wu, K.; Zeng, W.; Linhua, Y. Nature, **1995**, 373: 322--324.

4. MacDowell, J. F., *J. Am. Ceram. Soc.*, **1990**, 73(8), 2287.

5. Zhuralev, V. D., Fotiev, A. A., and Korablev, G. A., Rus. *J. Inorg. Chem.*, **1983**, 28(1), 115--117.

6. Weir, C. W. and Schroeder, R. A., *J. Res. Nat. Bur. Stand.*, **1964**, 68A, 466.

7. Keszler, D. A. Solid State & Materials Science **1996**, in press.

8. Yvon, K.; Jeitschko, W.; Parthe, E. *J. Appl. Cryst.* **1977**, *10*, 73.

9. ***POLSQ***: Least Squares Unit Cell Refinement, David Cahen, **1973**.

10. ***TEXSAN***, Structure Analysis Package, Molecular Structure Corp., MSC 3200A, Research Forest Drive, the Woodlands, TX 77381.

11. Sheldrick, G. M. In *Crystallographic Computing 3*; Sheldrick, G.M.; Krüger, C.; Goddard, R.; Eds.; Oxford Univ. Press, Oxford, U. K., **1985**, p 175.

12.Walker, N. and Stuart, D., *Acta Crystallogr.*, Sect. A, **1983**, 39, 158.

13. Shanon, R. D., , *Acta Crystallogr.*, Sect. A, **1976**, 32, 751.

14. O'Keeffe, M. and Brese, N. E., *J. Am. Chem. Soc.*, **1991**, 113, 3226--3229.

15. Brown, I. D. and Altermatt, D., *Acta Crystallogr.*, B41, **1981**, 244.

16. O'Keeffe, M. and Brese, N. E., *Acta Crystallogr.*, B47, **1991**, 192--197.

17. Schaffers, K. I., Doctoral Thesis, Oregon State University, **1992**, Chap. 1.

CHAPTER 6

$CaAl_2(BO_3)_2O$: CRYSTAL STRUCTURE

Ki-Seog Chang and Douglas A. Keszler*
Department of Chemistry and Center for Advanced Materials Research, 153 Gilbert Hall,
Oregon State University, Corvallis, OR 97331-4003

Mat. Res. Bull., **1997**

ABSTRACT

The structure of the aluminum borate $CaAl_2(BO_3)_2O$ has been established by single-crystal X-ray diffraction methods. It crystallizes in the trigonal space group Rc(h) (Z = 6) with unit-cell parameters a = 4.810(6) Å, c = 46.633(5) Å, and V = 934(1) $Å^3$. The structure was determined from 274 unique reflections and refined to the final residuals R = 0.024 and wR = 0.032. It is characterized by an association of BO_3 triangles, CaO_6 octahedra, AlO_4 tetrahedra, and unique, two-coordinate O atoms. Structural comparisons are made to Na^+ β-alumina.

KEYWORDS: A. optical materials B. oxides C. X-ray diffraction D. crystal structure

INTRODUCTION

The phase $CaAl_2(BO_3)_2O$ was first described by Schäfer and Kuzel, following a study of the ternary system $CaO\text{-}Al_2O_3\text{-}B_2O_3$ (1). They provided X-ray evidence for the existence of both high- and low-temperature forms of the compound. The high-temperature form was identified as an hexagonal material forming in space group $P6_322$ (a = 4.81(3), c = 15.55(3) Å). Later, MacDowell reported ultra-low thermal expansion in the series of glass ceramics $AEAl_2(BO_3)_2O$ (AE = Ca, Sr, Ba.) (2). You and Hong subsequently detailed the luminescence properties of Ce^{3+}-, Gd^{3+}-, and Tb^{3+}-doped $CaAl_2(BO_3)_2O$ powders (3). In a recent report, we described the crystal structure of the Sr analog, $SrAl_2(BO_3)_2O$ (4). This material crystallizes in a noncentrosymmetric structure having an arrangement of BO_3 groups that is favorable for high optical second-order nonlinear susceptibilities. Considering the structural characteristics of the Sr compound and the general interest in the Ca analog, we have crystallized the latter and determined its structure. It forms in the trigonal system with a tripling of the *c* axis relative to the value reported by Schäfer and Kuzel.

EXPERIMENTAL

A powdered sample of $CaAl_2(BO_3)_2O$ was prepared by heating a stoichiometric mixture of the reagents $CaCO_3$ (Cerac, 99.999%), Al_2O_3 (Alfa, 99.999%), and B_2O_3 (Alfa, 99.98%). The mixture was heated in a Pt crucible at 893 K for 1 h, cooled, ground at room temperature, and again heated in a Pt crucible at 1273 K for 12 h. An X-ray powder diffraction pattern of the product, obtained with a Philips diffractometer, matched that generated with the computer program LAZY-PULVERIX (5) and the results of the single-crystal X-ray study (*vide infra*). Since the compound decomposes at 1371 ± 10 K, crystals were grown in a Pt crucible from a melt containing 60 mol% $CaAl_2(BO_3)_2O$ and 40 mol% $LiBO_2$ (Alfa, 99.997%.) The melt was cooled at 4 K/h from 1273 to 800 K, and then 5 K/min to room temperature. A clear, colorless crystal was physically separated from the matrix for X-ray measurements.

The crystal was mounted on a glass fiber and analyzed on a Rigaku AFC6R X-ray diffractometer. Unit-cell parameters were derived from least-squares refinement with the setting angles of 19 automatically centered reflections in the range $30.0 < 2\theta < 36.0°$. Intensity data were collected at room temperature by using the ω-scan technique with a rate = 16° (ω)/min and peak widths = 1.50 + 0.30 tan θ. The cell constants and Laue symmetry m1 correspond to the trigonal system. The intensity data were collected over the range of indices $-6 \le h \le 6$, $0 \le k \le 6$, $-65 \le l \le 65$ to $2\theta_{max} = 60°$. From 2009 measured reflections, a total of 1361 were observed [$F_0^2 > 3\sigma(F^2)$]. The intensities of three standard reflections varied by an

average of 3% during the data collection.

The structure was solved and refined by using programs from the TEXSAN crystallographic software package (6) on a μ-VAX-II computer. The crystal exhibits the systematic conditions hkl: -h+k+l = 3n, hl: l = 2n. The space group Rc(h) has been chosen on the basis of the distribution of intensities and the successful solution and refinement of the structure. The atoms Ca and Al were located by using the direct methods program SHELXS (7). The remaining atoms were placed following analysis of difference electron density maps. After full-matrix, least-squares refinement of the model with isotropic displacement coefficients on each atom, an absorption correction was applied by using the program DIFABS (8) (transmission factors = 0.80 - 1); the data were then averaged (R_{int} = 0.06.) Final refinement with 274 averaged reflections and anisotropic displacement coefficients on each atom resulted in the residuals R = 0.024 and wR = 0.032. The largest peak in the final difference electron-density map corresponds to 2.1% of the Ca atom. Relevant crystallographic data and atomic parameters are listed in Table 6.1; anisotropic displacement coefficients are summarized in Table 6.2.

Table6.1 Crystallographic Data and Atomic Parameters for $CaAl_2(BO_3)_2O$.

a = 4.810(6) A, c = 46.633(5) Å, space group Rc(h) (no. 167), Z = 6

formula wt. = 227.66 u, $\mu = 6.23\ cm^{-1}$, $\rho_{calc} = 1.214\ g\ cm^{-1}$

274 averaged reflections, 19 variables, R =0.024, wR = 0.032

atom	x	y	z	B_{eq}
Ca	0	0	0	0.92(2)
Al	0	0	0.21426(1)	0.74(2)
O1	0.0310(2)	0.6274(2)	0.03158(2)	1.07(3)
O2	0	0	1/4	1.82(6)
B	0	0	0.13424(6)	0.81(5)

$$\beta_{eq}=8\frac{\Pi^2}{3}\sum_i\sum_j U_{ij}a_i^*a_j^*a_ia_j$$

Table 6.2 Anisotropic Displacement Coefficients for $CaAl_2(BO_3)_2O$.

atom	U_{11}	U_{22}	U_{33}	U_{12}	U_{13}	U_{23}
Ca	0.0116(3)	0.0116	0.0120(4)	0.0058	0	0
Al	0.0094(3)	0.0094	0.0093(4)	0.0047	0	0
O1	0.0100(5)	0.0121(5)	0.0175(5)	0.0049(4)	0.0016(3)	0033(3)
O2	0.030(1)	0.030	0.010(1)	0.015	0	0
B	0.0105(7)	0.0105	0.010(1)	0.005	0	0

Results and Discussion

The structure (Figure 6.1) of the title compound $CaAl_2(BO_3)_2O$ contains layers of planar BO_3 groups that are linked through Ca atoms in CaO_6 distorted octahedra and Al atoms in Al_2O_7 groups. The latter group is characterized by a linear Al-O2-Al interaction, where the unique O2 atom is bound only to the two Al atoms. The structure may also be described as a stacking of layers of $[Al_2B_2O_7]^{2-}$ blocks along the *c* axis in the sequence ABCABC . . . (*cf.* Figure 6.1a)

Selected interatomic distances and angles are listed in Table 6.3. The Ca atom is surrounded by six O1 atoms at the vertices of a distorted octahedron - site symmetry S_6. The Ca-O distance, 2.381(2) Å, is normal, and the O1-Ca-O1 angle, 94.22(6)°, is consistent with a small trigonal elongation of the octahedron. The distorted tetrahedral AlO_4 group exhibits C_3 point-group symmetry with three Al-O1 distances of 1.775(2) Å and one Al-O2 distance of 1.666(1) Å. These lengths are reflected in the angles O1-Al-O1, 103.56(5)°, and O1-Al-O2, 114.88(4)°. The B-O distance, 1.370(2) Å, in the trigonal BO_3 group is normal.

The linear Al-O2-Al columns are similar to those found in the ionic conductor Na^+ β-alumina (8). In the structure of this material (Figure 6.1b), spinel-type blocks are joined through linear Al-O-Al sticks. Planes of the linearly bound O atoms are spaced by approximately 11 Å along the *c* axis through the spinel blocks. In $CaAl_2(BO_3)_2O$, spacing of these O planes along the c axis is only 7.8 Å (*cf.* Figure 6.1a). In both $CaAl_2(BO_3)_2O$ and

β-alumina, the two-dimensional packing pattern and fraction of the two-coordinate

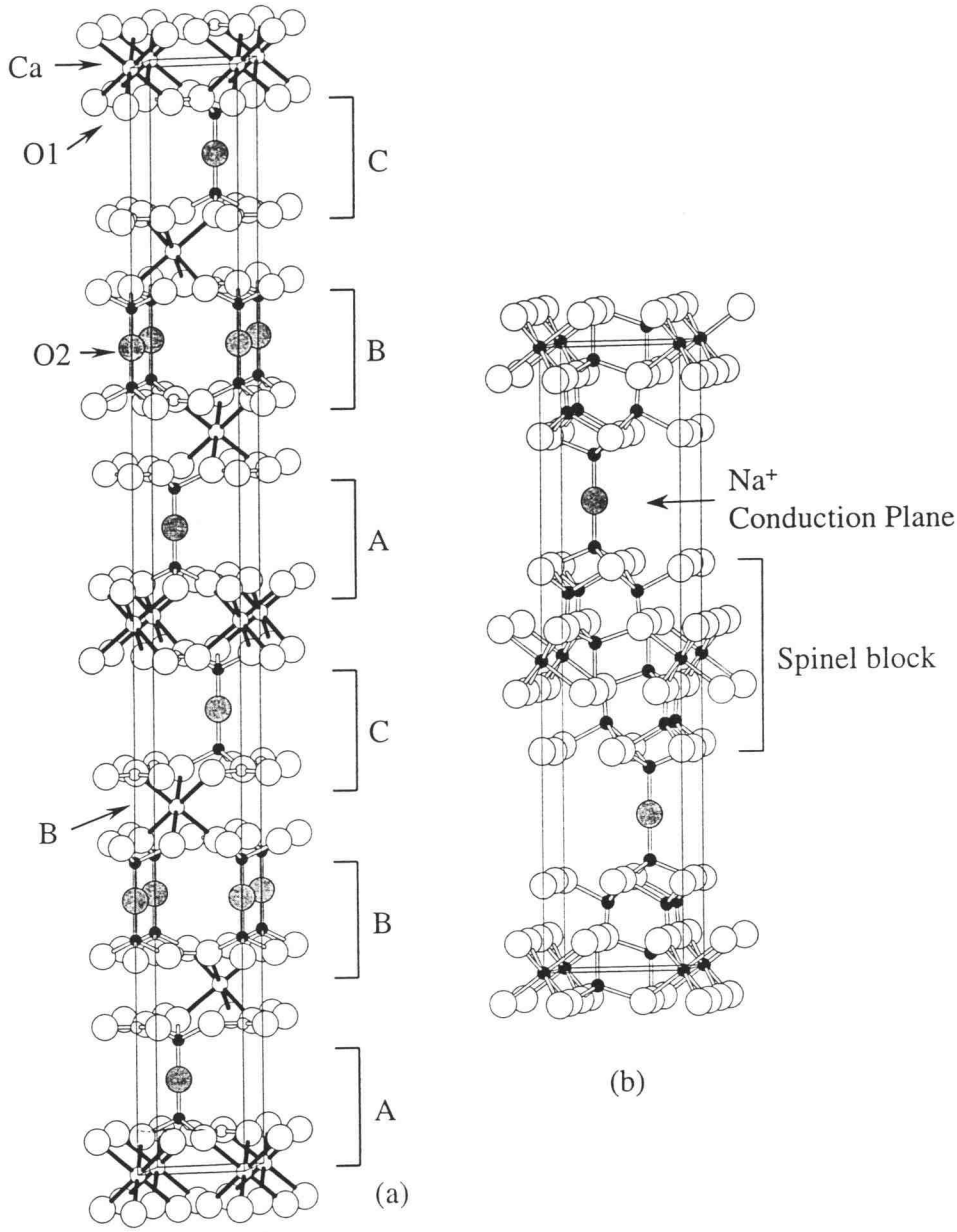

Figure 6.1 Crystal Structures of (a) $CaAl_2(BO_3)_2O$ and (b) Na^+-alumina.

O atoms in a given *ab* plane are identical. The packing density, however, is much higher in $CaAl_2(BO_3)_2O$ than in Na^+ β-alumina. For β-alumina, a = 5.69 Å, while for $CaAl_2(BO_3)_2O$, a = 4.8 Å. As a result, the two-dimensional packing density for $CaAl_2(BO_3)_2O$ is nearly 30% greater than that for Na^+ β-alumina.

Like Na^+ β-alumina, we have found that Na^+ ions can be substituted into sites within the planes of the linearly coordinated O atoms of $CaAl_2(BO_3)_2O$. This has been accomplished through charge compensation according to the formula $Ca_{1-x}Na_{2x}Al_2(BO_3)_2O$. As seen in Figure 6.2, substitution of Na^+ at x = 0.01, produces substantial changes in the powder X-ray diffraction pattern. The intensity of the strong reflection near 34.5° for $CaAl_2(BO_3)_2O$, for example, greatly diminishes with Na incorporation, whereas a new, strong reflection appears near 31°. The pattern for the phase containing Na can be indexed on the basis of a primitive hexagonal cell having a *c* axis that is approximately one-third that of $CaAl_2(BO_3)_2O$. In the Na phase, the packing of the $[Al_2B_2O_7]^{2-}$ layers is ABAB . . . (9), rather than the ABCABC . . . pattern of $CaAl_2(BO_3)_2O$. The cell parameters and space group $P6_322$ for the Na phase are consistent with the results previously reported by Schäfer and Kuzel for the α phase of $CaAl_2(BO_3)_2O$. We should also note that the diffraction pattern for the Na phase (Figure 6.2, bottom) is consistent with the data given on card no. 19-205 of the JCPDS Powder Diffraction File, which is labeled as α-$CaAl_2(BO_3)_2O$. High-purity reagents should be used for the preparation of

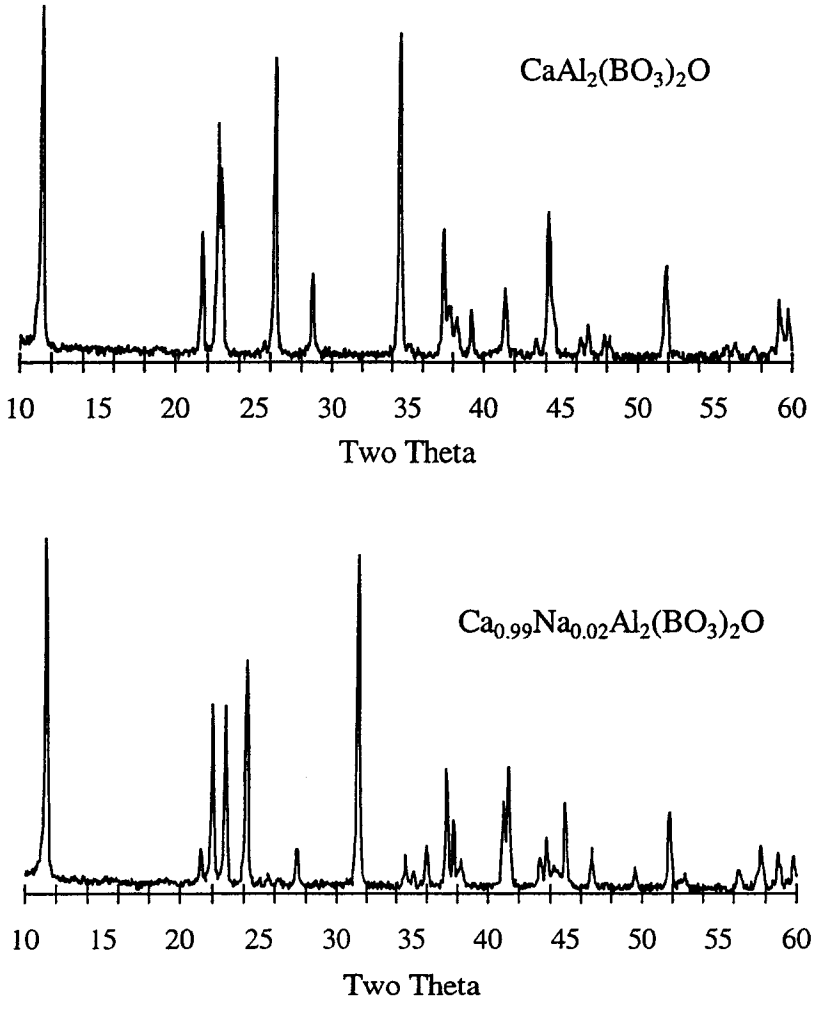

Figure 6.2 Top) Powder X-ray diffraction trace of $CaAl_2(BO_3)_2O$.
Bottom) Powder X-ray diffraction trace of $Ca_{0.99}Na_{0.02}Al_2(BO_3)_2O$.

Table 6.3 Selected Interatomic Distances and Angles for $CaAl_2(BO_3)_2O$.

Interatomic Distances (Å)		Interatomic Angles (°)	
Ca-O1(x 6)	2.381(2)	O1-Ca-O1	94.22(6)
Al-O1(x 3)	1.775(2)	O1-Al-O1	103.56(5)
Al-O2	1.6665(7)	O1-Al-O2	114.88(4)
B-O1(x 3)	1.370(2)	O1-B-O1	120

$CaAl_2(BO_3)_2O$; reagents containing low levels of Na impurities could lead to its incorporation and production of the altered structure.

The results of the structure determination also provide some insight into the small thermal expansion coefficient, 15 x 10^{-7}/°C, that has been reported by MacDowell (2). Two-coordinate bridging O atoms have been shown to be important for the negative thermal expansion in materials of the type ZrW_2O_8 and HfW_2O_8 (10). Here, transverse Zr(Hf)-O-W vibrations coupled with librations of the constituent metal-centered polyhedra and the cubic symmetry leads to isotropic thermal contraction. Similar processes may occur in the title compound, particularly along the *c* axis. Because the material is not isotropic, however, an overall small expansion is observed. Structural studies of the material at various temperatures are currently underway.

CONCLUSIONS

The borate oxide $CaAl_2(BO_3)_2O$ crystallizes in a unique structure containing $[Al_2B_2O_7]^{2-}$ layers with linear Al-O-Al sticks. While these sticks are reminiscent of those observed in Na^+ β-alumina, their much higher packing density may greatly limit ionic conduction. The low thermal-expansion coefficient may also derive from the presence of the two-coordinate O atoms.

ACKNOWLEDGMENTS

This work was supported by the National Science Foundation, Solid-State Chemistry Program. KSC thanks the Korean Air Force for a fellowship.

REFERENCES

1. V. L. Schäfer and H. J. Kuzel, Neues Jahrb. Mineral., Monatsh, 131 (1967).

2. J. F. MacDowell, *J. Am. Ceram. Soc.***73**, 2287 (1990).

3. H. You and G. Hong, *Mat. Res. Bull.* **32**, 78 (1997).

4. D. A. Keszler, *Curr. Opinion in Solid State & Mat. Sci.* **1**, 204 (1996).

5. K. Yvon, W. Jeitschko, and E. Parthe, *J. Appl. Cryst.* **73**, 10 (1977).

6. TEXSAN, Structure Analysis Package, Molecular Structure Corp., MSC 3200A, Research Forest Drive, The Woodlands, TX 77381.

7. G. M. Sheldrick, In Crystallographic Computing 3, G. M. Sheldrick, C. Krüger, and R. Goddard, Eds.; Oxford Univ. Press, Oxford, U. K., 1985, p 175.

8. N. Walker and D. Stuart, Acta Crystallogr., Sect. A **39**, 158 (1983).

9. K. S. Chang, Ph.D. dissertation, Oregon State University (1998); results to be published.

10. J. S. O. Evans, T. A. Mary, T. Vogt, M. A. Subramanian, and A. W. Sleight, *Chem.Mater.* **8**, 2809 (1996).

CHAPTER 7

SYNTHESIS, STRUCTURE, AND LUMINESCENCE OF $SrGa_2(B_2O_5)O_2$

Ki-Seog Chang and Douglas A. Keszler

To be submitted to Journal of Solid State Chemistry, **1998**

Abstract

The pyroborate oxide $SrGa_2(B_2O_5)O_2$ has been prepared and its structure determined by single-crystal X-ray diffraction methods. It crystallizes in the orthorhombic space group Cmcm (Z = 4) with unit-cell parameters a = 11.695(2), b = 8.351(1), c = 5.6916(5) Å, and V = 555.8 $Å^3$. The structure was determined from 386 unique reflections and refined to the final residuals R = 0.0206 and R_w = 0.0268. Pyroborate, B_2O_5, groups are linked by Sr-centered distorted trigonal prisms and Ga-centered distorted tetrahedra. Optical emission and excitation spectra are reported for undoped samples.

Introduction

Borates have long been important for the production of a variety of glasses. The glass-forming regions of alkaline-earth metal (Ca, Sr, Ba) aluminum borate systems were recently examined by MacDowell.[1] The materials of primary interest center near the 1 : 1 : 1 molar ratio of MO (M = Sr, Ba, or Ca) : Al_2O_3 : B_2O_3 where the glass - ceramics were highly crystalline. Results of an investigation of the Li_2O - Ga_2O_3 - B_2O_3 ternary system by DTA, X-ray phase analysis, and IR spectroscopy were also reported.[2] Crystal structure of di-strontium aluminum borate $Sr_2Al_2B_2O_8$ with R = 0.163 was reported by Nagai, T. and Ihara, M.[3] We have also recently synthesized and identified the compound $Sr_2Al_2B_2O_8$ with R = 0.059 as a new luminescent materials. The structure consists of 6-coordinated Sr atoms, AlO_4 tetrahedrons, and BO_3 triangles.

We also describe the undoped luminescence of $SrGa_2(B_2O_5)O_2$.

Experimental Section

Synthesis and Crystal Growth

A crystalline powder sample of $SrGa_2(B_2O_5)O_2$ is easily prepared by heating a stoichiometric mixture of the reagents $Sr(NO_3)_2$ (AESAR, reagent grade), Ga_2O_3 (Alfa, 99.999%), and B_2O_3 (Alfa, 99.98%). The mixture is heated in a Pt crucible at 893 K for 1 h, cooled and ground at room temperature, and again heated in a Pt crucible at 1173 K for 8 h. The powder diffraction pattern of the material, obtained with a Philips diffractometer, matches that generated from the results of the single-crystal study (*vide infra*) and the computer program LAZY-PULVERIX.[4] A crystal of $SrGa_2(B_2O_5)O_2$ was grown in a Pt crucible from a melt corresponding to the molar ratios 1 SrO : 1 Ga_2O_3 : 1.05 B_2O_3. The melts were cooled from 1293 to 873 K at 0.1 K/min, then 5 K/min to room temperature. A clear, colorless crystal of approximate dimensions 0.3 × 0.3 × 0.2 mm was physically separated from the matrix for X-ray measurements.

Crystallographic Study

The crystal was mounted on a glass fiber and analyzed on a Rigaku AFC6R X-ray diffractometer. Unit-cell parameters were derived from least-squares refinements with the setting angles of 23 automatically-centered reflections in the range of $30.0 < 2\theta < 36.0°$. Intensity data were collected at room temperature by using the ω-scan technique with a rate = 16.0°(ω)/min and peak widths = 1.60 + 0.30 tanθ. The cell constants and Laue symmetry *mmm* correspond to the

orthorhombic system. The intensity data were collected over the range of indices $0 \leq h \leq 16$, $0 \leq k \leq 14$, $-7 \leq l \leq 7$. From 1791 measured reflections, a total of 386 were observed [$F_0^2 > 3\sigma(F^2)$]. The intensities of three standard reflections were monitored throughout data collection; average fluctuations were 3.0%.

The atomic parameters were determined by using programs of the TEXSAN crystallographic software package[5] on a μ-VAX-II computer. The crystals exhibit systematic absences **hk0**: h+k = 2n+ 1 and **h0l**: l = 2n+1 that are consistent with the space group Cmcm. The atoms Sr and Ga were located by using the direct methods program SHELXS.[6] The remaining atoms were placed following analysis of difference electron density maps. After full-matrix, least-squares refinement of the model with isotropic displacement coefficients on each atom, an absorption correction was applied by using the program DIFABS.[7] The data were then averaged (R_{int} = 0.037). Final refinement with anisotropic displacement coefficients on each atom resulted in the residuals R = 0.0206 and R_w = 0.0268. Relevant crystallographic data, absorption characteristics, and final residuals are listed in Table 7.1. Atomic positional parameters and displacement coefficients are listed in Tables 7.2 and 7.3, respectively. The largest peak in the final difference electron density map corresponds to 1.84 % of a Sr atom.

Table 7.1 Crystallographic Data for $SrGa_2(B_2O_5)O_2$

chemical formula	$SrGa_2B_2O_7$
formula weight, u	360.68
Crystal system	orthorhombic
space group	Cmcm (No.63)
a	11.695(2) Å
b	8.351(1) Å
c	5.6916(5) Å
V	555.8(2) $Å^3$
Z	4
ρ_{calc}, g/cm^{-3}	4.310
F_{000}	664
radiation	Mo Kα (λ = 0.71069 Å) graphite monochromated
temperature, K	296
scan type	ω-2θ
scan rate, ° in ω	16
sin θ_{max}/λ	1.50
linear absorption coeff, cm^{-1}	188.59
transmission factors	0.80 - 1.14
secondary extinction coefficient	0.374×10^{-6}
total no. measured data	1791
no. observations	
$F_0^2 \geq 3\sigma(F_0^2)$	386
$R(F_o)^a$	0.021
$R_w(F_o)^b$	0.027
p factor	0.03
goodness of fit	1.177
maximum shift/error in final cycle	0.006

[a] $R = \Sigma \, | \, |F_o| - |F_c| \, | \, / \, \Sigma \, |F_o|$

[b] $R_w = [\, \Sigma w (\, |F_o| - |F_c| \,)^2 / \Sigma \, w \, |F_o|^2 \,]^{1/2}$

Table 7.2. Atomic Parameters for $SrGa_2(B_2O_5)O_2$

atom	x	y	z	β_{eq}^*
Sr	0	0.1884(2)	1/4	0.60(3)
Ga	0.2911(1)	0.4153(1)	1/4	0.43(3)
O1	0.1294(7)	0	0	0.6(1)
O2	0.1290(7)	0.4335(9)	1/4	1.2(1)
O3	-0.1989(8)	0.304(1)	1/4	1.0(1)
O4	0	-0.338(2)	1/4	1.5(2)
B	0.107(1)	0.595(2)	1/4	0.8(2)

$$*\beta_{eq}=8\frac{\Pi^2}{3}\sum_i\sum_j U_{ij}a_i^* a_j^* a_i a_j$$

Table 7.3. Anisotropic displacement coefficients for $SrGa_2(B_2O_5)O_2$

Atom	U_{11}	U_{22}	U_{33}	U_{12}	U_{13}	U_{23}
Sr	0.0130	0.0062	0.0088	0	0	0
Ga	0.0097	0.0066	0.0048	-0.0010	0	0
O1	0.0100	0.0119	0.0059	0	0	0
O2	0.0098	0.0102	0.0078	0	0	0
O3	0.0076	0.0158	0.0171	0	0	0
O4	0.0039	0.0070	0.0347	0	0	0
B	0.0143	0.0117	0.0030	0	0	0

Solid Solution

Samples in the solid-solution series $SrGa_{2-x}Al_x(B_2O_5)O_2$ were prepared by heating appropriate mixtures of the reagents $SrCO_3$, Ga_2O_3, Al_2O_3(Alfa, 99.999%), and B_2O_3. The mixtures were heated in Pt crucibles at 893 K for 1 h, cooled and ground at room temperature, and again heated in a Pt crucible at 1173 K for 22 h. X-ray powder diffraction patterns of the products were obtained with a Philips diffractometer. The peak positions were corrected by using an internal silicon powder standard, and unit-cell constants were calculated by using the least-squares computer program ***POLSQ***.[8]

Results and Discussion

Crystal Structure

A drawing of the contents of a unit cell for $SrGa_2(B_2O_5)O_2$ is given in Figure 7.1. The structure is characterized by a framework composed of layers B_2O_5 groups that extend in the ab plane and chains of vertex-sharing GaO_4 groups that extend along the c axis. (Figure 7.2) Sr atoms occupy distorted trigonal prismatic voids within the framework. Except for a shared O1···O2 edge between the Sr and Ga atoms, the metal-centered polyhedra share only vertices.

Selected interatomic distances and angles are listed in Table 7.4. The Sr atom is surrounded by four O1 and two O2 atoms in a distorted trigonal prismatic site, point group C_{2v}. (Figure 7.3) The interatomic Sr-O distances vary from 2.570(1) to 2.585(8) Å, averaging 2.580 ± 0.037 Å; the mean distance is comparable to the 2.52 Å length from calculated Shannon radii.[9] The O-Sr-O angles are 66.7(7), 71.6(5), and 106.9(1) ° for O1-Sr-O1 angles, 97.9(6) and 145.6(6) ° for O1-Sr-O2 angles, and 71.8(9) ° for O2-Sr-O2 angle. The O-O distances are 2.845(8) and 3.027(1) Å for O1-O1 and 3.054(6) and 3.211(7) Å for O1-O2. The GaO_4 group exhibits anion has distorted tetrahedral symmetry, point group C_s. The Ga-O distances - two at 1.840(7) Å for Ga-O1, 1.902(4) Å for Ga-O2, and 1.836(1) Å for Ga-O3 distance - are normal. The O-Ga-O angles are 101.2(5)° for O1-Ga-O1 angle, 118.1(8)° for O1-Ga-O2 angle, 110.5(9)° for O1-Ga-O3 angle, and 98.2(2)° for O2-Ga-O3 angle. All of the atoms of the B2O5 group lie in a mirror plane orthogonal to the c axis; the overall symmetry is C_{2v}. The B-O distances and O-B-O angles are normal (cf., Table 7.4) The central B-O4-B angle adopts an

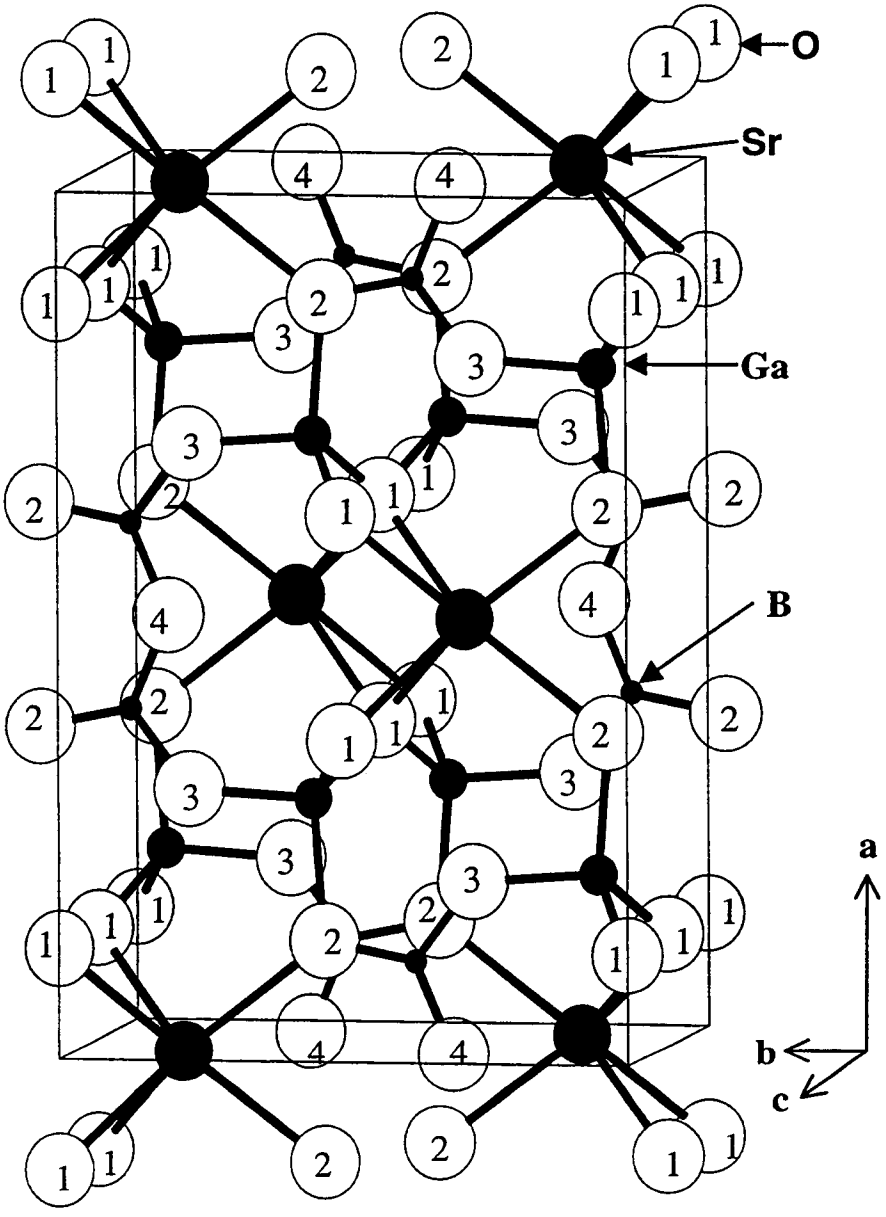

Figure 7.1 Drawing of the unit cell of $SrGa_2(B_2O_5)O_2$.

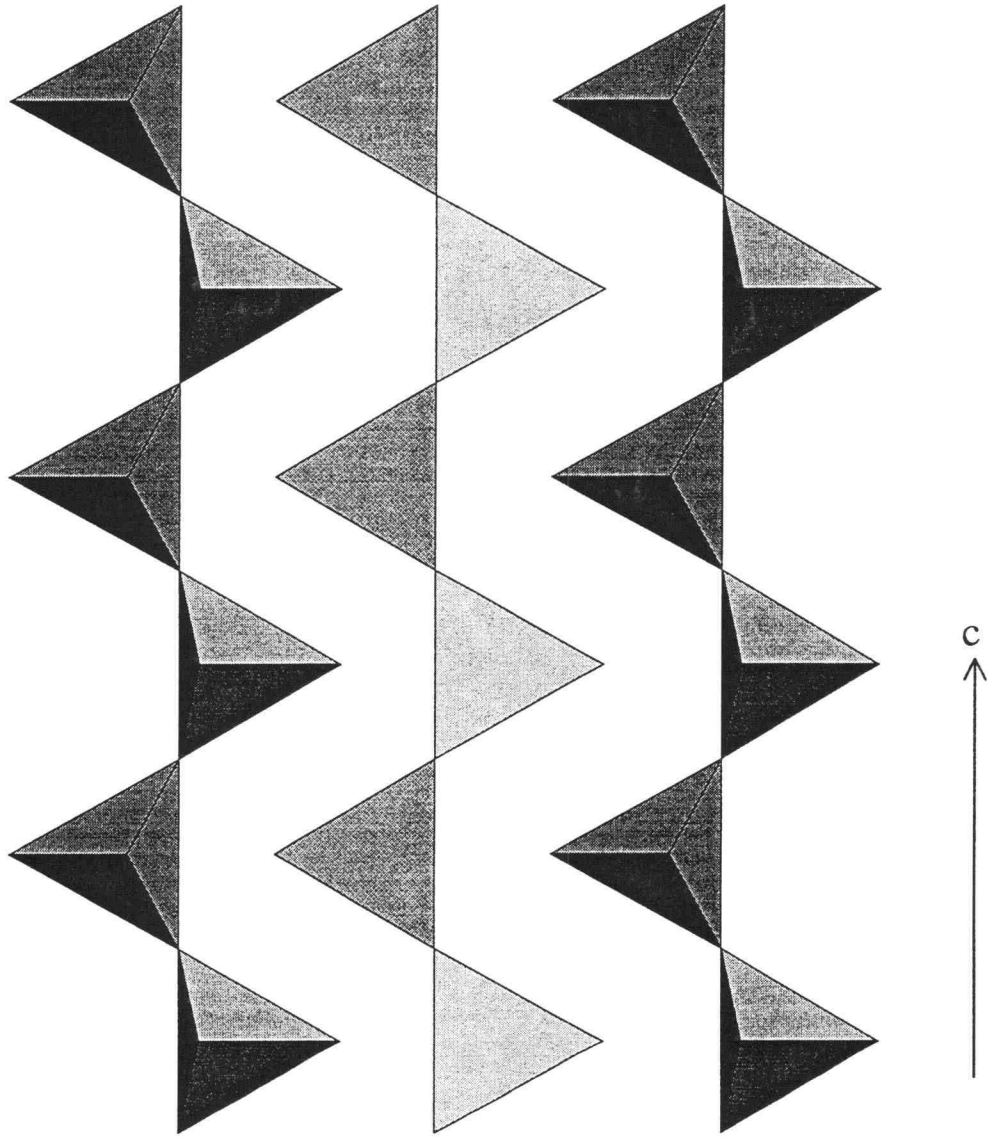

Figure 7.2 Drawing of the tetrahedral chains of Ga_2O_7 group as viewed along the c-axis

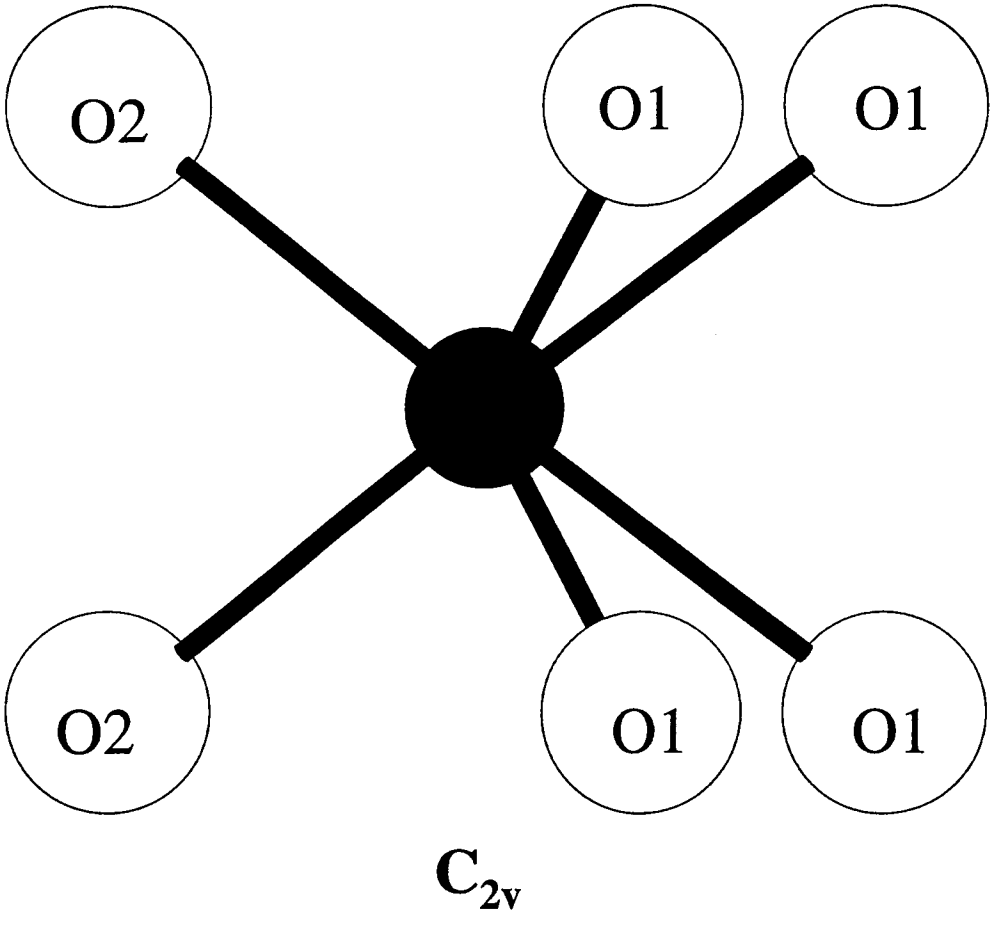

Figure 7.3 The Sr-centered trigonal prism in $SrGa_2(B_2O_5)O_2$.

intermediate, 132° (Figure 7.4), in comparison to values in other pyroborates that span the range 112-180.10

Solid Solutions

The formula $SrGa_2(B_2O_5)O_2 \equiv SrGa_2B_2O_7$ mimicks that of the known compound $SrAl_{x2}B_2O_7 \equiv SrAl_{x2}(BO_3)_2O$. While the structures of these two materials differ, limited solubilities of Al on the Ga sites in $SrGa_2B_2O_7$ and Ga on the Al sites in (V/Z) ration $SrAl_2B_2O_7$ are to be expected. Results from powder X-ray diffraction measurements covering the entire range $SrGa_{2-x}Al_xB_2O_7$ ($0 \leq x \leq 2$) are summarized in Figure 7.5. As seen from the steady decrease in unit-cell volume/Z (Z = the number of formula in the unit-cell) for x = 0 to ~1, a complete solid solubility of Al in $SrGa_2(B_2O_5)O_2$ exists in this range. As x decreases in the range 2 - 1.3, the V/Z ratio increases with partial substitution of Ga atoms on the Al site in $SrAl_2B_2O_7$. In the range 1 - 1.35, V/Z ratios remain constant, representing an equilibrium between the saturated Al form of $SrAl_2B_2O_7$ (x = 0.0) and (x = 0.7). We also observe a positive deviations from Vegard's law in the ranges $0 \leq x \leq 1.0$ and $1.3 \leq x \leq 2$, consistent with the general behavior for nonmetallic solid solutions.

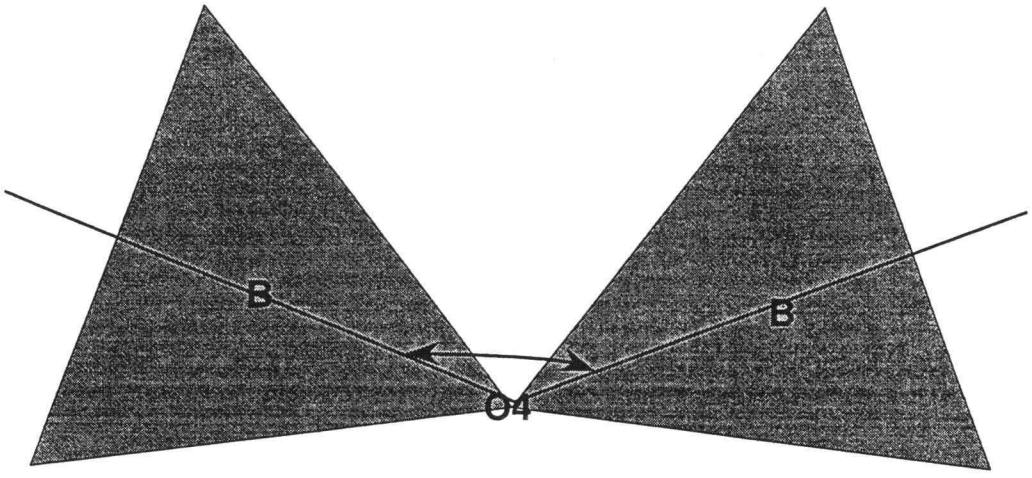

$\angle$ BO4B = 132(1)°

Figure 7.4 Polyhedral drawing of the isolated B_2O_5 group as viewed perpendicular to the c axis.

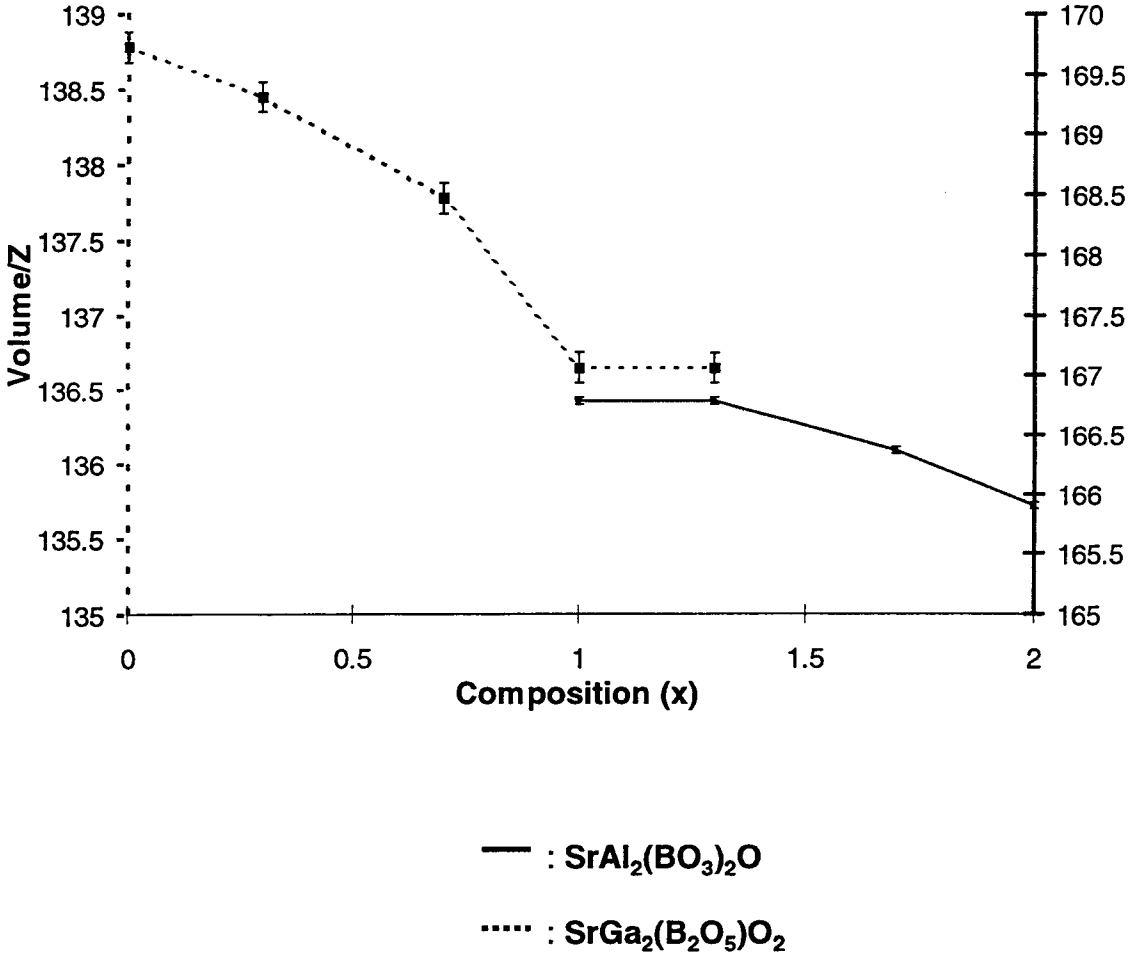

Figure 7.5 Graph of the unit-cell parameters of a solid solution system $SrAl_xGa_{2-x}B_2O_7$.

Table 7. 4. Selected Interatomic Distances (Å) and Angles (°) for $SrGa_2(B_2O_5)O_2$

Interatomic Distances (Å)		Interatomic Angles (°)	
Sr-O1(X4)	2.585(8)	O1-Sr-O1	66.7(7), 71.6(5), 106.9(1)
Sr-O2(X2)	2.570(1)	O1-Sr-O2	97.9(6), 145.6(6)
		O2-Sr-O2	71.8(9)
Ga-O1(X2)	1.840(7)	O1-Ga-O1	101.2(5)
Ga-O2	1.902(4)	O1-Ga-O2	118.1(8)
Ga-O3	1.836(1)	O1-Ga-O3	65.9(0), 82.0(6), 82.5(6), 110.5(9), 167.0(5)
		O2-Ga-O3	60.6(9), 71.6(7), 98.2(2)
B-O2	1.375(4)	O2-B-O2	74.5(8), 84.3(0), 92.4(4)
B-O3	1.361(3)		165.9(4)
B-O4	1.370(8)	O2-B-O3	88.9(8), 117.3(8), 168.0(3)
		O2-B-O4	49.8(5), 96.6(1), 124.4(4)
		O3-B-O4	118.1(8)

Table7.5 Lifetimes and maximum peak positions of the series $SrGa_{2-x}Al_xB_2O_7$

Composition (x)	Lifetime (ns)	Max. Peak(nm)	Phase
0	97	433	$SrGa_2(B_2O_5)O_2$
0.3	98	433	$SrGa_2(B_2O_5)O_2$
1.7	110	411	$SrAl_2(BO_3)_2O$
1.94	250	393	$SrAl_2(BO_3)_2O$

Luminescence

Under short-wavelength UV excitation, the title compound produces a bright blue-white emission. Luminescence excitation and emission spectra for this compound and Ga-doped sample of $SrAl_2(BO_3)_2O$ are given in Figure 7.6. As seen in this figure, the emission for the title compound peaks near 434 nm with a low-energy tail that extends through the greater portion of the visible region of the spectrum. The Ga^{3+}-doped sample of $SrAl_2(BO_3)_2O$ exhibits a much sharpen emission feature peaking near 393 nm. Additional data on luminescence lifetimes and wavelengths of maximum emission are summarized in Table 7.5.

Although d^{10} ions are generally not considered to be luminescent ions, their emission properties have been known for some time.[11] The gallium compounds $LnGa_3B_4O_{12}$ (Ln = Y, Sm, Eu, Gd, Tb, or Dy) exhibit a very broad emission band with a maximum near 450 nm. The emission has been ascribed to transitions within

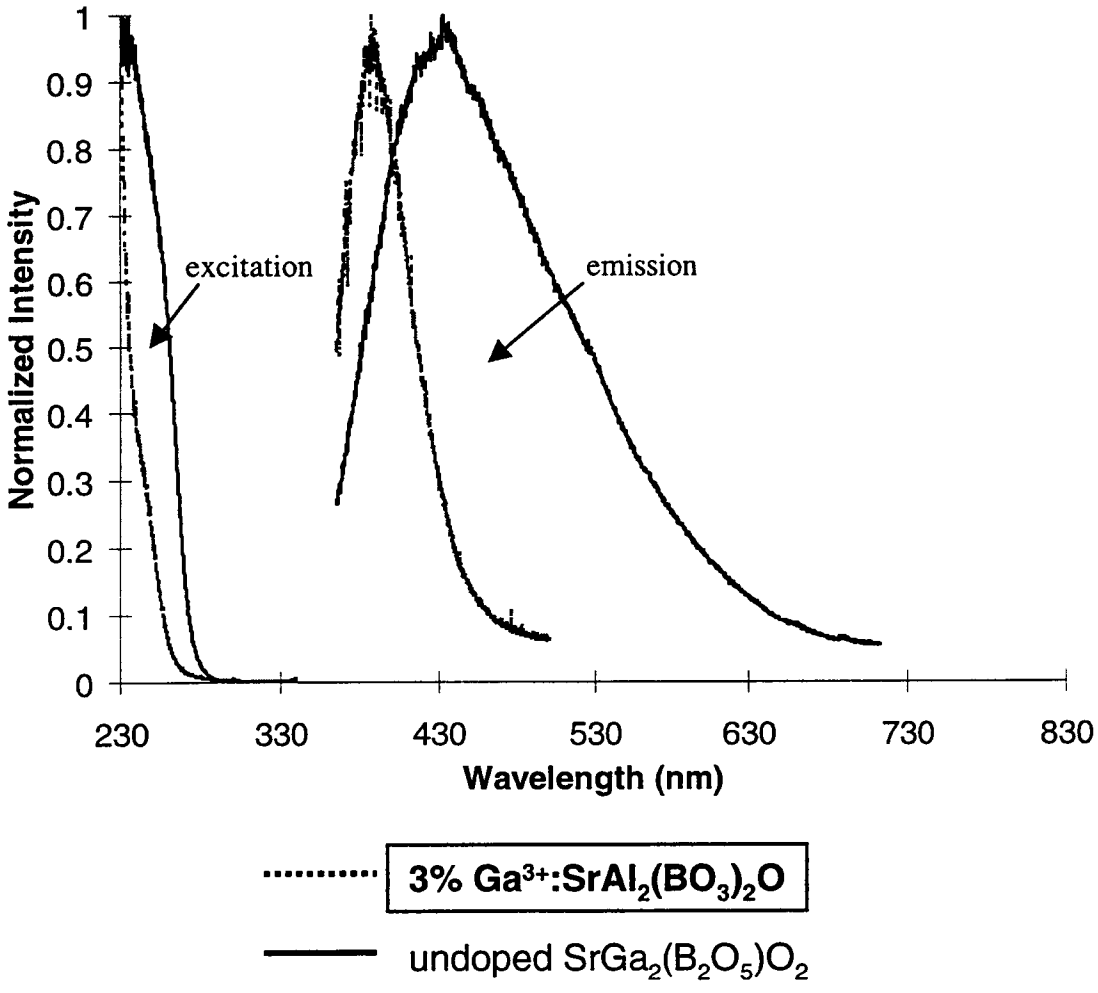

Figure 7.6 Excitation and emission spectra of the intrinsic luminescence of the undoped $SrGa_2(B_2O_5)O_2$ and 3% Ga^{3+}: $SrAl_2(BO_3)_2O$.

the GaO_6 octahedron. The possibility of emission from other defects or from an s, p-type conduction band has also been considered. Since emission from Sm, Eu, Tb, and Dy is not observed in these materials, it is clear that energy transfer from the GaO_6 group to the lanthanide ion is not very efficient.[12] The compound $MgGaBO_4$ also exhibits a blue luminescence under excitation by cathode rays with a maximum emission at 420 nm. Like the series $LnGa_3(BO_3)_4$, the Ga atom in this compound also occupies a distorted octahedral site.[13] The title compound appears to represent the first example of intrinsic emission from a borate containing distorted GaO_4 groups.

Acknowledgments

This research was supported by the National Science Foundation, Solid State Chemistry Program. We want to thank Dr. Diaz and Prof. Nibler for assistance with the lifetime measurement. KSC is grateful to the Korean Air Force for a graduate fellowship.

References

1. MacDowell, J. F., *J. Am. Ceram. Soc.*, **1990**, 73(8) 2287.

2. Abdullaev, G. K.; Rza - Zade, K. S., *Russian J. Inorg. Chem.*, **1984**, 29(9), 1365.

3. Nagai, T.; Ihara, M., *Yogyo - Kyokai - Shi*, **1972**, 80(11), 14.

4. Yvon, K.; Jeitschko, W.; Parthe, E., *J. Appl. Cryst.*, **1977**, *10*, 73.

5. TEXSAN, Structure Analysis Package, Molecular Structure Corp., MSC 3200A, Research Forest Drive, the Woodlands, TX 77381.

6. Sheldrick, G. M. In Crystallographic Computing 3; Sheldrick, G.M.; Krüger, C.; Goddard, R.; Eds.; Oxford Univ. Press, Oxford, U. K., **1985**, p 175.

7. Walker, N.; Stuart, D., *Acta Crystallogr.*, Sect. A **1983**, 39, 158

8. POLSQ: Least Squares Unit Cell Refinement, David Cahen, (1973).

9. Shannon, R. D., *Acta Crystallogr.*, **1976**, sect. A, 32, 751.

10. Thompson, P. D.; Huang, J.; Smith, R. W.; Keszler, D. A., *J. Solid State Chem.*, **1991**, 93, 430.

11. Blasse, G., *Chem. Phys. Letters*, **1990**, 175(3), 237.

12. Blasse, G.; Bril, A., *J. Inorg. Nucl. Chem.*, **1967**, 29, 266.

13. Blasse, G., *J. Inorg. Nucl. Chem.*, **1970**, 32, 700.

CHAPTER 8

SYNTHESIS AND STRUCTURE OF $Li_2Al(BO_3)O$ AND $LiAlB_2O_5$

Ki-Seog Chang and Douglas A. Keszler

To be submitted to J. Solid State Chem., **1997**

Abstract

The structures of the borate oxide $Li_2Al(BO_3)O$ and the pyroborate $LiAlB_2O_5$ have been established by single-crystal X-ray diffraction methods. The former crystallizes in the monoclinic space group $P2_1/c$ ($Z = 4$) with unit-cell parameters $a = 6.247(2)$, $b = 5.0562(9)$, $c = 10.258(2)$ Å, $\beta = 95.83(3)°$, and $V = 322.3(3)$ Å^3, and the latter forms in the monoclinic space group $C2/c$ ($Z = 8$) with unit-cell parameters $a = 9.903(1)$, $b = 10.052(1)$, $c = 9.347(1)$ Å, $\beta = 120.07(1)°$, and $V = 805.2(2)$ Å^3. The structure of $Li_2Al(BO_3)O$ was determined from 1037 unique reflections and refined to the final residuals $R = 0.036$ and $wR = 0.050$. It is characterized by an association of B_2O_5 pyroborates, two LiO_4 tetrahedra, and AlO_4 tetrahedra. The structure of $LiAlB_2O_5$ was determined from 2477 unique reflections and refined to the final residuals $R = 0.035$ and $wR = 0.044$. It is characterized by an association of two B_2O_5 pyroborate groups, one LiO_4 tetrahedron, and one AlO_4 tetrahedron.

Materials index: Lithium, Aluminum, Borate.

Introduction

The compound $Li_2Al(BO_3)O$ was first studied by Kim and Hummel (1). The $2Li_2O \cdot Al_2O_3 \cdot B_2O_3$ mixture, located within the non-glass-forming region of the ternary system Li_2O - Al_2O_3 - B_2O_3, melted at 870 ± 20°C according to differential thermal analysis. The compound $LiAlB_2O_5$ was also formed by Abdullaev et. al (2), with a melting point of 850°C. Its characteristic infrared bands are at the following approximate wavelengths: 1200, 1100, 770, 725, 630, 570, 525, 480, and 420 cm^{-1}. These show, according to Weir and Schroeder (3), that the boron atoms in this compound are three - coordinate as the boron oxygen radical $[B_2O_5]^{4-}$ of two triangles connected by common oxygen vertices.

Experimental

Synthesis and Crystal Growth

Powders of $Li_2Al(BO_3)O$ and $LiAlB_2O_5$ were prepared from stoichiometric mixture of the reagents Li_2CO_3 (Cerac, 99.99), Al_2O_3 (Alfa, 99.999%), and B_2O_3 (Alfa, 99.98%). The mixtures were heated in Pt crucibles at 893 K for 1 h, cooled and ground at room temperature, and again heated in the same crucibles at 1003 K for 12 h. X-ray powder diffraction patterns of the products, obtained with a Philips diffractometer, matched those generated with the computer program LAZY-PULVERIX (4) and the results of the single-crystal X-ray study (*vide infra*). Single crystals of $Li_2Al(BO_3)O$ were grown from a stoichiometric melt that was cooled from 1193 to 800 K at 4 K/h, and then 300 K/h to room temperature. A clear, colorless crystal of dimensions 0.6 mm × 0.1 mm × 0.3 mm was physically separated from the matrix for X-ray measurements. Single crystals of $LiAlB_2O_5$ were obtained from a stoichiometric melt by cooling from 1173 to 800 K at 4 K/h, and then 300 K/h to room temperature. A clear, colorless crystal of dimensions 0.15 mm × 0.07 mm × 0.1 mm was physically separated from the matrix for X-ray measurements.

X-ray Work

A crystal of $Li_2Al(BO_3)O$ was mounted on a glass fiber and analyzed on a Rigaku AFC6R X-ray diffractometer. Unit-cell parameters were derived from least-squares refinement with the setting angles of 25 automatically centered reflections in the range $30 < 2\theta < 36°$. Intensity data were collected at room temperature by

using the ω-2θ scan technique with a rate = 16.0°(ω)/min and peak widths = 1.50 + 0.30 tanθ. The cell constants and Laue symmetry *2/m* correspond to the monoclinic system. The intensity data were collected over the range of indices 0 ≤ h ≤ 8, 0 ≤ k ≤ 7, and -14 ≤ l ≤ 14 to $2\theta_{max}$ = 60.0°. From 1121 measured reflections, a total of 817 unique reflections were observed [$F_0^2 > 3\sigma(F^2)$]. The intensities of three standard reflections were monitored throughout data collection; average fluctuations were 3.0%.

The structure was solved and refined by using programs from the TEXSAN crystallographic software package (5) on a μVAX-II computer. The crystal exhibits the systematic absences h0l: l = 2n + 1 and 0k0: k = 2n + 1, consistent with thespace group $P2_1/c$. The Al atom was located by using the direct methods program SHELXS (6), and the remaining atoms were placed from analysis of difference electron density maps. After full-matrix, least-squares refinement of the model with isotropic displacement coefficients on each atom, an absorption correction was applied by using the program DIFABS (7). The data were then averaged (R_{int} = 0.061). Final refinement with anisotropic displacement coefficients on each atom resulted in the residuals R = 0.036 and wR = 0.050. The largest peak in the final difference electron density map corresponds to 3.5% of the Al atom.

A crystal of $LiAlB_2O_5$ was also mounted on a glass fiber and analyzed on the same diffractometer. Unit-cell parameters were derived from least-squares refinement of the setting angles of 21 automatically centered reflections in the range of 30 < 2θ < 36°. Intensity data were collected at room temperature by using

the ω-2θ scan technique with a rate = 16.0°(ω)/min and peak widths = 1.50 + 0.30 tanθ. The cell constants and Laue symmetry *2/m* correspond to the monoclinic system. The intensity data were collected over the range of indices $0 \leq h \leq 13$, $0 \leq k \leq 14$, and $-13 \leq l \leq 13$ to $2\theta_{max} = 60.0°$. From 2603 measured reflections, a total of 873 unique reflections were observed [$F_0^2 > 3\sigma(F^2)$]. The intensities of three standard reflections were monitored throughout data collection; average fluctuations were 3.0%.

The systematic absences hkl: h + k = 2n + 1 and h0l: l = 2n + 1 are consistent with space group C2/c. The Al atom was located by using the direct methods program SHELXS (6), and the remaining atoms were placed following analysis of difference electron density maps. After full-matrix, least-squares refinement of the model with isotropic displacement coefficients on each atom, an absorption correction was applied by using the program DIFABS (7). The data were subsequently averaged ($R_{int} = 0.071$), and final refinement with anisotropic displacement coefficients on each atom except for Li atoms, Li1 and Li2, resulted in the residuals R = 0.036 and wR = 0.050. The largest peak in the final difference electron density map corresponds to 2.5% of the Al atom. Relevant crystallographic data and atomic parameters for the two structures are listed in Tables 1, 2, 3, and 4, respectively.

Table 8.1Crystallographic Data for $Li_2Al(BO_3)O$ and $LiAlB_2O_5$

chemical formula	$Li_2Al(BO_3)O$	$LiAlB_2O_5$
formula weight, u	115.671	135.540
Crystal system	monoclinic	monoclinic
space group	$P2_1/c$ (No. 14)	C2/c (No. 15)
a	6.247(2) Å	9.903(1) Å
b	5.056(1) Å	10.052(1) Å
c	10.258(2) Å	9.347(1) Å
β	95.83(3)°	120.07(1)°
V	322.3(3) $Å^3$	805.2(2) $Å^3$
Z	4	8
ρ_{calc}, gcm^{-3}	2.161	1.014
F(000)	196	588
radiation	Mo Kα (λ = 0.71069 Å) graphite monochromated	
temperature, K	296	
scan type	ω-2θ	
scan rate, ° in ω	16	
sin θ_{max}/λ	1.22	
linear absorption coeff, cm^{-1}	4.23	5.08

Table 8.1 (Continued)

secondary extinction coefficient	0.333×10^{-7}	-----
total data	1037	2477
obsvd data, $F_o^2 \geq 3\sigma(F_o^2)$	817	873
$R(F_o)$[a]	0.036	0.035
$wR(F_o)$[b]	0.050	0.044
p factor	0.03	0.03
GOF	2.12	1.277
Δ/σ	0.07337	0.05466

---

[a] $R = \Sigma \, | \, |F_o| - |F_c| \, | \, / \, \Sigma \, |F_o|$

[b] $wR = [\, \Sigma w (\, |F_o| - |F_c| \,)^2 / \Sigma \, w \, |F_o|^2 \,]^{1/2}$

Table 8.2 Positional parameters and β_{eq} for $Li_2Al(BO_3)O$

atom	x	y	z	β_{eq}*
Al	-0.0021(1)	0.1454(1)	0.15932(5)	0.77(2)
O1	-0.0974(2)	-0.1475(3)	0.2153(1)	1.01(5)
O2	-0.1988(2)	0.3008(3)	0.0522(1)	1.20(5)
O3	0.2340(2)	0.0868(3)	0.0802(1)	0.92(5)
O4	-0.4475(2)	0.2984(3)	-0.1392(1)	1.11(5)
B	-0.2971(3)	0.1757(4)	-0.0583(2)	0.83(7)
Li1	0.3978(6)	0.3609(7)	0.2114(4)	1.6(1)
Li2	-0.2723(6)	-0.3336(7)	0.0714(3)	1.2(1)

$$*\beta_{eq}=8\frac{\Pi^2}{3}\sum_i\sum_j U_{ij}a_i^* a_j^* a_i \cdot a_j$$

Table 8.3 Positional parameters and β_{eq} for $LiAlB_2O_5$

atom	x	y	z	β_{eq}*
Al	0.19510(8)	0.15209(7)	0.15156(9)	0.85(2)
O1	0.1866(2)	0.1075(2)	-0.0315(2)	1.11(5)
O2	0.3789(2)	0.2054(2)	0.3128(2)	1.09(5)
O3	0.1574(2)	0.0166(2)	0.2436(2)	1.27(5)
O4	0.3585(2)	-0.0724(2)	0.0174(2)	1.36(5)
O5	0.0565(2)	0.2764(2)	0.1069(2)	1.20(5)
B1	0.2317(3)	0.0059(3)	-0.0934(3)	1.00(7)
B2	0.4317(3)	0.1710(3)	0.4716(3)	0.99(7)
Li1	0	0.3799(7)	1/4	1.9(1)
Li2	0	-0.1608(7)	1/4	1.6(1)

$$*\beta_{eq}=8\frac{\Pi^2}{3}\sum_i\sum_j U_{ij}a_i^* a_j^* a_i a_j$$

Table 8.4 Anisotropic Displacement Coefficients for $LiAlB_2O_5$

ATOM	U_{11}	U_{22}	U_{33}	U_{12}	U_{13}	U_{23}
Al	0.0109(3)	0.0109(3)	0.0110(3)	0.0016(3)	0.0058(3)	0.0004(3)
O1	0.0152(8)	0.0124(8)	0.0158(8)	0.0042(6)	0.0088(7)	0.0003(6)
O2	0.0131(7)	0.0148(8)	0.0136(7)	-0.0019(6)	0.0068(6)	0.0026(6)
O3	0.0166(8)	0.0152(8)	0.0133(8)	-0.0045(7)	0.0052(7)	0.0013(6)
O4	0.0189(9)	0.0184(9)	0.0131(7)	0.0104(7)	0.0071(7)	0.0005(7)
O5	0.0136(8)	0.0168(9)	0.0133(7)	0.0065(7)	0.0054(7)	0.0014(6)
B1	0.011(1)	0.013(1)	0.016(1)	0.002(1)	0.008(1)	0.000(1)
B2	0.011(1)	0.012(1)	0.015(1)	-0.000(1)	0.007(1)	0.001(1)
Li1	0.024(1)					
Li2	0.020(1)					

Results and Discussion

Structure

As seen in Figure 8.1, the structure of $Li_2Al(BO_3)O$ is built from BO_3 triangles and distorted LiO_4 and AlO_4 tetrahedra. The BO_3 groups are loosely packed in planes that stack parallel to (101) (cf., Figure 8.2). The BO_3 groups bridge the Li and Al atoms through O atoms, O2, O3, and O4. In addition to binding a B atom, atom O2 is shared one Al and Li2; O3 is shared by one Al and Li2; and O4 is shared by one Li2 and two Li1. Atom O1 is unique in not binding to the B atom - it binds one Li1, one Li2, and two Al. The distorted AlO_4 tetrahedra O1 atoms to form an $(AlO_3)_\infty^1$ chain (Figure 8.3) that extends along the *b* axis. The presence of the unique O1 atom leads to the more descriptive formulation of this material as the borate oxide - $Li_2Al(BO_3)O$.

The interatomic distances and angles listed as Table 5 are consistent with previously observed values (8). The range of distances for a given metal-O interaction is consistent with the unique coordination environment of each O atom. Hence, the valence (9, 10) of each atom has been computed to be within 4% of commonly accepted integral values.

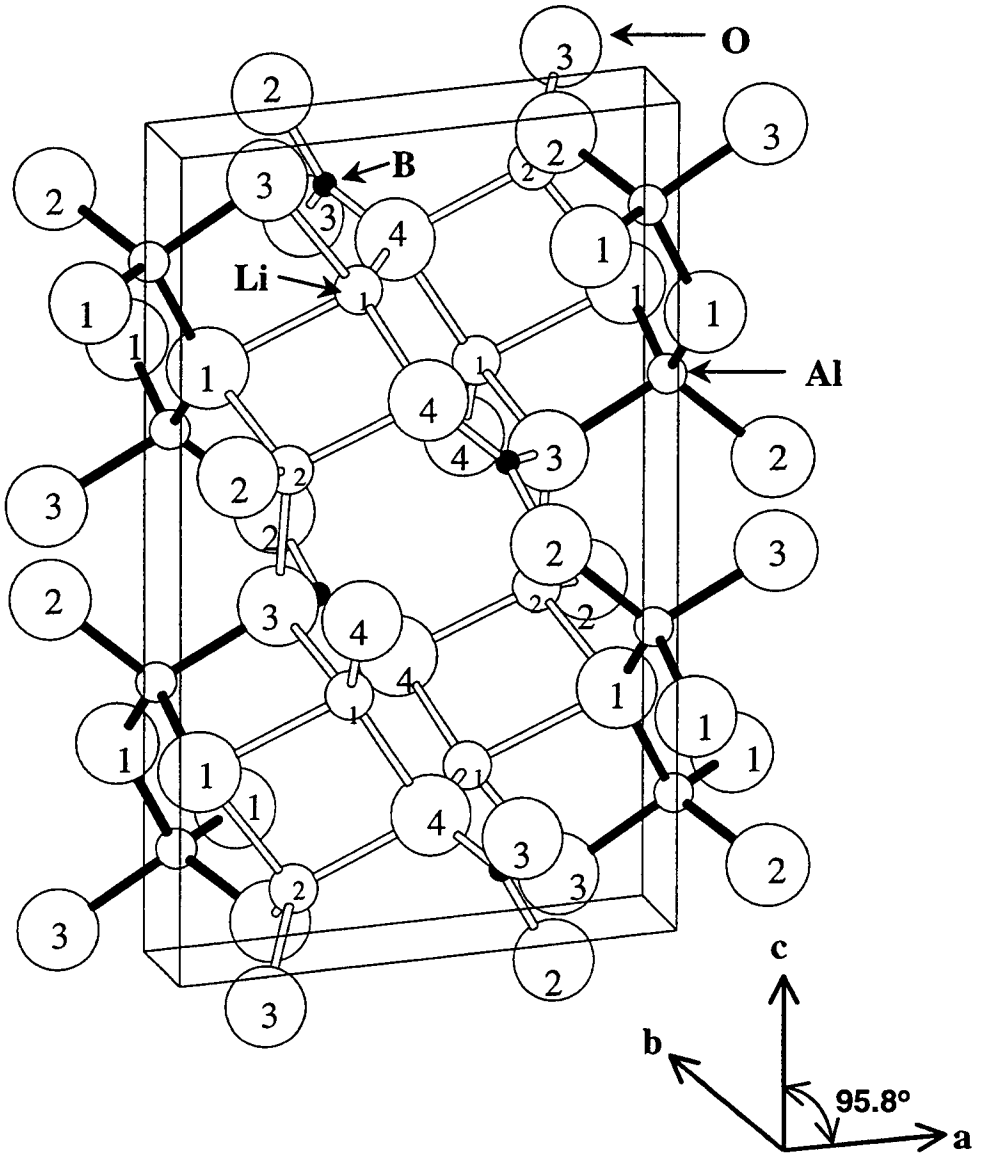

Figure 8.1 Drawing of the unit cell of $Li_2Al(BO_3)O$.

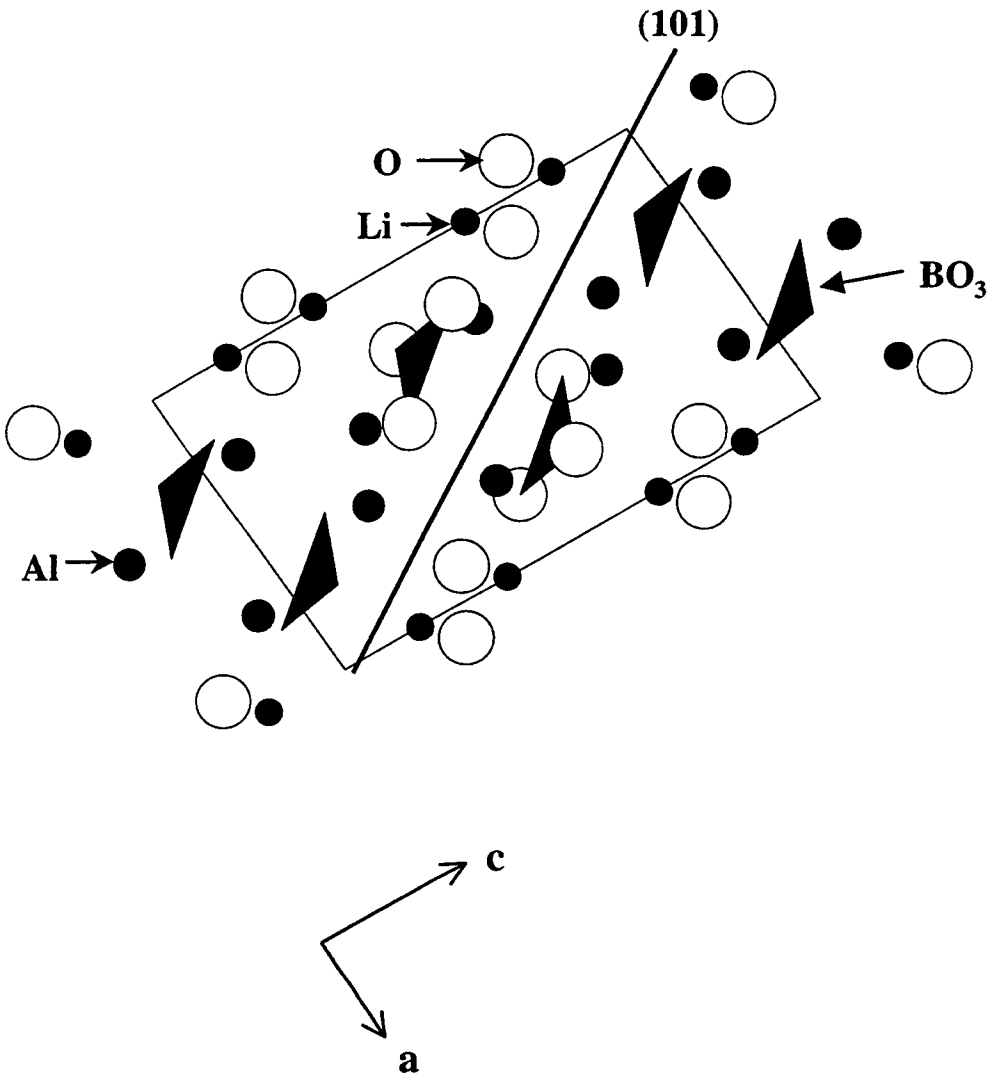

Figure 8.2 The triangular BO_3 groups of $Li_2Al(BO_3)O$ are loosely packed in distorted planes that stack along (101).

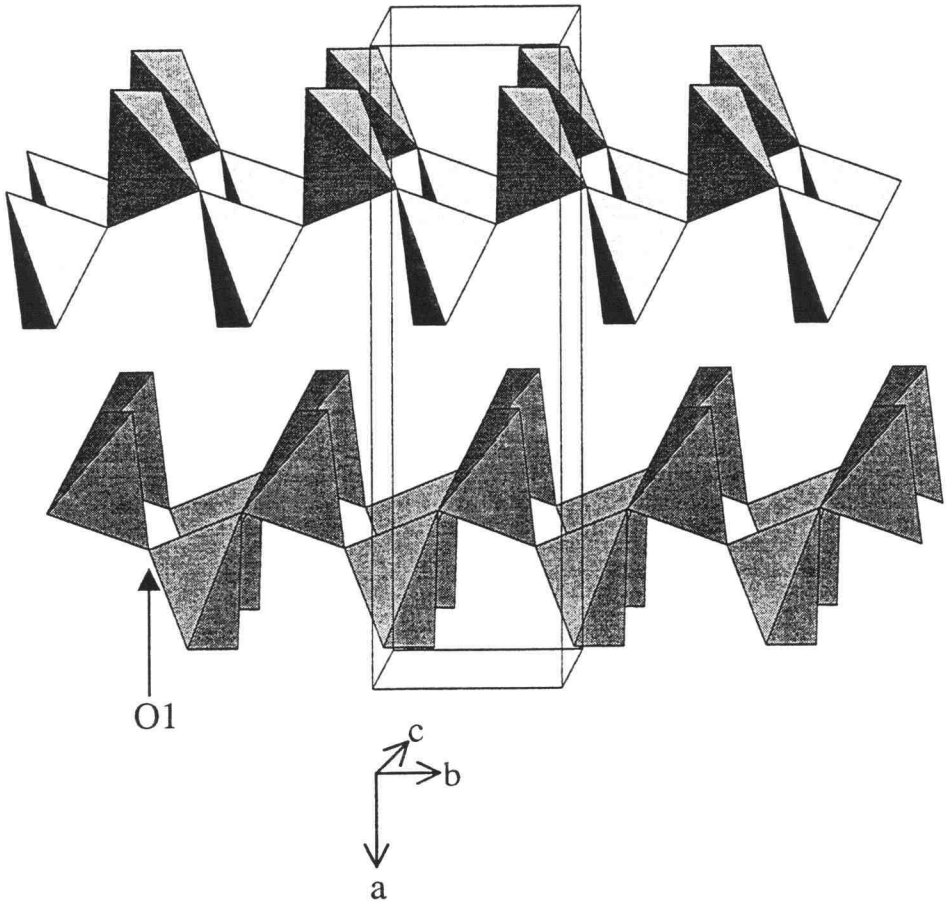

Figure 8.3 The distorted AlO_4 terahedra share atom O1 to an (AlO_3) chain that extends along the b axis in $Li_2Al(BO_3)O$.

Table 8.5 Selected Interatomic Distances (Å) and Angles (°) for $Li_2Al(BO_3)O$

Interatomic Distances (Å)		Interatomic Angles (°)	
Al-O1(×2)	1.721(2)	O1-Al-O1	111.87(7), 112.66(4)
Al-O2	1.750(2)	O1-Al-O2	110.63(7)
Al-O3	1.779(2)	O1-Al-O3	100.88(7), 109.93(7)
		O2-Al-O3	110.49(7)
B-O2	1.386(3)	O2-B-O3	116.9(2)
B-O3	1.409(2)	O2-B-O4	121.3(2)
B-O4	1.341(3)	O3-B-O4	121.8(2)
Li1-O1	2.091(4)	O1-Li1-O3	79.8(1)
Li1-O3	2.122(4)	O1-Li1-O4	95.9(2), 110.1(2)
Li1-O4(×2)	1.909(4)	O3-Li1-O4	114.0(2), 115.4(2)
		O4-Li1-O4	127.1(2)
Li2-O1	1.982(4)	O1-Li2-O2	114.5(2)
Li2-O2	1.920(4)	O1-Li2-O3	100.4(2)
Li2-O3	2.027(4)	O1-Li2-O4	97.9(2)
Li2-O4	1.956(4)	O2-Li2-O3	117.8(2)
		O2-Li2-O4	110.8(2)
		O3-Li2-O4	113.3(2)

Condensation of AlB_2O_7 rings in $LiAlB_2O_5$, which is similar to condensation of B_3O_7

The structure of $LiAlB_2O_5$ has layers of isolated pyroborate B_2O_5 groups and tetrahedral LiO_4 and AlO_4 groups. The common feature of simple borate structures is shown in Figure 8.4. The structure contains two type of B atoms, two 4-coordinate Li atoms, and a 4-coordinate Al atom. A isolated pyroborate B_2O_5 groups with 6d connected to Al-centered oxygen tetrahedron chains. The isolated B_2O_5 groups also bridged to Li-centered oxygen tetrahedrons.

The interatomic distances and angles listed as Table 6 are consistent with previously observed values (8). The range of distances for a given metal-O interaction is consistent with the unique coordination environment of each O atom.

The contents of the unit cell of $LiAlB_2O_5$ are depicted in Figure 8.4. The structure is a new type comprising distoted tetrahedral LiO_4 and AlO_4 groups and $AlBO_3$ triangles. Like many polyborates, the structure may described as the condensation product of simple ring system. The ring, AlB_2O_7(Figure 8.5), is comprised of one AlO_4 groupand two fused BO_3 groups. As such, it is a direct analog of the B_3O_7 rings found in the materials LiB_3O_5(9), CsB_3O_5(10), $SrLi(B_3O_5)_3$(11), $Na_4Li(B_3O_5)_5$(12), $CsLi(B_3O_5)_2$(13). The Al atom is simply substituted for the B atom on the four-coordinate site. In all of these systems, the rings condense via the four terminal O atoms to give the observed formulas $AlB_2O_3O_{4/2} \equiv AlB_2O_5$ and $B_3O_3O_{4/2} \equiv B_3O_5$.

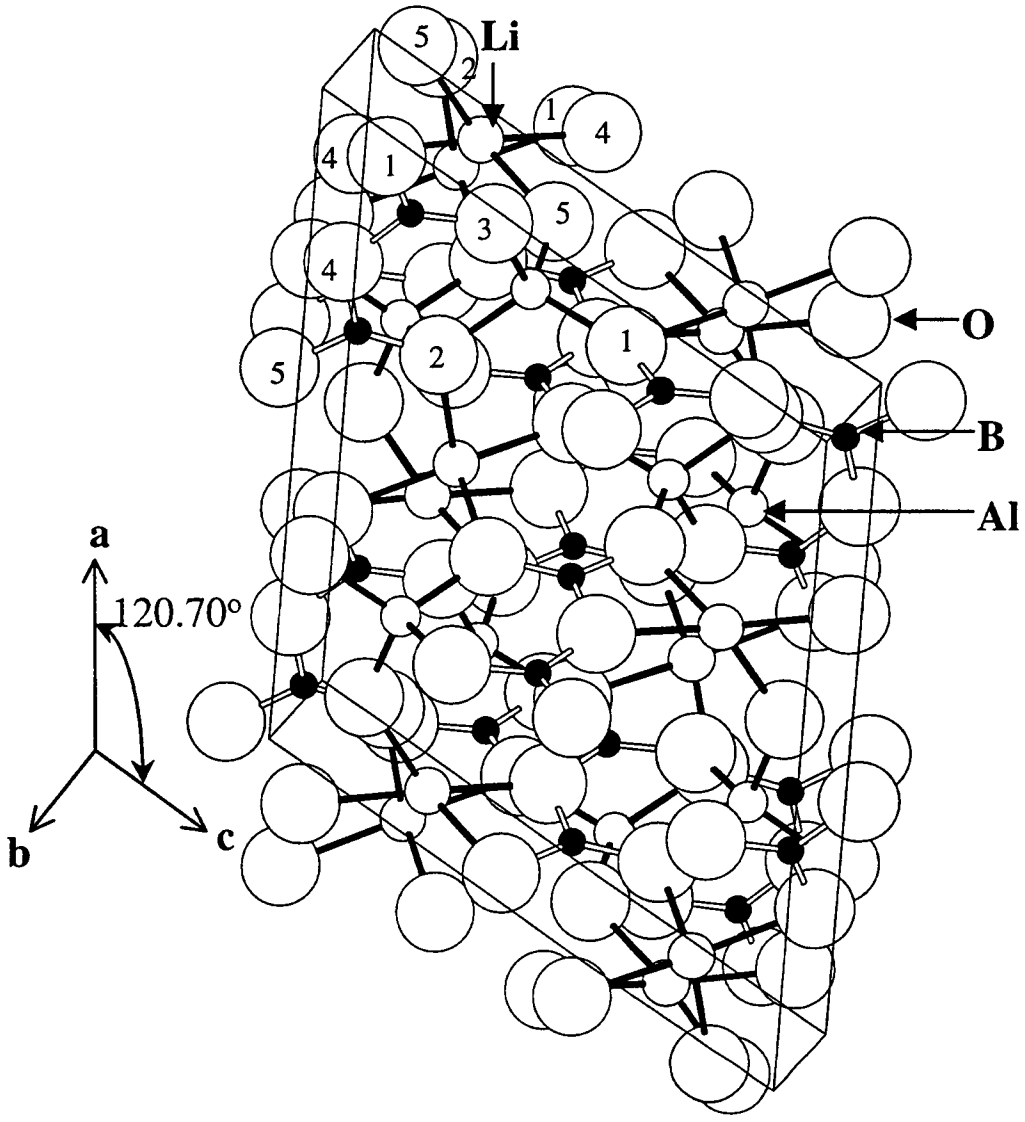

Figure 8.4 Drawing of the unit cell of $LiAlB_2O_5$

Table 8.6 Selected Interatomic Distances (Å) and Angles (°) for $LiAlB_2O_5$

Interatomic Distances (Å)		Interatomic Angles (°)	
Al-O1	1.729(2)	O1-Al-O2	116.20(8)
Al-O2	1.767(2)	O1-Al-O3	111.60(9)
Al-O3	1.748(2)	O1-Al-O5	107.83(8)
Al-O5	1.745(2)	O2-Al-O3	101.49(8)
		O2-Al-O5	109.72(9)
		O3-Al-O5	109.84(9)
B1-O1	1.355(3)	O1-B1-O3	120.2(2)
B1-O3	1.339(3)	O1-B1-O4	118.2(2)
B1-O4	1.402(3)	O3-B1-O4	121.6(2)
B2-O2	1.349(3)	O2-B2-O4	122.5(2)
B2-O4	1.414(3)	O2-B2-O5	126.5(2)
B2-O5	1.356(3)	O4-B2-O5	111.0(2)
Li1-O4(×2)	1.967(2)	O4-Li1-O4	151.8(4)
Li1-O5(×2)	1.984(4)	O4-Li1-O5	126.0(1), 70.60(8)
		O5-Li1-O5	116.8(4)
Li2-O1(×2)	2.023(2)	O1-Li2-O1	149.3(4)
Li2-O2(×2)	2.073(5)	O1-Li2-O2	104.5(1), 95.3(1)
		O2-Li2-O2	99.1(3)

Pyroborates containing the unit B_2O_5 that consists of two triangles joined by a common oxygen atom. The pyroborate group consists of two joined BO_3 triangles sharing one corner oxygen and the boron atoms are in the plane defined by the three surrounding oxygens. Triborates are containing B_3O_7 rings that comprise pyroborate-two triangular BO_3 and one tetrahedral BO_4 group. The pyroborate groups of triborates, LiB_3O_5, $SrLi(B_3O_5)_3$, $Na_4Li(B_3O_5)_5$, $CsLi(B_3O_5)_2$, were found with a oxygen bond angle of the central B-O-B system. The oxygen bond angles were 118.8(5)° in LiB_3O_5, 118.0(3)° and 120.4(3)° in $Na_4Li(B_3O_5)_5$, 120.2(6)° in $SrLi(B_3O_5)_3$, and 124.0(4)° in $CsLi(B_3O_5)$. In the title compound $LiAlB_2O_5$, the B1-O4-B2 angle is 125.1(2)° (Figure 8.5). According to the atomic radii of metals this angle is common.

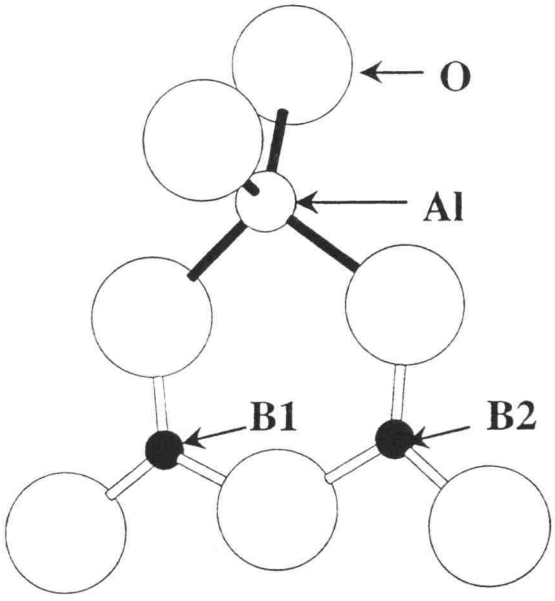

$$\angle B1O4B2 = 125.1(2)^{o}$$

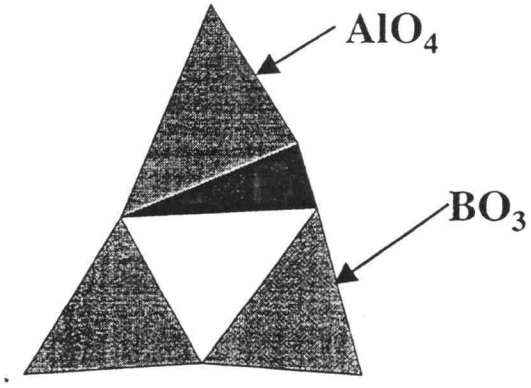

$$B_3O_{3+4/2} \rightarrow AlB_2O_{3+4/2}$$

Figure 8.5 Drawing of the B1-O4-B2 angle and the ring AlB_2O_7 group in the $LiAlB_2O_5$, which is similar to condensation of B_3O_7.

Acknowledgments

This work was supported by the National Science Foundation, Solid State Chemistry Program.

References

1. Kim, K. H.; Hummel, F. A., *J. Amer. Ceram. Soc.*, **45**, 487 (1962).

2. Abdullaev, G. K., Rzade, P. F.; Mamedov, Kh. S., *Russ. J. Inorg. Chem.*, **28(3)**, 428 (1983).

3. Weir, C. E.; Schrooder, R. A., *J. Res. Nat. Bur. Stand.*, **68A**, 465 (1964).

4. Yvon, K.; Jeitschko, W.; Parthe, E., *J. Appl. Cryst.* **10**, 73 (1977).

5. ***TEXSAN***, Structure Analysis Package, Molecular Structure Corp., MSC 3200A, Research Forest Drive, the Woodlands, TX 77381.

6. Sheldrick, G. M., In *Crystallographic Computing 3*; Sheldrick, G.M.; Krüger, C.; Goddard, R.; Eds.; Oxford Univ. Press, Oxford, U. K., 175 (1985).

7. Walker; Stuart, *Acta Crystallogr., Sect. A,* **39**, 158 (1983).

8. Shannon, R. D., *Acta Crystallogr., Sect. A,* **32**, 751 (1976).

9. Konig, V. H.; Hoppe, R., *Z. Anorg. Allg. Chem.,* **439**, 71 (1978).

10. Krogh-Moe, J., *Acta Crystallogr.,* **13**, 889 (1960).

11. Schaffers, K. I., Ph.D. Thesis, Oregon state University (1992).

12. Tu, T., Ph.D. Thesis, Oregon state University (1996).

13. Tu, J.; Keszler, D. A., *Mat. Res. Bull.*, **30**, 209 (1995).

BIBLIOGRAPHY

Aalst, W. V.; Hollander, J. D.; Peterse, A. M.; and Wolff, P. M. *Acta Crystallogr.,* **1976**, Sect. B, *32*, 47.

Akella, A., Ph.D. Thesis, Oregon State University, **1996**.

Akella, A.; Tu, J.; Keszler, D. A.,to be sumitted to *Inorg. Chem.* **1995**.

Alekel III, T. Ph.D. Thesis, Oregon State University, **1993**.

Bordui, P. F., *Annu. Rev. Mater. Sci.,* **1993**, *23*, 321.

Blasse, G.; Bril, A.; Vries, J. de., *J. Electrochem. Soc.: Solid State Science*, **1968**, *115(9)*, 977.

Blasse, G.; Grabmaier, B. C., *Luminescent Materials,* Springer-Verlag, **1994**.

Brese, N. E.; O'Keeffe, M. *Acta Crystallogr.* Sect. B, **1991**, *47*,192.

Chen, C.; Wang, Y.; Xia, Y.; Wu, B.; Tang, D.; Wu, K.; Wenrong, Z.; Yu, L., *J. Appl. Phys.*, **1995**, 77, 2268--2272

Chen, C.; Wang, Y.; Wu, B.; Wu, K.; Zeng, W.; Linhua, Y., *Nature*, **1995**, 373, 322--324

Chen, C.; Liu, G. *Ann. Rev. Mater. Sci.,* **1985**, *16*, 203.

Chen, C.; Wu, B.; Jiang, A.; You, G. *Sci. Sin., Ser B* **1985**, *28*, 235.

Chen, C.; Wu, Y.; Li, R. *J. Crystal Growth,* **1990**, *99*, 790.

Chen, C.; Wu, Y.; Jiang, A.; Wu, B.; You, G. *J. Opt.Soc.Am.* **1989**, B *6(4)*, 616.

De Villiers, J. P. R., *American Mineralogist,* **1971**, *56*, 758.

Diaz, A., Ph.D. Thesis, Oregon State University, **1997**.

Diaz, A; Keszler, D. A., *Mat. Res. Bull.***1996**, 31, 147.

Dirksen, G. J.; Blasse, G. *J. Solid State Chem.*, **1991**, *92*, 591.

Dubbeldam, G. C.; Wolff, P. M. *Acta Crystallogr.,* **1969**, *25*, 2665.

BIBLIOGRAPHY (Continued)

Eckardt, R. C.; Masuda, H.; Fan, Y. X.; Byer, R. L. *IEEE J. Quantum Electron.* **1990**, *26*, 922.

Eimerl, D.; Davis, L.; Velsko, S.; Graham, E. K.; Zalkin, A. *J. Appl. Phys.* **1987**, *62*, 1968.

Fan, S.; Shen, G.; Wang, W.; Li, J.; Le, X. *J. of Crystal Growth,* **1990**, *99*, 811.

Fouassier, C.; Latourrette, B.; Portier, J.; Hagenmuller, P., *Mat. Res. Bull.,* **1976**, *11*, 933.

Franken, P.; Hill, A.; Peters, C.; Weinreich, G. *Phys. Rev. Lett.* **1961**, *7*, 118.

Gatehouse, B. M.; Lloyd, D. J. *J. Chem. Soc. Dalton,* **1973**, 70.

Horrestam, R., *Z. Kristallogr.,* **1989**, *187*, 103-110.

Hyman, A.; Perloff, A.; Mauer, F.; Block, S., *Acta Crystallogr.,* **1968**, Sect. B, *24*, 179.

International Tables for X-ray Crystallography .Vol. IV. Birmingham: Kynoch, Press, **1974.**

Kato, K. IEEE *J. Quantum Electron.* **1990**, *26*, 1173.

Keszler, D. A., *Solid State & Materials Science*, **1996**, in press.

Keszler, D. A.; Akella, A.; Schaffers, K. I.; Alekel III, T. *Mater. Res. Soc. Symp. Proc.* **1994**, *15,* 329.

Keszler, D. A., unpulished results. (Dept. Chem. Oregon State Uni. Corvallis, OR 97331)

Konig, H.; Hoppe, A. *Z. Anorg. Allg. Chem.* **1978**, *439*, 71.

Krogh-Moe, J., *Acta Crystallogr.,***1965**, Sect. B, *18*, 77.

Krogh-Moe, J., *Acta Crystallogr.,***1968**, Sect. B, *24*, 179.

Krogh-Moe, J., *Acta Crystallogr.,***1969**, Sect. B, *25*, 2153.

Krogh-Moe, J., *Acta Crystallogr.* **1972**, Sect. B, *28*, 3089.

BIBLIOGRAPHY (Continued)

Krogh-Moe, J., *Acta Crystallogr.*,**1974**, *Sect.B, 30*, 1178.

Kurtz, S. W.; Perry, T. T., *J. Appl. Phys.* **1968**, *39*, 3798.

Laser Foocus World, **1994**, *30*, 24.

Leskelä, M.; Keskentalo, T.; Blasse, G. *J. Solid State Chem.* **1985**, *59*, 272.

Lloyd, MM. D.; Levesseur, J. A.; Fouassier, C., *J. Solid State Chem.* **1973,** *6*, 179.

MacDowell, J.F., *J. Am. Ceram. Soc.*, **1990**, 73(8), 2287.

Meijerink, A.; Blasse, G, *J. Phys. Condens. Matter*, **1990,** *2*, 3169.

Meijerink, A.; Van Heek, M. M.; Blasse, G. *J. Phys.Chem. Solids,* **1993,** *54*, 901.

Molecular Structure Corporation, *TEXSAN,* Structure Analysis Package, MSC (3200A,Godard. R., Eds.; Oxford Univ. Press, Oxford, U. K., **1985**; pp175-189. Muckenheim, W. Lokai, P. Burghardt, B. and Besting, B. *Appl. Phys.* **1988**, B *45,* 259.

Nagai, T.; Ihara, M., *Yogyo-Kyoshi-Shi*, **1972**, 80(11), 14.

Nebel, A. Beigang, R. *Opt. Lett.* **1991**, *16*, 1729.

Norrestam, R., *Z. Kristallogr.*,**1989**, *187*, 103.

POLSQ: Least Square Unit Cell Refinement, David Cahen, **1973**.

Sasaki, T.; Kuroda, I.; Nakajima, S.; Watanabe, S.; Mori, Y.; Nakai, S. *Advanced Solid-State Lasers Conference,* **1995**.

Saubut, B.; Fouassier, C.; Hagenmuller, P., Mater. Res. Bull. **1981**, *16*, 193.

Schaffers, K.I. PhD thesis, Oregon State University, **1992**.

Schaffers, K. I.; Keszler, D. A. *Chem. Mat.* to be submitted. Chapter2, Schaffers, K.I., Ph.D thesis, Oregon State University, **1992**.

Schaffers, K. I. Ph.D. Thesis, Oregon State University, **1992**.

BIBLIOGRAPHY (Continued)

Schläger, M.; Hoppe, R. *Aust. J. Chem.* **1992**, *45*, 1427.

Schläger, M.; Hoppe, R. *Z. anorg. allg. Chem.* **1993**, *619,* 976.

Shannon, R. D., *Acta Crystallogr.,***1976**, Sect. A, *32*, 751.

Sheldrick, G, M., in 'Ctrystallographic Computing 3"(Sheldrick, G.M.; Krüger, C.R.; Godard. Eds.), Oxford Univ. Press, Oxford, **1975,** 175.

Sheldrick, G, M. In Ctrystallographic Computing 3; Sheldrick, G.M., Krüger, C., and Smith, R.W. and Keszler, D.A., *Mat. Res. Bull.* **1989**, *24*, 725.

Soules, T. F.; Hoffman, M. V. *Kirk-Othmer: Encyclopedia of Chemical Technology*; John Wiley & Sons, Inc. **1981**, *14*, 527.

Stevels, A. L. N. *J. Luminescence,* **1976**, *12/13*, 97.

Sun, H.; Keszler, D. A., unpublished results. Sun, H.; Ph.D thesis, Oregon State University, **1989**.

TEXSAN, Structure Analysis Package, Molecular Structure Corp., MSC (3200A, Research Forest Drive, the Woodlands, TX 77381. International Tables for X-ray Crystallography. Vol. IV. Birmingham: Kynoch Press, 1974.

Thompson, P. D.; Huang, J.; Smith, R. W.; Keszler, D. A., *J. Solid State chem.,* **1991**, *95*, 126.

Thompson, P. D.; Keszler, D. A., *Chem. of Mat.*, **1989**, *1*, 292.

Tu, J., Ph.D. Thesis, Oregon State University, **1996**.

Vegas, A.; Cano, F. H.; Garcia-Blanco, S.*J. Solid State Chem.,* **1976**, *17*, 151.

Velsko, S. P.; Webb, M.; Davis, L.; Huang, C. *IEEE J. Quant. Electron.* **1991**, *27*, 2128.

Vendenberghe, K., M.S. Thesis, Oregon State University, **1997**.

Verwey, J. W.; Fayos, J.; Howie, R. A.; Glasser, F. P.. *Acta Cryst.,* Sect.C, **1985**, *41,* 1394.

Walker, N.; Stuart, D. *Acta Crystallogr.,* **1983**, Sect. A, *39*, 158-166.

BIBLIOGRAPHY (Continued)

Weber, M. J. *CRC Handbook of Laser Science and Technology*, "Section 1:Nonlinear Optical Materials", Boca Raton, Fla.: CRC Press, **1986**.

Welker, T, *J. Luminescence*, **1991**, *48 & 49*, 49.

Wells, A. F. Structural Inorganic Chemistry, **1984**, Clarendon Press. p 1065.

Wen-Tian, F.; Fouassier, C.; Hagenmuller, P. *Mat. Res. Bull.* **1987**, *22*, 899.

Xia, Y.; Chen, C.; Tang, D.; Wu, B., *Adv. Mater.*, **1995**, 7, 79--81.

Yakubovich, O. V.; Yamnova, N. A.; Shchedrin, B. M.; Simonov, M. A.; Belov, N. V., *Dokl. Akad. Nauk SSSR*, **1975**, *228*, 842.7.

Yvon, K.; Jeitschko, W.; Parthe, E. *J. Appl. Crystallogr.* **1977**, *10*, 73.

APPENDIX

APPENDIX

CURRICULUM VITAE

KI-SEOG CHANG

EDUCATION: Ph.D. Chemistry, Oregon State University (OSU), Corvallis, OR. 1993-1998
Major in Solid-State Materials/Inorganic Chemistry

M.S. Organic Chemistry, Pohang Institute of Science & Technology (POSTEC), Pohang, Korea. 1988-1990

B.S. Chemistry, Seoul National University (SNU), Seoul, Korea. 1984-1987

B.S. Mechanical Engineering, Republic of Korea Air Force Academy (KAFA), Seoul, Korea. 1978-1982

WORK EXPERIENCE:

Republic of Korea Air Force Academy, Department of Chemistry, Chungju, Korea. 1990-1993

Republic of Korea Air Force Academy, Department of Chemistry, Chungju, Korea. 1987-1988

Republic of Korea Air Force Training Corps, Daejeon, Korea. 1982-1984

PROFESSIONAL MEMBERSHIP:

Korean Chemical Society (KCS).

PUBLICATIONS: $CaAl_2(BO_3)_2O$: Crystal Structure, Ki-Seog Chang and Douglas A. Keszler, *Mat. Res. Bull.*, 1997, in press.

Synthesis, Structure, Nonlinerity, and Thermal Expansion of $SrAl_2(BO_3)_2O$, Ki-Seog Chang and Douglas A. Keszler, To be submitted to *J. Solid State Chem.*

Synthesis, Structure, and Luminescence of $SrAlBO_4$, Ki-Seog Chang and Douglas A. Keszler, To be submitted to *Acta Crystallographica C.*

Synthesis, Structure, and Luminescence of $SrGa_2(B_2O_5)O_2$, Ki-Seog Chang and Douglas A. Keszler, To be submitted to *J. Solid State Chem.*

Synthesis and Structure of $Li_2Al(BO_3)O$ and $LiAlB_2O_5$, Ki-Seog Chang and Douglas A. Keszler, To be submitted to *J. Solid State Chem.*

Comparative Synthesis of (R)- and (S)-Glycerol Acetonide in Synthetic Studies on Phospholipid Derivatives (May, 1991, KCS, Korea)

The Study on the Biochemical Properties of the Toxic Agents. (April, 1991, KAFA, Korea)

Synthetic Studies of Phosphatidyl Choline Analogs. (October, 1990, POSTEC, Korea)

Synthetic Studies of 2-Amidophosphatidyl Choline and its Derivatives. (March, 1990, M.S. Thesis, Korea)

CONFERENCES: Structure and Properties of Alkaline-earth metal Aluminum borates, D. A. Keszler and K. S. Chang, 213th American Chemical Society national Meeting, April 13-17, 1997, USA

High Optical Nonlinearities in Aluminum Borate Crystals, Douglas A. Keszler and Ki-Seog Chang, International Union of Crystallography (IUCr) XVII, August 8-17, 1996, USA

New System of Borate Nonlinear Optical Materials, D. A. Keszler and K. S. Chang, 51st American Chemical Society (ACS) Northwest Regional Meeting, June 19-22, 1996, USA

Total Synthesis of Phospholipidyl Choline (May, 1991, KCS, Korea)